

**ACOUSTIC AND THERMODYNAMIC STUDY OF
GLYCOL ETHERS IN AQUEOUS SOLUTION OF
SUGAR ALCOHOLS**

Thesis Submitted for the Award of the Degree of

DOCTOR OF PHILOSOPHY

in

Physics

By

Harsimaran Kaur

Registration Number: 12105329

Supervised By

Dr. Kailash Chandra Juglan (11468)

Professor & Associate Dean



**LOVELY PROFESSIONAL UNIVERSITY, PUNJAB
2025**

DECLARATION

I, hereby declared that the presented work in the thesis entitled “**Acoustic and Thermodynamic Study of Glycol Ethers in Aqueous Solution of Sugar Alcohols**” in fulfilment of degree of Doctor of Philosophy (Ph. D.) is outcome of research work carried out by me under the supervision of Dr. Kailash Chandra Juglan, working as Professor, in the Department of Physics of Lovely Professional University, Punjab, India. In keeping with general practice of reporting scientific observations, due acknowledgements have been made whenever work described here has been based on findings of other investigator. This work has not been submitted in part or full to any other University or Institute for the award of any degree.



(Signature of Scholar)

Name of the scholar: Harsimaran Kaur

Registration No.: 12105329

Department/school: Physics/ School of Chemical Engineering and Physical Sciences

Lovely Professional University,

Punjab, India

CERTIFICATE

This is to certify that the work reported in the Ph. D. thesis entitled “**Acoustic and Thermodynamic Study of Glycol Ethers in Aqueous Solution of Sugar Alcohols**” submitted in fulfillment of the requirement for the award of degree of **Doctor of Philosophy (Ph.D.)** in the Department of Physics, is a research work carried out by Harsimaran Kaur, 12105329, is bonafide record of his/her original work carried out under my supervision and that no part of thesis has been submitted for any other degree, diploma or equivalent course.



(Signature of Supervisor)

Name of supervisor: Dr. Kailash Chandra Juglan

Designation: Professor and Associate Dean

Department/school: Physics/School of Chemical Engineering and Physical Sciences

University: Lovely Professional University, Phagwara, Punjab

ABSTRACT

The ultrasonic technique has come out as an effective tool in many research projects, which provide a detailed and accurate approach to understanding different behaviours and properties of different liquid mixes. This method allows the investigation of molecular interactions between the different components, providing crucial insights into the microscopic structure as well as the arrangement of the molecules in a liquid mixture. The behavior of ultrasonic waves while passing through the medium can help in understanding the physicochemical properties of the component molecules. The technique is recognized for its accuracy and non-destructive nature that makes it suitable for the evaluation of the physicochemical properties of different liquid mixes. Ultrasonic analysis is utilized largely in the pharmaceuticals, cosmetics, and food processing industries, and various industrial sectors, where there is an interest in getting intermolecular forces appropriate chemical process optimization because knowledge about it can give important insight into these forces. Thesis deals with the acoustical and thermodynamic properties of ternary mixtures consisting of polyol components maltitol, erythritol, and inositol with water, as well as six different glycol ethers. The aim is to understand the interactions and behavior of these mixtures, which are relevant for applications in various sectors. Experimental density measurements and sound speed data were obtained at various quantities and thermal conditions. Through experimentally obtained data, several properties were calculated, i.e., transfer properties, apparent as well as various partial molar properties, and spectroscopic studies were also investigated to assess the different association types among different molecules. The outcome suggests that the polyol-glycol ether systems consist of predominantly H-bonding and C-H bonds, hydrophobic interactions that are influenced by the varying structure and molecular polarity of the glycol ethers. In addition, this contribution builds upon the existing understanding of molecular dynamics within ternary systems and, furthermore, covers the way for the optimization of the formulation of alloys for different industries. In section 1, in problem 1, the ultrasonic velocity and density values for 2-ME and 2-EE in aqueous inositol solution are determined via experimental measurements. The liquid states of the systems, along with the respective spectroscopic measurements, were performed at a pressure of 0.1

MPa and $T = (288.15\text{-}318.15\text{ K})$. The additional properties that were measured using ultrasonic velocity and density values were measured for the (2-ME/2-EE + water + inositol) in order to obtain their interactions. Additionally, E_{ϕ}^0 and $(\partial E_{\phi}^0/\partial T)_p$ were also determined. The results were studied to decipher the various kinds of existing interactions in liquid mixtures. Also, FTIR spectroscopic study was performed for a simple binary system consisting of inositol and water to examine the interactions for solutes within a solvent. Section II, Problem 2, sound speeds and density values obtained for 2-BE and 2-PhE in $(0.01, 0.02, \text{ and } 0.03)\text{ mol} \cdot \text{kg}^{-1}$ aqueous maltitol solutions. The measurements were done under different thermal conditions and 0.1 MPa pressure. The numerous parameters, such as V_{ϕ} , $K_{\phi,s}$, V_{ϕ}^0 , and $K_{\phi,s}^0$ were obtained from the experimental data. It is helpful in understanding the solvation behavior of maltitol, the important constituent of sugar-free products. Further, with the help of the co-sphere overlap model, a study of intermolecular interactions within the ternary systems was carried out. Partial molar expansibilities, (E_{ϕ}^0) , and their first-order derivatives $(\partial E_{\phi}^0/\partial T)_p$ were calculated to determine the structure-making and breaking properties of different solutes. Additionally, we also carried out spectroscopic studies for both binary and ternary mixtures. The observed different molar properties designate the existence of significant interactions among the solute-solvent components. This is further supported by the positive values of E_{ϕ}^0 . Moreover, the mixture's partial molar properties strongly imply the occurrence of H-bond formation. In problem 3, sound speeds and density values for the (DEGMME/DEGMEE + maltitol (aq)) mixtures were obtained. Based on the obtained data, various apparent molar parameters for the mixture of DEGMME/DEGMEE in aqueous maltitol solutions were estimated along with partial molar and transfer properties. The interaction coefficients, thermal expansion coefficient, and specific volume further contributed to a deeper understanding of the nature of the interactions within the solution. Furthermore, in section III, in problem 4, using values of densities and sound speeds values, for a ternary mixture (erythritol+ water + DEGMME/ DEGMEE) this study calculates various properties at $T=(288.15\text{-}318.15\text{ K})$. Unlike previous research, which primarily focused on binary mixtures, this study delves into a more complex system, and providing valuable insights into solvation behaviour and molecular interactions. These results, derived from precise

measurements using a density and sound analyzer (DSA), that provide an inclusive interpretation on associations type and behaviour, also structural changes within the studied systems. The thesis primarily provides an extensive overview of the experimental data and calculated parameters and in-depth critical analysis of the underlying molecular mechanisms and theoretical implications. Additionally, the study successfully presents comprehensive data and highlights trends in solute-solvent interactions, further interpretation and comparison with existing literature could strengthen the analytical depth of the work.

ACKNOWLEDGMENT

I am deeply grateful to God, the Almighty, for His continuous blessings and guidance throughout my research journey. It is by His grace that I have been able to successfully complete this work. I am deeply indebted to my esteemed supervisor, Dr. Kailash Chandra Juglan, Professor, Department of Physics, and Associate Dean of the School of Chemical Engineering and Physical Sciences of Lovely Professional University, Punjab, India, for providing me the opportunity to carry out my research under his excellent mentorship. His vision, dedication, and unwavering support have been a constant source of inspiration for me. I am sincerely grateful for his persistent encouragement, insightful advice, and patience throughout the course of my Ph.D. I feel truly fortunate to have had the opportunity to work under his guidance.

I would also like to extend my sincere thanks to Dr. Vikramjit Singh, Associate Professor, and the Late Dr. Harsh Kumar Manchanda, Associate Professor, Department of Chemistry, National Institute of Technology, Jalandhar, and Dr. Tejwant Singh Kang, Associate Professor from Guru Nanak Dev University, Amritsar, for graciously allowing me to conduct my experimental work in their labs. I am also thankful for their exceptional guidance, critical insights, and for providing an excellent research environment. Their expertise and support were invaluable throughout the various stages of my research. My special thanks to Dr. Nabaparna Chakraborty, Assistant Professor, Department of Physics, Lovely Professional University, Phagwara, for her continuous support, insightful suggestions, and dedicated assistance throughout my research.

Finally, I would like to acknowledge the most important people in my life, my family, for their unwavering love and support. I owe my deepest gratitude to my father, S. Harvinder Singh, and my grandfather, the late S. Sewa Singh, for their strength, wisdom, and encouragement. Their sacrifices and belief in my potential have been the foundation of my academic journey. I am forever thankful to them for always showing me the light at the end of the tunnel and for being my pillars of strength. My sincere thanks also go to my colleagues and friends for their support, camaraderie, and invaluable assistance throughout this journey.

Thank you all for making this journey possible.

Harsimaran Kaur

TABLE OF CONTENTS

Sr. No.	Title	Page No.
1	Declaration	i
2	Certificate	ii
3	Abstract	iii-v
4	Acknowledgement	vi
5	Table of contents	vii-ix
6	List of Tables	x-xiii
7	List of Figures	xiii-xvii
8	List of Abbreviations	xvii-xviii
CHAPTER 1		
INTRODUCTION		1-10
1.1	Ultrasonic Research	
1.2	Applications of ultrasonic research	
1.3	Ultrasonication	
	1.3.1 Through-transmission technique/ Piezo-Electric Method	
1.4	Chosen system for present study	
	1.4.1 Sugar Alcohols	
	1.4.1.1 <i>myo</i> -Inositol	
	1.4.1.2 Maltitol	
	1.4.1.3 Meso-erythritol	
	1.4.2 Glycol ethers	
	1.4.2.1 Ethylene glycol monomethyl ether (EGMME)	
	1.4.2.2 Ethylene glycol monoethyl ether (EGMEE)	
	1.4.2.3 Ethylene glycol monobutyl ether (EGMBE)	
	1.4.2.4 Ethylene glycol monophenyl ether (EGMPE)	
	1.4.2.5 Diethylene glycol monomethyl ether (DEGMME)	
	1.4.2.6 Diethylene glycol monoethyl ether (DEGMEE)	
1.5.	Importance of binary and ternary mixture	

References		11-13
CHAPTER 2		
REVIEW OF LITERATURE		14-26
References		27-31
CHAPTER 3		
OBJECTIVES AND EXPERIMENTAL PROCEDURES		32-41
3.1	Research Objectives	
3.2.	Research Methodology	
	3.2.1. Preparation of samples	
	3.2.2 Measurements of experimental densities and speed of sound	
	3.2.3. Theory of density speed of sound measurement	
3.3.	Fourier Transform Infrared Spectrometer	
3.4.	Chemical structures	
3.5.	Specifications of the Chemicals	
3.6.	Calculation of Acoustics parameters	
	3.6.1 Acoustic impedance	
	3.6.2 Adiabatic compressibility	
	3.6.3 Wada's constant	
	3.6.4 Rao's Constant	
	3.6.5 Intermolecular free length	
	3.6.6 Vander Waal's constant	
3.7.	Apparent molar, Partial molar and Transfer properties	
	3.7.1 Apparent molar volume	
	3.7.2 Partial molar volume	
	3.7.3 Partial molar volume of transfer	
	3.7.4 Temperature dependent partial molar volume	
	3.7.5 Apparent molar isentropic compression	
	3.7.6 Partial molar isentropic compression	
	3.7.7 Partial molar isentropic compression of transfer	
	3.7.8. Pair and triplet interaction coefficients	

	3.7.9. Apparent specific volume	
3.8.	Isobaric thermal expansion coefficients	
3.9.	FTIR spectroscopy	
CHAPTER 4		
RESULTS AND DISCUSSION		
Section I		
Problem 1	Volumetric and Ultrasonic Studies on Interactions of 2-Methoxyethanol/ 2-Ethoxyethanol in Aqueous Solutions of Inositol at Different Temperatures	42-68
References		69-71
Section II		
Problem 2	Thermodynamic and physicochemical characteristics of 2-Butoxyethanol/ 2-Phenoxyethanol in aqueous Maltitol solutions	72-101
Problem 3	Characteristics of a temperature dependent aqueous solution of Maltitol with DEGMME/ DEGMEE: An acoustic and volumetric approach	102-123
References		124-126
Problem 4	Study of Thermodynamic and Acoustic Properties of DEGMME/ DEGMEE in aqueous Erythritol solutions at different temperatures	127-151
References		152-153
Summary and Conclusions		154-157
Future Scope of Research work		158
List of publications		159-161
List of conferences attended		162

LIST OF TABLES

Table No.	Caption of Tables
CHAPTER 3	
Objectives and Experimental Procedures	
Table 3.1	List of chemical structures
Table 3.2	Chemicals name along with their specifications
CHAPTER 4	
Results and Discussion	
Section I	
Problem 1	
Table 4.1	Density measurements of 2-ME and 2-EE in inositol (aq) at 0.1 MPa pressure and different thermal conditions.
Table 4.2	Speed of sound measurements of 2-ME and 2-EE in inositol (aq) at 0.1 MPa pressure and at different thermal conditions.
Table 4.3	Values of V_ϕ , for 2-ME /2-EE in inositol (aq) mixtures at constant frequency and different temperatures.
Table 4.4	Values of V_ϕ^0 and S_V^* with standard deviations of linear regression of 2-ME and 2-EE in inositol (aq) mixes at pressure of 0.1 MPa.
Table 4.5	Values of ΔV_ϕ^0 of 2-ME and 2-EE in inositol (aq) solutions at pressure, $p=0.1$ MPa.
Table 4.6	Values a, b, and c of 2-ME and 2-EE in inositol (aq) solutions along with R^2 and ARD (deviations).
Table 4.7	Values of E_ϕ^0 for 2-ME and 2-EE in inositol (aq) solutions at different thermal conditions.
Table 4.8	Values of $K_{\phi,s}$, 2-ME and 2-EE in inositol (aq) solution at, $p = 0.1$ MPa.
Table 4.9	FTIR spectra for a binary mixture (Inositol + water).(black: 0.01, red: 0.03, and green: 0.05 mol · kg ⁻¹ inositol).
Table 4.10	Values of $\Delta K_{\phi,s}^0$ for 2-ME and 2-EE in inositol (aq) solutions.
Table 4.11	Interaction coefficients of 2-ME and 2-EE in aqueous solutions of inositol at different temperatures.

Table 4.12	Isothermal expansion coefficients for 2-ME and 2-EE in Inositol (aq) solutions at different temperatures.
Section II	
Problem 2	
Table 4.13	Densities (ρ) values and apparent molar volumes (V_ϕ) values were measured for solutions of 2-BE/2-PhE in maltitol aqueous solutions at pressure, $p = 0.1$ MPa.
Table 4.14	Values of V_ϕ for aqueous maltitol solutions of different concentrations.
Table 4.15	Values of V_ϕ^0 , experimental slopes, S_V^* , with standard deviations of linear regression and partial molar volume of transfer, ΔV_ϕ^0 of 2-BE/ 2-PhE in water and Maltitol (aq) solutions.
Table 4.16	Empirical parameters of Eq. 4.4, for 2-BE and 2-PhE in Maltitol (aq) solutions at different temperatures along with R^2 and ARD (deviations).
Table 4.17	Values of E_ϕ^0 , for 2-BE and 2-PhE in Maltitol (aq) solutions at different temperatures.
Table 4.18	Isothermal expansion coefficients for 2-BE and 2-PhE in Maltitol (aq) solutions at different temperatures.
Table 4.19	Values of the 'c' and $K_{\phi,s}$, for 2-BE and 2-PhE in aqueous Maltitol solutions at different temperatures.
Table 4.20	Values of $K_{\phi,s}^0$, experimental slopes, S_K^* , and $\Delta K_{\phi,s}^0$, for 2-BE and 2-PhE in aqueous Maltitol solutions at different temperatures.
Table 4.21	Interaction coefficients for 2-Butoxyethanol and 2-Phenoxyethanol in aqueous maltitol at different temperatures.
Table 4.22	Functional Group and its quantified frequencies from the FTIR data.
Problem 3	
Table 4.23	Density and calculated V_ϕ values for (DEGMME/ DEGMEE + maltitol) at 0.1 MPa pressure.
Table 4.24	Calculated partial molar volume (V_ϕ^0) values along with experimental slope (S_V^*) for (DEGMME/ DEGMEE + maltitol) at (288.15- 318.15) K temperatures.

Table 4.25	Calculated ΔV_{ϕ}^0 values for (DEGMME/ DEGMEE + maltitol) at 0.1 MPa pressure.
Table 4.26	Calculated values for empirical parameters for (DEGMME/ DEGMEE + maltitol) at (288.15- 318.15) K temperatures.
Table 4.27	Calculated partial molar expansibilities, (E_{ϕ}^0) values for (DEGMME/ DEGMEE + maltitol) at 0.1 MPa pressure.
Table 4.28	Values of sound speeds and $K_{\phi,S}$ values for (DEGMME/ DEGMEE + Maltitol).
Table 4.29	Calculated partial molar isentropic compression ($K_{\phi,S}^0$) values along with experimental slope (S_K^*) for (DEGMME/ DEGMEE + maltitol) at (288.15- 318.15) K temperatures.
Table 4.30	Calculated $\Delta K_{\phi,S}^0$ values for (DEGMME/ DEGMEE + maltitol) 0.1 MPa pressure.
Table 4.31	Pair (V_{AB} , K_{AB}) and triplet (V_{ABB} , K_{ABB}) interaction coefficients for (DEGMME/ DEGMEE + maltitol) at 0.1 MPa pressure.
Table 4.32	Calculated isothermal expansion coefficients for (DEGMME/ DEGMEE + maltitol).
Section III	
Problem 4	
Table 4.33	Values of ρ and V_{ϕ} for solutions of DEGMME/ DEGMEE in erythritol aqueous solutions.
Table 4.34	Partial molar volumes, V_{ϕ}^0 , and parameters S_V^* , and C with standard deviations, for DEGMME/ DEGMEE in erythritol (aq) solutions at p=0.1 MPa.
Table 4.35	Values of ΔV_{ϕ}^0 , of DEGMME/ DEGMEE in aqueous solutions of erythritol.
Table 4.36	Values of empirical constants for DEGMME/ DEGMEE in aqueous solutions of erythritol at p=0.1Mpa along with R^2 and ARD (deviations).

Table 4.37	Partial molar expansibilities, E_{ϕ}^0 for DEGMME/ DEGMEE in erythritol (aq) solutions at different temperatures.
Table 4.38	Values of c , and $K_{\phi,S}$ of DEGMME/ DEGMEE in water and aqueous solutions of erythritol.
Table 4.39	Values of $K_{\phi,S}^0$, experimental slopes, S_K^* , of DEGMME/ DEGMEE in water and erythritol (aq) solutions at $p=0.1$ MPa.
Table 4.40	Values of ΔK_{ϕ}^0 of DEGMME/ DEGMEE in erythritol (aq) solutions at different for temperatures.
Table 4.41	Pair (V_{AB} , K_{AB}) and triplet (V_{ABB} , K_{ABB}) interaction coefficients of DEGMME and DEGMEE in erythritol (aq) mixes.
Table 4.42	Isothermal expansion coefficients for DEGMME/ DEGMEE in erythritol (aq) solutions.

LIST OF FIGURES

Figure No.	Caption of Figures
CHAPTER 1	
INTRODUCTION	
Figure 1.1	Application of ultrasonic research
Figure 1.2	Use of Ultrasound
Figure 1.3	Through-transmission technique/ Piezo electric method
Figure 1.4	myo-Inositol
Figure 1.5	Maltitol
Figure 1.6	Meso-erythritol
Figure 1.7	EGMME
Figure 1.8	EGMEE
Figure 1.9	EGMBE
Figure 1.10	EGMPE
Figure 1.11	DEGMME
Figure 1.12	DEGMEE
Figure 1.13	Different binary and ternary mixtures

CHAPTER 3	
Objectives and Experimental Procedures	
Figure 3.1	Sartorius CPA-225 D electronic weighing balance
Figure 3.2.	Preparation of samples
Figure 3.3	Density and sound velocity analyser
Figure 3.4	Schematic representation of Anton Paar DSA 5000 M
Figure 3.5	Fourier Transform Infrared Spectrometer
CHAPTER 4	
Results and Discussion	
Section I	
Problem 1	
Figure 4.1	2-ME/ 2-EE and Inositol interactions.
Figure 4.2	Comparison graph of (a) density and (b) speed of sound for a binary mixture (Inositol + water) at different temperatures.
Figure 4.3	Comparison graph of density (a) Water + 2-ME and (b) Water + 2-EE at different temperatures.
Figure 4.4	Comparison graph of speed of sound (a) Water + 2-ME and (b) Water + 2-EE at different temperatures.
Figure 4.5	Plots of the variations in V_ϕ of 2-ME (I) and 2-EE (II) in (a) $0.00 \text{ mol} \cdot \text{kg}^{-1}$ inositol, (b) $0.01 \text{ mol} \cdot \text{kg}^{-1}$ inositol, (c) $0.03 \text{ mol} \cdot \text{kg}^{-1}$ inositol and (d) $0.05 \text{ mol} \cdot \text{kg}^{-1}$ inositol.
Figure 4.6	Plots of the variations in partial molar volume, V_ϕ^0 , of 2-ME (red) and 2-EE (blue) in an inositol aqueous solution at various temperatures.
Figure 4.7	Plots of the variations of $K_{\phi,s}$, of (a) 2-ME and (b) 2-EE in an Inositol (aq) solutions. (Symbol: red = 288.15K, green = 298.15K, blue = 308.15K, and yellow = 318.15K).
Figure 4.8	Variations of $K_{\phi,s}^0$ versus molality ($\text{mol} \cdot \text{kg}^{-1}$) of (a) 2-ME and (b) 2-EE in aqueous Inositol solutions at different temperatures.

Figure 4.9	FTIR spectra for a binary mixture (Inositol + water).(black: 0.01 mol · kg ⁻¹ , red: 0.03 mol · kg ⁻¹ , and green: 0.05 mol · kg ⁻¹ inositol).
Section II	
Problem 2	
Figure 4.10	The density of a binary mixture (Maltitol + water) was plotted at various temperatures using both experimental and literature values.
Figure 4.11	Plots depicting the changes in apparent molar volumes of (I) 2-BE and (II)-PhE when transitioning from water to an aqueous Maltitol solution at varying temperatures, specifically for (a) 0.00 Maltitol, (b) 0.01 Maltitol, (c) 0.02 Maltitol, and (d) 0.03 Maltitol (mol · kg ⁻¹).
Figure 4.12	2-BE/ 2-PhE and Maltitol interactions.
Figure 4.13	Plots illustrating the changes in partial molar volume, V_{ϕ}^0 , for 2-BE (blue) and 2-PhE (red) within an Maltitol aqueous solution at various temperatures.
Figure 4.14	Plots illustrating the changes in $K_{\phi,s}$, of (a) 2-BE and (b) 2-PhE within an aqueous Maltitol solution, for concentrations of 0.00 Maltitol (in black), 0.01 Maltitol (in blue), 0.02 Maltitol (in red), and 0.03 Maltitol (in green), at various temperatures. (squares: 288.15K, circles: 293.15K, upward triangles: 298.15K, downward triangles: 303.15K, and diamonds: 308.15K).
Figure 4.15	Plots showing the changes in $K_{\phi,s}^0$ with respect to the molality of (a) 2-BE and (b) 2-PhE in aqueous solutions of Maltitol at different temperatures.
Figure 4.16	FTIR spectra for 2-Butoxyethanol (2-BE)/ 2- Phenoxyethanol (2-PhE) having molality (0.1-0.5) mol · kg ⁻¹ in (0.01, 0.02, and 0.03) mol · kg ⁻¹ maltitol solutions (I) Maltitol + Water (black: 0.01 maltitol, Blue: 0.02 Maltitol, red: 0.03 Maltitol) (II) (a) 2-BE in 0.1-0.5 mol · kg ⁻¹ (b) 2-PhE in 0.1-0.5 mol · kg ⁻¹ in 0.01 maltitol

	<p>solution. (III) 2-BE in 0.1-0.5 $\text{mol} \cdot \text{kg}^{-1}$ (b) 2-PhE in 0.1-0.5 $\text{mol} \cdot \text{kg}^{-1}$ in 0.02 maltitol solution. (IV) 2-BE in 0.1-0.5 $\text{mol} \cdot \text{kg}^{-1}$ (b) 2-PhE in 0.1-0.5 $\text{mol} \cdot \text{kg}^{-1}$ in 0.03 maltitol solution. (Black: 0.1, blue: 0.2, red: 0.3, green: 0.4, sky blue: 0.5) $\text{mol} \cdot \text{kg}^{-1}$ of 2-BE/ 2-PhE.</p>
Problem 3	
Figure 4.17	Comparison of density of maltitol + water at different temperatures with literature values.
Figure 4.18	Plot of V_ϕ of (I) DEGMME and (II) DEGMEE at different temperatures and different concentrations of Maltitol: (a) 0.00 Maltitol, (b) 0.04 Maltitol, (c) 0.06 Maltitol, and (d) 0.08 Maltitol ($\text{mol} \cdot \text{kg}^{-1}$).
Figure 4.19	Partial molar volume, V_ϕ^0 , for DEGMME (red) and DEGMEE (sky blue) within an maltitol aqueous solution at various temperatures.
Figure 4.20	Plot of 'c' values for Maltitol + water with existing previous values [41].
Figure 4.21	Plot of $K_{\phi,s}$, v/s molality, for (a) DEGMME and (b) DEGMEE at different temperatures and concentrations ($\text{mol} \cdot \text{kg}^{-1}$), 0.04 Maltitol (purple), 0.06 Maltitol (black), and 0.08 Maltitol (red).
Figure 4.22	Plot of $K_{\phi,s}^0$ v/s molality, for (a) DEGMME and (b) DEGMEE in maltitol (aq) solutions at different temperatures.
Problem 4	
Figure 4.23	Experimental (line + symbol) and literature values (scatter) of density for erythritol + water at different temperatures.
Figure 4.24	Experimental (line + symbol) and literature values (scatter) of density for (a) DEGMME and (b) DEGMEE at different temperatures.
Figure 4.25	Plot of V_ϕ for (I) DEGMME and (II) DEGMEE at different temperatures and different concentrations of erythritol: (a) 0.1 Erythritol, (b) 0.2 Erythritol, and (c) 0.3 Erythritol ($\text{mol} \cdot \text{kg}^{-1}$).

Figure 4.26	Interactions between DEGMME/DEGMEE and Erythritol.
Figure 4.27	Partial molar volume, V_{ϕ}^0 , for DEGMME (red) and DEGMEE (blue) within an Erythritol aqueous solution at various temperatures.
Figure 4.28	Experimental (line + symbol) and existing values (scatter) [2] of speed of sound for erythritol + water.
Figure 4.29	Experimental (line + symbol) and literature values(scatter) [4,5] of speed of sound for (a) DEGMME and (b) DEGMEE at different temperatures.
Figure 4.30	Values of $K_{\phi,s}$, v/s molality, for (a) DEGMME and (b) DEGMEE at different temperatures and concentrations, ($mol \cdot kg^{-1}$), 0.1 Erythritol (Square), 0.2 Erythritol (Star), and 0.3 Erythritol (circle).
Figure 4.31	Plot of $K_{\phi,s}^0$ v/s molality, for (a) DEGMME and (b) DEGMEE in erythritol (aq) solutions at different temperatures.

LIST OF ABBREVIATIONS

c	Speed of sound
ρ	Density of material
K	Kelvin (Temperature in absolute)
Z	Acoustic impedance
β	Adiabatic compressibility
L_f	Intermolecular free length
R	Rao's constant
W	Wada's constant
b	Vander Waal's Constant
V_{ϕ}	Apparent molar volume
m_A	Molality of the solute
m_B	Molal concentration of co-solute
p	Pressure
Pa	Pascal
T	Temperature

V_{ϕ}^0	Partial molar volume
ΔV_{ϕ}^0	Partial molar volume of transfer
a, b, c	Constants of least square fitting of equation 4.4
E_{ϕ}^0	Partial molar expansibility
$K_{\phi,s}$	Apparent molar isentropic compression
K_S	Isentropic compressibility
$K_{\phi,s}^0$	Partial molar isentropic compression
ΔK_{ϕ}^0	Partial molar isentropic compression of transfer
S_V^*, S_K^*	Experimental Slopes
V_{AB}	Pair interaction coefficient for volume
K_{AB}	Pair interaction coefficient for isentropic compression
V_{ABB}	Triplet interaction coefficient for volume
K_{ABB}	Triplet interaction coefficient for isentropic compression
ASV	Apparent specific volume
α_p	Isobaric thermal expansion coefficients
EGMME	Ethylene glycol monomethyl ether
EGMEE	Ethylene glycol monoethyl ether
EGMBE	Ethylene glycol monobutyl ether
EGMPE	Ethylene glycol monophenyl ether
DEGMME	Diethylene glycol monomethyl ether
DEGMEE	Diethylene glycol monoethyl ether

CHAPTER 1

INTRODUCTION

1.1 Ultrasonic Research

Ultrasonic investigation is a technique that use high-frequency sound waves, that are particularly in the range of 1 MHz to 20 MHz. Studying the physical as well as chemical properties of various materials and mixtures is highly beneficial. These waves travel through different media, such as liquids, solids, and gases, and their interaction with the medium mainly provides a great understanding into molecular interactions, structure, and other important properties of mixtures and materials [1-5]. This method is widely used in many fields such as chemistry, physics, biology, material science, and engineering, because of its non-destructive nature as well as it produces precise data about the composition and behaviour of substances. In the case of ultrasonic investigations, the frequency typically ranges between 1 MHz and 20 MHz, that allows for high-resolution probing of molecular-level interactions. These waves can travel through a medium by causing periodic compression and rarefaction of particles, as well as their velocity and absorption properties depend on the molecular composition, structure, and physical state of the mediums (solid, liquid, or gas). When ultrasound waves travel through a medium, it interacts with the molecules present in the medium, that cause changes in wave velocity and amplitude, that depend on the characteristics of the medium such as ultrasonic velocity, viscosity, and densities. Understanding how these waves react in binary and ternary systems become useful in the elucidation of some considerable phenomena, especially molecular interactions and other thermodynamic properties [6-8]. The primary purpose for which ultrasonic waves are employed is to study liquids, particularly mixtures, and to understand the interactions present widely in the liquids. They are also applied to get comprehensive data related to physical and chemical characteristics of various liquid combinations. This research is quite useful and the practice of ultrasonic waves gives how different work out with each other to form a mixture [9-11]. For instance, in binary or ternary mixtures, the extensive study of ultrasonic waves explains the constituent component angling of the molecules for solvent-solute, solute-solute and solvent-solvent. These variations are indicative of molecular attractions, repulsion, H-bonding, Van der Waals forces and ion-dipole interactions present among the mixture participants. Also, this study allows

to measure the sound speeds and the densities of the mixes by how this ultrasonic wave propagates within the medium. Normally denser materials slow down the speed of propagation of the ultrasonic wave since more energy will be required to shift the particles in the medium [12-15]. As an additional component, sound speed refers to the velocity at which sound waves travel in any given medium. These parameters present very vital information concerning the composition of the mixture and the relationship between the components within the mixture. Ultrasonic velocity in liquids is determined by the medium of the liquid, which may include density, compressibility, and the manner of the molecule's interaction. In more compact and organized liquids, sound transmission is slower because waves are obstructed by closely arranged organized structures. On the contrary, less dense or broad-range compression mixtures allow relatively faster sound wave propagation. It is possible to deduce effects related to the ordering of molecules in a compound by simply determining the sound speed in that compound. In addition, ultrasonic investigation discloses more useful data relating to the bonding and arrangement of atoms [16-20]. The degree, for instance, to which sounds are absorbed or transmitted throughout a medium is dependent on the medium's physical characteristics including the presence or absence of strong hydrogen bonds and activity by dipoles, ion and hydrophilic and other such union interactions. Considerable evidence about structural principles like packing of the molecules, the strength of the molecular association, and the extent of different species' interactions can be provided by studying the scattering and absorption of sound in a mixture. Such techniques are especially useful to understand these effects due to the fact that one is able to visualize the structure around solute molecules in the presence of solvent and more importantly, how ultrasonic waves propagate through a given mixture-solute and solvent eluding to the concept of solvation dynamics [21-26]. Ultrasonic techniques are valuable in fields like chemistry, physics, and pharmaceuticals, where solvation impacts the stability and reactivity of compounds. Mixtures help reveal molecular structures and interactions, with higher ultrasonic velocities indicating tightly packed, stiff architectures, and lower velocities reflecting looser packing and weaker interactions. As ultrasonic waves pass through a medium, energy is lost via absorption or scattering, and this attenuation provides insights into internal friction and viscosity-high attenuation typically suggests higher viscosity and stronger intermolecular forces.

Adiabatic compressibility reflects how much a material's structure compresses under sound waves. Overall, ultrasound is a safe, efficient, and non-intrusive tool for probing molecular interactions and assessing the physicochemical and thermal properties of liquid-liquid systems [27,28].

1.2 Applications of ultrasonic research

This technique is applicable in many sectors, mainly textiles, pharmaceuticals, chemicals, cosmetics, biotechnology, automotive, healthcare, etc., where this method is helpful. Moreover, this research studies a lot of liquid mixtures, which proves to be useful and important in many aspects. In addition, studies of binary and ternary mixtures by ultrasonic methods have numerous useful uses. Ultrasonic methods are

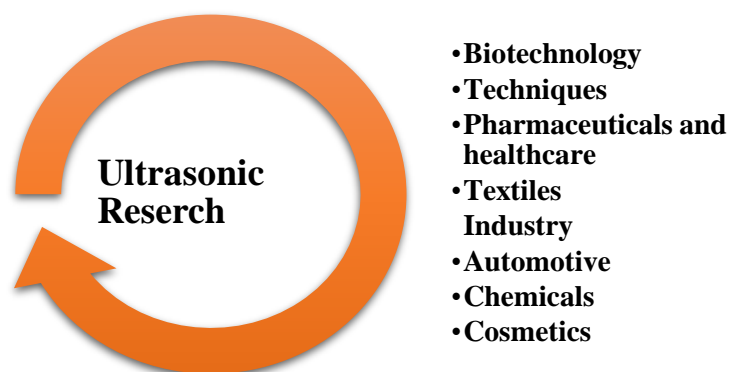


Figure 1.1 Application of ultrasonic research

primarily applied for the understanding of the resolution of solute-solvent associations, phase behaviour, and the arrangement of molecules in the solution. These are valuable for drug formulation, emulsions, and mixtures used in chemical processes. Ultrasonic investigations are also helpful in characterising materials, composites, and mixtures, particularly in understanding their mechanical and thermal properties [29-31]. This study is applied to analyse the structure and interactions in food emulsions, suspensions, and solutions, leading to better product formulations. Moreover, ultrasound is used in cleaning, detection of cracks, echocardiography, ultrasonography, sound navigation, and ranging etc.

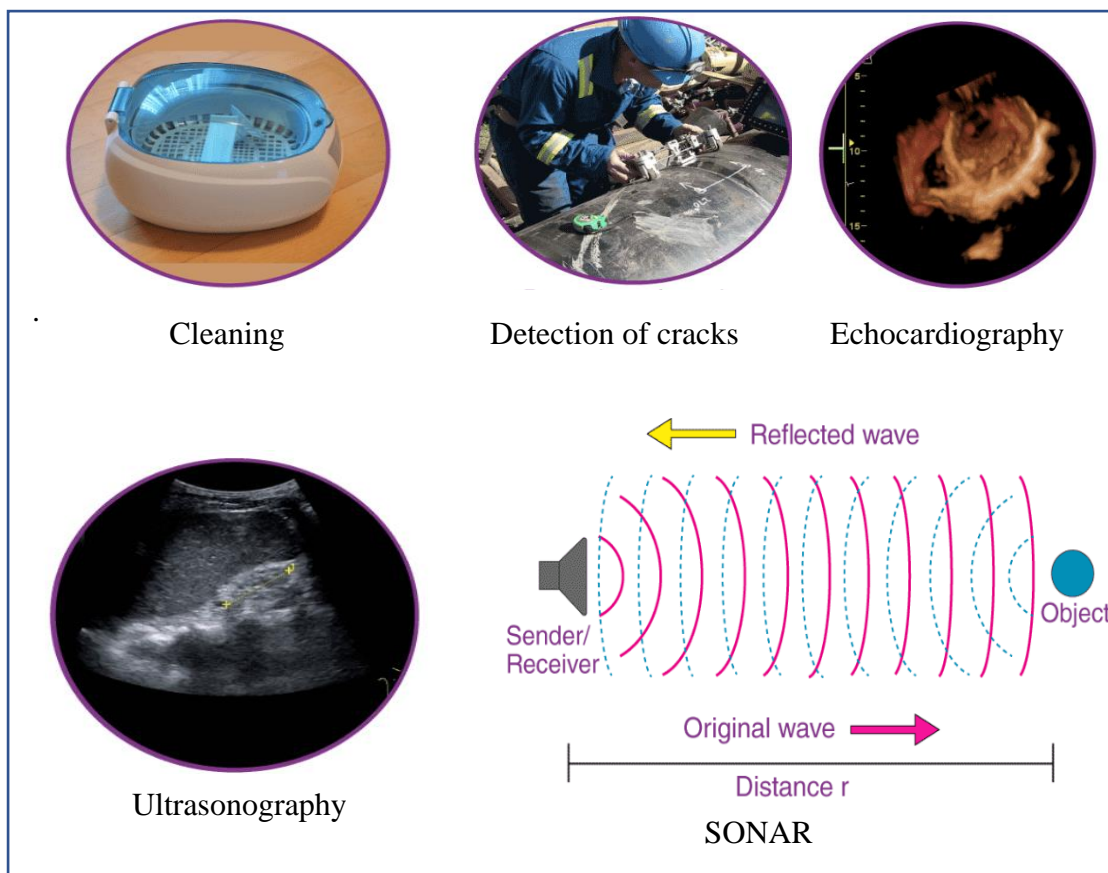


Figure 1.2. Use of Ultrasound

1.3 Ultrasonication

Ultrasonication is a process of agitating samples using high-frequency sound energy. The Anton Paar DSA 5000 M effectively utilizes this principle by applying high-frequency sound waves that generate significant impact energy on liquid particles. The DSA 5000 M is equipped with advanced ultrasonic transducers that produce consistent high-frequency sound waves that ensure efficient agitation and dispersion of particles within the base fluid. Different types of ultrasonication setups, such as probe-type and bath-type sonicators are available, but pulse-echo methods are more advantageous and accurate.

1.3.1 Through-transmission technique/ Piezo-Electric Method

In the through-transmission technique, an ultrasonic pulse is sent from a transmitter transducer. This pulse travels through the material or medium under investigation and is received by a receiver transducer on the opposite side. The time taken for the ultrasonic wave to pass through the sample and the changes in the wave (such as amplitude reduction or phase shifts) provide valuable information about the material's

internal structure and physical properties. A transmitting transducer generates high-frequency ultrasonic waves. This transducer converts an electrical signal into mechanical vibrations (ultrasound), which then propagate through the medium and

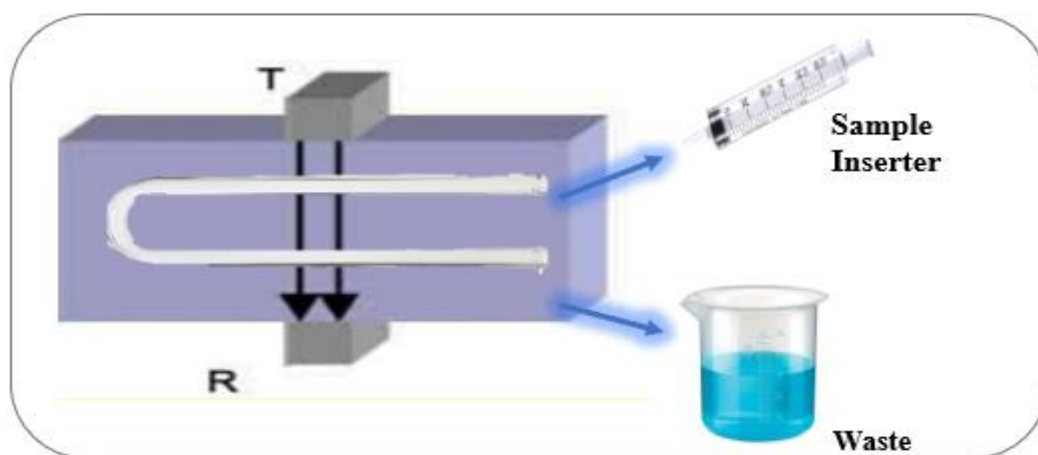


Figure 1.3 Through-transmission technique

receiving transducer that is placed directly opposite to the transmitting transducer. This device captures the ultrasonic waves after they have passed through the sample. The receiving transducer converts the sound waves back into electrical signals for analysis.

1.4 Chosen system for present study

This investigation focuses on sugar alcohols and glycol ethers due to their unique properties and widespread industrial use. Sugar alcohols such as inositol, erythritol, and maltitol are valued for their low caloric content, minimal impact on blood glucose, and benefits to oral health, making them ideal sugar substitutes. Glycol ethers, known for their low volatility and high solvency, are commonly used in paints, coatings, and cleaning agents. This study explores potential interactions between these compounds to develop innovative formulations that promote health, improve product stability, and enhance sensory qualities.

1.4.1 Sugar Alcohols

These compounds are mainly carbohydrates that own molecular structures with features of both sugars as well as alcohols. These compounds are commonly used as low-calorie sweeteners and provide a taste the same as sugar but with fewer calories. Since sugar alcohols are not fully absorbed by the body, they impact blood sugar levels little, making them a popular choice for sugar-free and reduced-calorie products.

Additionally, sugar alcohols can be useful for weight management and dental health, but consuming them in excess may lead to digestive discomfort, such as bloating and gas problems. One of their key benefits is that they do not lead to tooth decay like regular sugars do. In this study, three sugar alcohols are used that are as follows:

1.4.1.1 *myo*-Inositol

Myo-inositol is a naturally occurring carbocyclic sugar alcohol found in high amounts in the brain and various mammalian tissues. It plays a crucial role in maintaining cellular function by regulating osmotic balance and transmitting signals in response to hormones, growth factors, and neurotransmitters. It has about half the sweetness of sucrose and is synthesized in the body from glucose, with the kidneys producing around 2 grams daily. In the brain, myo-inositol supports the interaction between steroid hormones and neurotransmitters with their receptors, contributing to hormonal and neurological health. In recent years, it has gained recognition for its safety and effectiveness in managing polycystic ovary syndrome (PCOS), making it a widely accessible therapeutic option [32,33].

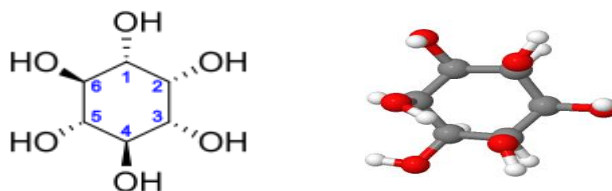


Figure 1.4 *myo*-Inositol

1.4.1.2 Maltitol

A sugar alcohol, “maltitol” provides about 75% to 90% of the sweetness of sucrose but has fewer calories and a negligible effect on blood sugar levels, which makes it a popular choice in sugar-free and reduced-calorie items. Unlike sucrose, maltitol does not brown during cooking, yet its similar taste and texture make it ideal for use in many products [34]. Chemically known as 4-O- α -glucopyranosyl-D-sorbitol, maltitol is produced by hydrogenating maltose, and it is derived from the hydrolysis of starch, mainly corn syrup. Beyond its use in food, maltitol is mainly used in the pharmaceutical industry in syrups, where its non-crystallizing nature prevents bottle caps from sticking, and it also acts as a humectant and plasticizer in gelatin capsules [35].

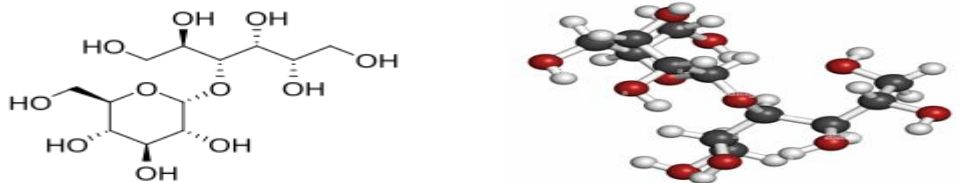


Figure 1.5. Maltitol

1.4.1.3 meso-Erythritol

Erythritol provides about 60–70% of the sweetness of sucrose with almost no calories, making it ideal for those managing sugar intake or weight. Unlike other sugar alcohols, it's absorbed and excreted unchanged, with minimal impact on blood sugar or insulin-suitable for diabetics [36]. Found naturally in fruits like grapes and melons, it's commercially produced by fermenting glucose. Erythritol is widely used in sugar-free gums, candies, baked goods, and drinks. It rarely causes digestive issues and doesn't contribute to tooth decay, adding to its appeal as a sugar alternative [37,38].

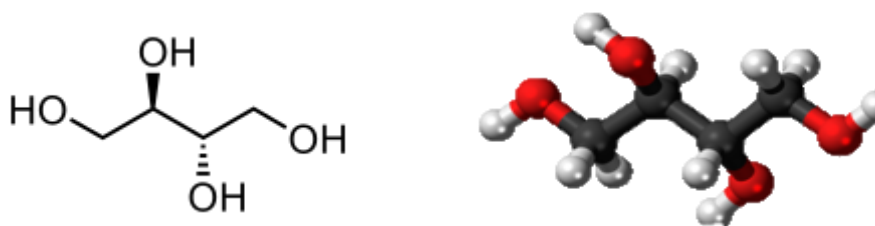


Figure 1.6. Erythritol

1.4.2. Glycol ethers

In the current study, a wide range of fluids is used to make different mixtures. However, based on a comprehensive review of existing literature, five specific solutes were selected for this study. These solutes were chosen for their established effectiveness in various industries. The main focus and aim of these selected glycol ethers is to enhance the quality and consistency of the mixtures, contributing to improved performance in various industrial and chemical applications.

1.4.2.1 Ethylene glycol monomethyl ether (EGMME)

It is also known as 2-methoxyethanol, it is a highly versatile solvent that is known for its ability to dissolve in both water and organic compounds effectively. This dual solubility makes EGME suitable for various applications, including paints, coatings, and industrial cleaners. Its balanced evaporation rate and solvent strength are very important in formulations that demand effective dissolution in diverse environments

without rapid drying. Like several compounds that provide similar solubility and performance in various industrial settings, EGMME is well regarded for its efficiency in maintaining smooth and stable solutions [39,40].

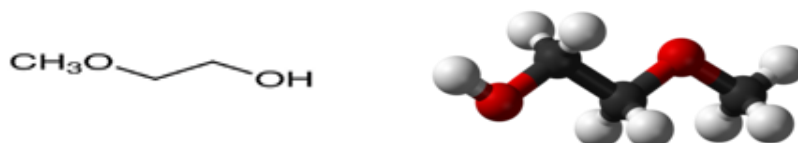


Figure 1.7 EGMME

1.4.2.2 Ethylene glycol monoethyl ether (EGMEE)

It is also referred as 2-ethoxyethanol, this solvent possesses outstanding solubility characterized by an intermediate volatility and solvent strength making it suitable for coatings, lacquers, and varnishes. Like other compounds it is used to improve the texture in formulations, EGMEE helps retain uniformity without much development of crystals and any sudden loss of moisture. It can also be found in industrial cleaning products and surface finishing [41,42].



Figure 1.8 EGMEE

1.4.2.3. Ethylene glycol monobutyl ether (EGMBE)

It is also known as 2-butoxyethanol. This compound has become quite popular owing to its efficient solvent strength and evaporation rate. Its regular release properties are valued in paints and coatings and industrial cleaning agents where an even and consistent application is required. Moreover, EGMBE possesses the quality of long-term solvency akin to the controlled release of certain other materials used in the formulation to avoid ingredient crystallization and keep the mixture uniform. However, it is commonly used in adhesives and hydraulic fluids, though it must be handled with care due to potential irritant effects [43,44].

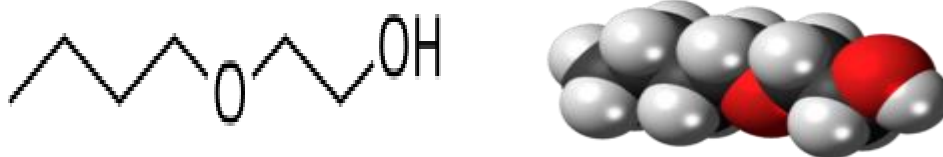


Figure 1.9 EGMBE

1.4.2.4 Ethylene glycol monophenyl ether (EGMPE)

More familiar as 2-phenoxyethanol, this highly functional compound has been effective in the dissolution of crenophilic substances (e.g., dyes, inks) and coatings. Its solvent properties are similar to those of substances used to maintain the uniformity and consistencies of numerous chemical preparations. EGMPE's phenyl group mainly enhances its ability to interact with aromatic compounds, making it very useful in specialized industries. Additionally, it also provides a unique advantage in formulations where stability and prolonged performance are critical [45,46].

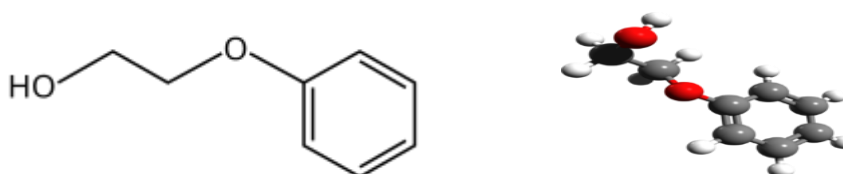


Figure 1.10. EGMPE

1.4.2.5 Diethylene glycol monomethyl ether (DEGMME)

It is also referred to as 2-methoxyethanol and is recognized for its high solvency properties, particularly in the formulation requiring stability over a prolonged period and low volatility. More formulations intended for slow-releasing activity performance, this compound is used in coatings, cleaning agents, and hydraulic fluids because of its low evaporation rate. Due to its water miscibility, it is also widely used in the formulation of paints and surface treatments, where it plays an important role in improving the performance and stability of the end product [47,48].



Figure 1.11 DEGMME

1.4.2.6. Diethylene glycol monomethyl ether (DEGMEE)

It is also referred to 2-2-ethoxyethanol, which has outstanding compatibility with water, and it mainly provides a long evaporation rate and ensures effective use in several industries. It is incorporated in formulations for consistency, and it is rendering capability without drying too quickly. Due to these properties, it is used in paints, coatings, cosmetics, and pharmaceutical products, where active ingredient stability and effectiveness are essential. Additionally, DEGMEE's effectiveness in water and organic compounds significantly contributes to its usefulness across industries [49,50].

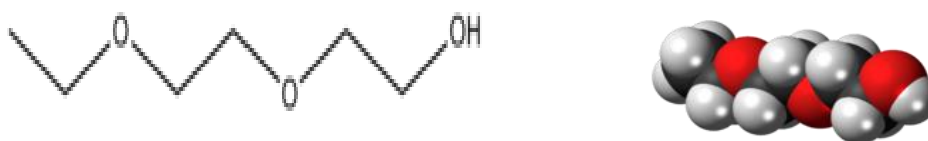


Figure 1.12 DEGMEE

1.5. Importance of binary and ternary mixtures

Binary (water and sugar alcohols/glycol ethers) and ternary (water, sugar alcohol, and glycol ethers) mixtures play a vital role in enhancing product performance across industries. These combinations leverage the water compatibility of sugar alcohols and the solvency and controlled evaporation of glycol ethers, improving solubility, stability, and viscosity. Such properties make them ideal for use in pharmaceuticals, cosmetics, coatings, and adhesives [51–54]. Adjusting the component ratios allows manufacturers to fine-tune properties like drying time, solvent strength, and cooling effects.

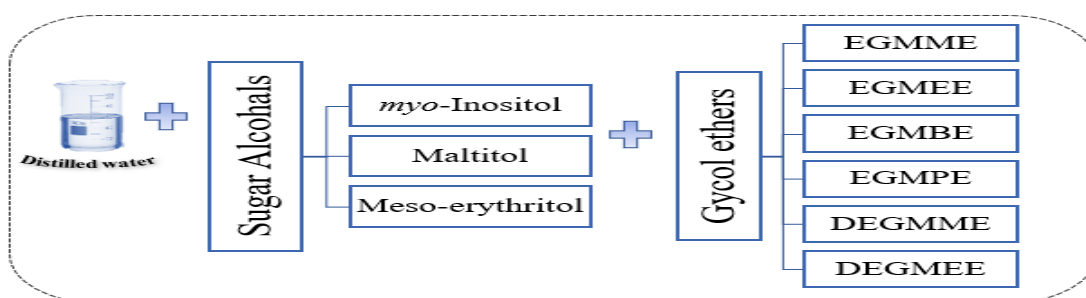


Figure 1.13 Different binary and ternary mixtures

Temperatures of 288.15 to 318.15 K were chosen to observe temperature-dependent behaviors under realistic industrial and environmental conditions, ensuring practical relevance and broad applicability.

References

1. H. Kumar, M. Singla and R. Jindal, *Monatsh. Chem.* 145, 1063-1082 (2014).
2. H. Kumar and I. Behal, *J. Mol. Liq.* 219, 756-764 (2016).
3. H. Kumar, M. Singla and R. Jindal, *J. Mol. Liq.* 199, 385-392 (2014).
4. T.S. Banipal, D. Kaur, P.K. Banipal and G. Singh, *J. Chem. Thermodyn.* 39, 371-384 (2007).
5. R. Sadeghi and A. Gholamireza, *J. Chem. Thermodyn.* 43, 200-215 (2011).
6. S.S. Dhondge, R. Paliwal and N.S.S. Bhawe, *J. Chem. Thermodyn.* 59, 158-165 (2013).
7. A.K. Nain, R. Pal and Neetu, *J. Chem. Thermodyn.* 64, 172-181 (2013).
8. N. Chakraborty, K.C. Juglan, H. Kumar and M. Singla, *J. Chem. Thermodyn.* 174, 106876 (2022).
9. C.M. Romero and F. Negrete, *Phys. Chem. Liq.* 42, 261-267 (2004).
10. S. Baluja and S. Oza, *Fluid Phase Equilibria* 178, 233-238 (2001).
11. M.T. Zafarani-Moattar and S. Sarmad, *J. Chem. Thermodyn.* 42, 1213 (2010).
12. A. Salabat, L. Shamshiri and F. Sahraei, *J. Mol. Liq.* 118, 67-70 (2005).
13. R. Sadheghi and F. Ziamajidi, *J. Chem. Eng. Data* 52, 1037-1044 (2007).
14. W.G. McMillan, J.E. Mayer, *J. Chem. Phys.* 13, 276-305 (1945).
15. H.L. Friedman and C.V. Krishnan, *J. Sol. Chem.* 2, 37-51 (1973).
16. A.V. Rajulu and P.M. Sab, *Bull. Mater. Sci.* 18, 247-253 (1995).
17. K.N. Mehrotra and S.K. Upadhyaya, *Phys. Chem. Liq.* 19, 47-57 (1989).
18. K.C. Rao, S.V. Naidu and A.V. Rajulu, *Eur. Polym. J.* 26, 657-659 (1990).
19. A. Thakur, H. Kumar, K.C. Juglan and K. Kaur, *J. Mol. Liq.* 288, 111014 (2019).
20. L.D. Jennifer, V.N. Nathaniel, A.S. Kim and J.M. Vanderkooi, *J. Phys. Chem. B* 109, 24152 (2005).
21. J. McDuffie, R.G. Quinn and T.A. Litovitz, *J. Chem. Phys.* 37, 239-242 (1962).
22. S.K. Begum, R.J. Clarke, M.S. Ahmed, S. Begum and M.A. Saleh, *J. Mol. Liq.* 177, 11-18 (2013).
23. R.A. Durst and J.K. Taylor, *J. Res. Natl. Bur. Stand.* 68, 625-630 (1964).
24. D.H. Dagade, S.P. Shinde, K.R. Madkar and S.S. Barge, *J. Chem. Thermodyn.* 79, 192-204 (2014).
25. Ernst and B. Jewowska-Trzeblalowska, *J. Phys. Chem.* 79, 2113-2116 (1975).

26. Ashima, K.C. Juglan and H. Kumar, *J. Chem. Thermodyn.* 140, 105916 (2020).
27. X. Jiang, C. Zhu, and Y. Ma, *J. Chem. Eng. Data* 58, 2970-2978 (2013).
28. C. Zhu, X. Ren and Y. Ma, *J. Chem. Eng. Data* 62, 477-490 (2017).
29. H. Kumar and I. Behal, *J. Chem. Thermodyn.* 102, 48-62 (2016).
30. A. Ali, S. Hyder and A.K. Nair, *J. Mol. Liq.* 79, 89-99 (1999).
31. K. Kaur, K.C. Juglan, H. Kumar and I. Behal, *J. Chem. Eng. Data* 63, 3237-3251 (2018).
32. C.M. Romero, M.S. Paez and M.J. Puchana, *J. Mol. Liq.* 223, 1192-1196 (2016).
33. M.B. Blodgett, S.P. Ziemer, B.R. Brown, T.L. Niederhauser and E.M. Woolley, *J. Chem. Thermodyn.* 39, 627-644 (2007).
34. X. Jiang, C. Zhu and Y. Ma, *J. Mol. Liq.* 188, 67-73 (2013).
35. C.M. Romero, J.M. Lozano and G.I. Giraldo, *Phys. Chem. Liq.* 46, 78-85 (2008).
36. C. Zhu, Y. Ma and C. Zhou, *J. Chem. Eng. Data* 55, 3882-3885 (2010).
37. U. Shahazidy, M.A. Jamal, M. Muneer, B. Naseem and A.K. Qureshi, *J. Mol. Liq.* 350, 118543 (2022).
38. C.G. Awuchi and K.C. Echeta, *Int. J. Adv. Acad. Res.* 5, 1-33 (2019).
39. A. Boruń, A. Florczak and A. Bald, *J. Mol. Liq.* 149, 74-80 (2009).
40. H. Kumar, K. Kaur, S. Arti and M. Singla, *J. Mol. Liq.* 221, 526-534 (2016).
41. P.J. Carvalho, C.H. Fonseca, M.L.C. Moita, A.F. Santos and J.A. Coutinho, *J. Chem. Eng. Data* 60, 3721-3737 (2015).
42. I. Cibulka, *J. Chem. Thermodyn.* 125, 240-249 (2018).
43. A. Boruń, A. Florczak and A. Bald, *J. Chem. Eng. Data.* 55, 3725-3730 (2010).
44. I. Cibulka, *J. Chem. Eng. Data* 62, 2649-2658 (2017).
45. H. Makhoulouf, N. Munoz-Rujas, F. Aguilar, B. Belhachemi, E.A. Montero, I. Bahadur and L. Negadi, *J. Chem. Thermodyn.* 128, 394-405 (2019).
46. J. Wang, Y. Liu, W.R. Kam, Y. Li and D.A. Sullivan, *Experi. Eye Res.* 196, 108057 (2020).
47. G.P. Dubey, K.K. Mehra and M. Sharma, *J. Chem. Thermodyn.* 42, 234-243 (2010).
48. C.P. Pandhurnekar, D.V. Parwate and S.S. Dhondge, *J. Mol. Liq.* 183, 94-101 (2013).

49. S.S. Dhondge, C.P. Pandhurnekar and D.V. Parwate, *J. Chem. Thermodyn*, 41, 577-585 (2009).
50. P. Suneetha, T.S. Krishna, M. Gowrisankar and D. Ramachandran, *J. Mol. Liq.* 238, 170-183 (2017).
51. R. Rani, A. Kumar, T. Sharma, T. Sharma and R.K. Banezai, *J. Chem. Thermodyn.* 135, 260-277 (2019).
52. G.I. Egorov, D.M. Makarov and A.M. Kolker, *Russ. J. Gen. Chem.* 80, 1267-1275 (2010).
53. N. Chakraborty, K.C. Juglan, H. Kumar and M. Singla, *J. Chem. Eng. Data* 6, 2292-2306 (2022).
54. V. Dhasi, R. Wadhwani, Y. Akhtar, J.D. Pandey and V. Vyas, *Acta Acustica united with Acustica*, 84, 976-979 (1998).

CHAPTER 2

REVIEW OF LITERATURE

Reddy et al. (1994) had investigated properties of aqueous 1,2-ethanediol and alkoxy alcohols at $T = 308.15$ K. Their research revealed that the excess volumes and compressibility deviations in these mixtures were negative, whereas deviations in viscosity were consistently positive across all the systems analyzed. [1]

Aminabhavi and Gopalakrishna (1995) had examined several binary mixtures that included water and various solvents such as N,N-dimethylacetamide, acetonitrile, EG, DEG, 1,4-dioxane, tetrahydrofuran, 2-ME, and 2-EE at a temperature of 298.15 K. They focused on properties like densities, ultrasonic velocity, and viscosity that provide valuable insight into the molecular interactions occurring within these mixtures. [2]

Aralaguppi et al. (1996) had investigated binary mixtures of 2-ethoxyethanol with dioxane, acetonitrile, and tetrahydrofuran. binary mixtures of 2-ethoxyethanol with dioxane, acetonitrile, and tetrahydrofuran. Their focus was on measuring properties such as density, refractive index, viscosity, and ultrasonic velocity and acquiring data therefrom to work out values that give important information relating to the kind of interaction at the molecular level going on in such systems. [3]

Magazu et al. (1997) had studied the density and ultrasonic velocity of α - α -trehalose in water-based solutions through ultrasonic measurements. From their study, it came out that these solutions failed to exhibit ideal mixing behavior. Through excess compressibility analysis, it was understood that, at higher concentration, the molecules of solutes are likely to show intramolecular H-bonds. [4]

Eliassi and Modarres (1998) had studied the densities of binary mixtures of water with PEG 400, 4000, and 6000 at different temperatures. This work provides valuable insight into the molecular interactions occurring within these mixtures. [5]

Tamura et al. (1998) had worked upon the properties of ethoxyethanol and H_2O mixtures. Their work consisted of the determination of excess enthalpy and heat capacity. They have also derived density data for three different temperatures and ultrasonic velocity at 298.15K temperature that provides much better insight into the behavior of the mixture at different temperatures. [6]

Ali et al. (1999) had studied viscosities, densities, and ultrasonic velocities for some pure compounds, such as 1-octanol, ethanol, acetonitrile, and 1-hexanol. From these data, they reported values of several physical properties that provided evidence related to the molecular association between molecules in those compounds. [7]

Moattar and Mehrdad (2000) had presented experimental values of density measurements in two kinds of mixtures, namely in aqueous polymer mixtures in the presence of dissolved salts and in aqueous-salt mixtures, wherein the apparent molar volumes of these systems had been determined. [8]

Tamura et al. (2000) had studied the various physical properties of mixes composed of 2-glycol ethers and n-octane. In that study, they showed that the excess isobaric thermal expansivities were greatly positive, which is an indication of a typical behavior of the polar mixes, but the excess isothermal and isentropic compressibilities were found to be of small values. [9]

Baluja and Oza (2001) had investigated various thermodynamic properties, such as Gibbs free energy, specific impedance, several excess molar properties, and isentropic compressibility. The study was conducted on methanol and anisole-dimethylformamide and anisole-chloroform mixtures. [10]

Ebner et al. (2002) had studied the D-Panthenol properties, which were used in cosmetic and pharmaceutical formulations and were claimed to have a positive impact. [11]

Graber et al. (2002) had investigated the data for viscosity, density, and refractive index in blend of H₂O, PEG, and sodium nitrate at varying temperatures and calculated the excess molar volumes of the liquid combinations. [12]

Sorenson et al. (2003) had investigated the apparent molar volume as well as the heat capacity of L-proline (aq) mixes, including solutions with equimolar HCl/NaOH under a pressure of 0.35 MPa. Results from their research, particularly on NaProl (aq) mixes, employed Young's Rule to account for species variation. [13]

George and Sastry (2003) had studied the different binary mixes containing 2-ME, 2-EE, and 2-BE, mixed with various aromatic and cyclic hydrocarbons, including benzene, toluene, different isomers of xylene (o-, m-, and p-), ethylbenzene, and cyclohexane. At various temperatures, measured properties such as density, excess

molar properties, viscosities, ultrasonic velocity, and relative permittivity's provide great understanding of the behaviour of liquid system. [14]

Sastry and Patel (2003) had examined densities, sound speed, various excess molar properties, and relative permittivity of different mixes of alkyl acetates with glycols, their study provided a qualitative assessment of deviations and excess functions to better understand the interactions present within these mixtures at various temperatures. [15]

Schmelzer et al. (2004) had performed measurements of ultrasonic velocity and densities of the mixtures of water and polyethylene glycol (PEG). Using experimental data, they derived various acoustic properties, including adiabatic compressibility calculated via Laplace's equation. [16]

Syal (2005) has studied the viscosity, sound velocity, and density of PEG solutions in water and acetonitrile at a constant temperature. Using the data obtained from it, several acoustic parameters have been calculated. [17]

Zwirbla et al. (2005) had investigated the densities and ultrasonic velocities in mixtures of water with EG and PEG 200 and 400 at various temperatures. They had calculated adiabatic compressibility and determined the variation of density and velocity with temperature and concentration. [18]

Blodgett et al. (2007) have studied the apparent molar properties and heat capacity of several sugar alcohol (aq) solutions. With the densimeter for density measurements and the fixed-cell temperature scanning calorimeter for heat capacity, they could study the molecular interaction in the solutions. [19]

Roy et al. (2007) had studied the viscosities and densities of formamide with compounds like 2-ME, acetophenone, acetonitrile, 1,2-dimethoxyethane, and dimethyl sulfoxide. Their results proved very informative on the types of interactions prevailing in these systems [20].

Ayranci and Sahin (2008) had measured ultrasonic velocity and densities of PEG and EG. Several parameters obtained from these measurements were calculated and plotted graphically, which provided information about the behavior of these substances. [21]

Palani and Geetha (2008) had studied the ultrasonic velocity, viscosity, and density of aqueous PG in combination with tetrahydrofuran, dimethylformamide, dimethyl

sulfoxide, and 1,4-dioxane at different temperatures. Data gave a chance to compute a set of excess properties and interaction parameter (d). [22]

JianBan et al. (2008) had analyzed the density of a water-ethylene glycol binary system to determine the excess molar volume. FTIR spectra were also analyzed, paying special attention to the OH-stretching vibrations linked to the interaction between water and alcohol as well as to bending vibrations of water. [23]

Romero et al. (2008) had investigated the density of various aqueous compounds such as 1-propanol, 1,2, 1,3 and 1,2,3 propanediol across a range of temperatures. By analyzing the data, they calculated partial and excess molar properties, providing insight into the molecular interactions within these mixtures. [24]

Kinart et al. (2008) had studied the properties of n-alkoxyethanols combined with sulfolane, focusing on density, viscosity, and relative permittivity at 303.15 K. Their findings highlighted the role of intermolecular forces and structural aspects of these binary mixtures. [25]

Zhao et al. (2009) had investigated the apparent molar volumes from density values of inositol in both H₂O and MCl₂ (aq) solutions. The results showed that the V_ϕ increased along with higher salt concentrations and temperatures. [26]

Dhondge et al. (2009) had investigated the sound speed, densities, refractive indices, as well as optical properties of aqueous ethylene glycol ether solutions at 298.15 K. Their study provided valuable insights into hydrogen bonding and the interactions between solute and solvent. [27]

Sadeghi et al. (2009) had investigated density and ultrasonic velocity for a ternary mixture consisting of water, polypropylene glycol, and phosphate salts (including sodium dihydrogen phosphate, disodium hydrogen phosphate, and trisodium hydrogen phosphate) across different temperatures, maintaining constant pressure. They used experimental data to derive thermodynamic parameters like isentropic compressibility, apparent specific volume, and deviations in compressibility and volume. [28]

Patil (2010) had conducted a study to measure viscosity, ultrasonic velocity, and density in binary mixtures of 1-hexanol and 1-heptanol with nitrobenzene over varying temperatures and at atmospheric pressure across all mole fractions. By using the R-K equation, various different parameters were calculated from the experimental data. [29]

Raman et al. (2010) had studied the velocity, viscosity, and data for the density of D-arabinose (aq). From this, they calculated many thermodynamic parameters like shear relaxation time, classical sound absorption, intermolecular free length, hydration number, and isentropic compressibility. [30]

Zorebski et al. (2010) had investigated the sound velocities and densities of different compounds with water. This measurement was conducted at 298.15 K. Using pulse-echo-overlap techniques and a vibrating tube densitometer, they obtained data that enabled the calculation of excess. [31]

Pan et al. (2010) had conducted a study on the electrical conductivity, viscosity, and density of a ternary mixture made up of water, nicotinic acid, and polyethanol. Further, measurements were used to determine dissociation levels, partial molar volumes, and viscosity coefficients, providing insights into the interactions within the system. [32]

Zhu et al. (2010) had studied the viscosities and densities of solutions of aqueous sugar alcohols. They found a direct proportionality between the density data and temperature or concentration and used a linear equation to correlate the experimental densities with minimal deviation. [33]

Sinha et al. (2011) had investigated the viscosity and density of L-alanine in silver sulphate (aq) blends at varying temperatures. Their findings suggested strong interactions among solute-solvent molecules. [34]

Li et al. (2011) had investigated viscosities and densities of EGMME with water. The findings indicated that the interactions between EGMME and water were relatively weak as compared to those observed with DEGMME or TEGMME when mixed with water. [35]

Pal et al. (2011) had performed experiments to measure the ultrasonic velocity and density of liquid ternary mixes, which included water, 2-aminopropanoic acid, and either fructose, D-cellobiose, or D-melezitose, over various temperatures. The data allowed for the calculation of thermodynamic parameters, including apparent, partial, and partial molar transfer properties, shedding light on the different nature of interactions within these mixtures. [36]

Sadeghi et al. (2011) had investigated density data and sound speeds of binary mixes comprising polyvinylpyrrolidone with solvents at atmospheric pressure. From this data,

they derived several thermodynamic properties, including apparent specific volume, K_S , etc. [37]

Yang et al. (2011) had investigated the electrical conductivity and density data of a ternary mixture composed of H_2O , dextran, and nicotinic acid at various temperatures. Their analysis involved calculating linear coefficients, partial molar volumes, linear molar conductance, dielectric coefficients, and viscosity coefficients (A and B) based on the collected data. [38]

Awasthi and Awasthi (2012) had examined the sound speed data and density of formamide with 2-ME and 2-EE at different concentrations and three distinct temperatures. They assessed various parameters to understand the behavior of the system under varying temperature conditions. [39]

Dhondge et al. (2012) had analyzed the density and viscosity of various drug solutions in water across different temperatures. Their study focused on different properties such as apparent and partial molar properties, and expansivity, that provide insights into the molecular interactions present in these solutions. [40]

Jiang et al. (2013) have studied the viscosities and densities of binary mixtures as well as ternary and solutions containing erythritol, xylitol, or D-mannitol with L-ascorbic acid and water. Their work targeted the evaluation of apparent as well as partial molar volumes, besides transfer properties toward understanding properties of these mixtures. [41]

Pal et al. (2013) have calculated densities and sound velocities in the mixtures of ionic liquid [bmim][Br] with alkoxyalkanols and water at various thermal conditions. The present study proved informative concerning the bonding as well as non-bonding interactions between the under-study molecules. [42]

Pandhurnekar et al. (2013) studied the density, refractive index, and sound speed of several glycol ethers with H_2O . They obtained various volumetric, acoustic, and optical properties that enhance the knowledge of the system. [43]

Shah et al. (2014) has conducted studies on the densities, viscosity, and ultrasonic velocity in dextrose, fructose, and inositol (aq) at a temperature of 398.15 K. Their findings included thermodynamic parameters that provide insights into molecular interactions. [44]

Dixit et al. (2014) had performed their study on the ultrasonic velocity, density, and viscosity of butanol (C_4H_9OH), H_2O , and acetic acid (CH_3COOH) at a constant temperature of 289 K. Using ultrasonic techniques, they determined various acoustical parameters and also the constants such as Rao's and Wada's in order to observe molecular interactions in the mixture. [45]

Kumari et al. (2014) had investigated viscosity, density, and ultrasonic velocity of a tyrosine derivative in a non-aqueous solution of DMSO across various concentrations, maintaining a temperature of 290 K. They used the gathered data to calculate acoustic and thermodynamic parameters, helping them analyze solute-solvent interactions. [46]

Banipal et al. (2015) had studied the density and viscosity of ternary mixtures containing ammonium bromide (NH_4Br), polyhydroxy compounds, and water across different temperatures and atmospheric pressures. They calculated partial properties at infinite dilution, Jones-Dole B-coefficients, and transfer properties to explore the kosmotropic and chaotropic behaviors of the solutes and co-solutes. [47]

Jengathe et al. (2015) had investigated ultrasonic velocity and density for DPH in H_2O , NaCl and myo-inositol (aq) mixtures. They computed various parameters, including partial molar properties, transfer properties, molar expansion, and Hepler's constant, to better understand the interactions between solutes and solvents. [48]

Singh et al. (2015) had studied the behavior of ascorbic acid in protic ionic fluid mixes. It dealt with the molecular interaction involving the ternary solutions using partial molar and transfer properties along with interaction coefficients. [49]

Romero et al. (2016) had examined the density and viscosity of EG, glycerol, and sugar alcohols. Their results providing an insight into the solute-solvent interactions. [50]

Reddy et al. (2016) had investigated ultrasonic velocity density of pure [Emim][EtSO₄], 2-PE, and in aqueous solution. The results indicated strong interactions between the components, as suggested by the calculated excess and deviation properties. [51]

Reddy et al. (2016) had investigated the ultrasonic velocity as well as the density, of pure [Emim][EtSO₄], 2-EE, and their binary mixtures. The analysis of various parameters, such as the internal pressure, free volume, and excess properties, reveals that stronger intermolecular interactions take place among the components. [52]

Naseem et al. (2016) had obtained two physical quantities of polyols in DMSO and in H₂O. Data obtained from their experiments were used to analyse a range of acoustic and thermodynamic properties. [53]

Reddy et al. (2016) had studied the density, refractive index, and sound velocity of various pure compounds such as [Emim][EtSO₄], 2-ME, and their binary mixtures. Their acoustic and thermodynamic parameters analysis showed significant interactions between the different components. [54]

Kumar et al. (2016) had studied diverse properties of D-(+)-glucose and D-(-)-fructose along with mixtures with aqueous trisodium citrate. The results that were obtained had indicated the stereoscopic property of the solute(s) as well as an insight into the mixture interactions. [55]

Kumar et al. (2016) had studied the thermodynamic behavior of SDS in alkoxyalkanols (aq) mixes at different temperatures, which emphasizes ion-2 and ion-solvent associations among the molecules. [56]

Krishna et al. (2017) had analyzed the density, refractive index, and speed of sound for the mixed solvents of [Bmim][PF₆] with 2-ME and 2-EE. The FTIR spectra of these mixed solvents at 298.15 K indicated very intense ion-dipole and hydrogen bonding between the [Bmim][PF₆] and alcohol molecules. [57]

Zhang et al. (2017) had analyzed data in myo-inositol (aq) mixes at four different temperatures. Their results, based on volumetric and viscometric analyses, gave an idea about the interaction between solute molecules and solvent molecules. [58]

Ghanta et al. (2017) had investigated binary mixtures of [Bmim][NTf₂] with 2-ME. The deviation among considered and excess value, gives insight into the molecular interactions occurring between [Bmim][NTf₂] and 2-ME. [59]

Jengathe et al. (2017) had studied densities and ultrasonic velocity of NaSl in aqueous sodium chloride solution and myo-inositol solution of concentration 0.06 mol·kg⁻¹ at three different temperatures. Their findings exhibited mixed interactions between NaSl that involved –COO– and phenolic OH groups and NaCl ions with the –OH group of myo-inositol. [60]

Srinivasu et al. (2017) had analyzed binary mixes of 1,4-butanediol with 2-ME and 2-PE at varying temperatures to calculate excess properties. The study found that these parameters increased with the alkyl chain length of the alkoxyethanols. [61]

Kaur et al. (2017) had investigated the densities and sound velocities of glycols in sorbitol (aq) mixtures. Their findings provided understandings into the associations among molecules in the solutions. [62]

Sharma and Thakur (2017) had studied the physiochemical properties of nicotinic acid in D-lactose (aq) mixes. Utilizing Masson's equation for data interpretation, they concluded that nicotinic acid functions as a structure maker in these particular mixtures. [63]

Bergua et al. (2018) had studied the density and ultrasonic velocity solutions that included two solvents, reline and glyceline. Their results, which were analyzed based on temperature and composition, showed that ionic-hydrophilic and hydrophilic-hydrophilic interactions dominated these systems. [64]

Prasad et al. (2018) had investigated the molecular interactions of [Bmim][NTf₂] with 2-PE and determined several properties at different thermal conditions. [65]

Kaur et al. (2018) had analyzed density data and sound velocity data for PEGs in sorbitol (aq) mixtures. An analysis revealed significant ionic-hydrophilic and hydrophilic-hydrophilic interactions. [66]

Omar et al. (2018) had investigated the densities and other apparent molar properties and α_p of binary mixes containing piperazine with H₂O, methanol, and acetone at different thermal conditions. [67]

Bernal et al. (2019) had investigated the density data and ultrasonic velocity of sugar alcohols (aq) solutions at different temperatures, after that utilizing this data to derive various volumetric parameters. [68]

Shakila et al. (2019) had examined the densities data and ultrasonic speeds of tetrahydrofuran (THF) with 4-methoxybenzyl alcohol and phenylmethanol (C₆H₅CH₂OH), at several temperatures. From the data, they calculated a few excess properties. [69]

Ankita and Nain (2019) had examined the ultrasonic velocity, densities, and viscosities of drug solutes dissolved in aqueous D-sucrose or D-glucose solutions, measuring these properties at T = (293.15-318.15) K. They derived various parameters, such as V_ϕ and compressibility's, by employing viscosity data to calculate Falkenhagen coefficients. [70]

Thakur et al. (2019) had investigated properties for EG, HG, and PG in methanol solutions containing methylparaben. They measured ultrasonic velocity and density at different temperatures, allowing to compute apparent molar volumes and isentropic compressibility. [71]

Yan et al. (2019) had analyzed the physicochemical properties of benzalkonium chloride in relation to biomolecules by measuring densities, conductivities, fluorescence, and UV absorption in mixed solutions. They subsequently calculated partial molar volumes and critical micellar concentrations. [72]

Rani et al. (2019) had focused on measuring properties in thiamine (aq) mixtures. They analyzed viscometric, acoustic, and volumetric properties to determine properties, as well as specific coefficients derived from the viscosity data. [73]

Abella and Romero (2019) had investigated the interactions of α -chymotrypsinogen in water and aqueous EG, glycerol, and sugar alcohols. Measurements taken at 298.15 K played a crucial role in establishing preferential interaction parameters. [74]

Makhlouf et al. (2019) had studied the physicochemical properties of mixtures containing 2-PE combined with propanol and butanol. Their focus was on the intermolecular interactions and structural characteristics present within these binary mixtures. [75]

Kumar and Sharma (2020) had investigated the molecule's interactions in aqueous ternary mixtures containing the ionic liquid and amino acids. They utilized volumetric, acoustic, and spectroscopic property data to elucidate the effects of the amino acids. [76]

Shi et al. (2020) had investigated the densities, viscosities, and various properties of maltitol in aqueous glycylglycine mixtures to understand different molecular interactions occurring within these mixtures. [77]

Ankita and Nain (2020) had investigated densities, sound speed, and viscosities of sodium salicylate in water as well as in D-glucose or D-sucrose aqueous solutions at varying temperatures. Their findings indicated notable different types of interactions in these solutions. [78]

Nain (2020) had studied the ultrasonic velocity and density for aqueous L-arginine, L-histidine, and gentamicin sulfate, to identifying significant interactions between solute-solute and solute-solvent. [79]

Chand and Nain (2020) had explored the properties such as density, viscosity and ultrasonic speed, for semi carbazide hydrochloride in H₂O as well as in D-xylose/L-arabinose aqueous blends. This research provides a comprehensive understanding of hydrophilic-hydrophilic interactions, as well as the structure-modifying effects of the drug. [80]

Kaur et al. (2020) had focused on the density, ultrasonic speed, and related parameters of glycols in glutaraldehyde (aq) mixes at various T, and explaining the solute-solvent interactions present in these mixtures. [81]

Chakraborty et al. (2021) had examined the ultrasonic velocity and densities data of polyethylene glycols in aqueous niacin solutions. Their study provided significant understandings into the molecular associations occurring in this ternary system. [82]

Rajput et al. (2021) the ultrasonic velocity, density, and viscosity of nucleic acid bases, and adenine (aq) mixes and inositol (aq). These measurements elucidate the intermolecular interaction between these mixtures. [83]

Asghar et al. (2021) had measured the viscosities, velocities, and densities of a binary mixture consisting of phenol and acetaldehyde at 303 K. Their findings enabled the calculation of various excess properties and standard deviation coefficients. [84]

Vankar and Rana (2021) had studied the velocity, viscosity, and density of binary mixtures of methanol and 3-bromoanisole over a range of temperatures while utilizing their results to obtain excess molar properties. [85]

Sharma et al. (2021) had studied the speed of sound, and density mixtures of n-hexane with 2-chlorotoluene, 4-chlorotoluene, and 1,3-dichlorobenzene as a function of T. Their investigation proved useful for the determination of several derived thermodynamic parameters, viz., intermolecular free length, available volume, excess isentropic compressibility, viscosity deviation, and excess molar volumes. [86]

Dhivya et al. (2021) had determined the refractive indices, velocity, viscosity, as well as density of a binary mixs of water and PEG 200 at 303 K. [87]

Dubey and Dhingra (2021) had explored similar properties for mixtures of 2-butoxyethanol with dipropylamine, dimethylamine, and trimethylamine at different temperatures. [88]

Diaz and Navaza (2021) had examined the surface tension, viscosity, velocity, and densities data for ternary mixes composed of water, ethanol, and hexamethylenetetramine across various temperatures. [89]

Amirchand et al. (2021) had studied the different interactions influencing the hydration behavior of saccharides such as D-glucose, sucrose, and D-lactose monohydrate in calcium salt (aq) solutions at atmospheric pressure. [90]

Kaur et al. (2022) had focused on the thermodynamic and acoustic properties derived from density and sound velocity data for a ternary system involving hexylene or propylene in aqueous glutaraldehyde solutions. Their results indicated strong solute-solvent interactions, suggesting a structured arrangement of water molecules in bulk while showing reduced compressibility for charged groups within the system. [91]

Chakraborty et al. (2022) had explored the density and ultrasonic speeds of PEGs in solutions of Vitamin B₅ (aq) across various T. This study provided insight into molecular interactions within these ternary solutions. [92]

Bandral et al. (2022) had investigated the properties of two amino acids, L-threonine and L-histidine, in both (aq) and binary aqueous hydrochloride media. They measured density, ultrasonic velocity, and viscosity, subsequently apparent and partial molar properties and transfer parameters, and hydration numbers. [93]

Bandral et al. (2022) had investigated ultrasonic velocity, density, and viscosity of glycine and glycyglycine in betaine aqueous hydrochloride liquid mixtures. They derived several volumetric, compressibility, and rheological parameters from their findings. [94]

Shahazidy et al. (2022) had investigated sound speeds and densities of meso-erythritol (aq) and water-DMSO mixtures. The calculated values from such data explained the different properties behind the solvation behavior of compounds. [95]

Bhakri et al. (2023) had studied the sound speeds and densities data of glycols in gluconolactone (aq) mixtures at different thermal conditions. The study gave important information about hydrophobic hydration in these mixtures. [96]

Pathania et al. (2023) had studied several properties of RNH₃ClO₄ in acetonitrile and dimethyl sulfoxide over a range of temperatures. The study has measured sound velocity, density, and conductivity to determine the effects of the solute. [97]

Khajuria et al. (2023) had analyzed the properties of L-ascorbic acid in L-histidine (aq) mixes, focusing on densities and sound speeds across temperature range of 298.15 to 313.15 K. The results provided data on thermodynamic parameters, including apparent molar volumes and isentropic compressibility. [98]

Gaba et al. (2023) had studied ternary mixtures containing sugar alcohol and choline chloride with the study of the density and ultrasonic velocity. This paper calculated numerous apparent molar properties that explored the interaction in mixtures of erythritol and water, both in their binary and ternary versions, at different temperatures. [99]

Lamba et al. (2024) had focused on the density and ultrasonic speed of aqueous disodium EDTA in mixtures with PEG's 400/4000 across multiple temperatures, providing insights into molecular interactions in ternary solutions. [100]

Monira et al. (2024) had studied properties of caesium niobite (CsNbO_3) using a first-principles method, examining the effects of temperature as well as pressure on these properties. [101]

Panda et al. (2024) had investigated the behavior of electrolytes in aqueous dimethyl sulphoxide solutions. The study measured density, ultrasonic velocity, and viscosity, utilizing this data to calculate adiabatic compressibility and other properties, shedding light on solute-solvent interactions. [102]

Godhani et al. (2024) measured ultrasonic velocities, densities, and viscosities in binary mixtures containing pyrimidine-substituted azetidinone. The research focused on understanding acoustical and thermodynamic properties, providing insights into the interactions within these mixtures. [103]

So, vast studies have been done on physicochemical, acoustic, and thermodynamic properties (density, viscosity, ultrasonic velocity, refractive index, conductivity, etc.) of binary, ternary, and aqueous mixtures, involving alcohols, glycols, polyols, amino acids, ionic liquids, and sugars, often under temperature variations. But there is no study has been done sugar alcohols with glycol ether. So present study has been done to enhance the applications of these compounds. This investigation also aims to bridge the existing research gap and provide valuable insights into molecular interactions and solvation behaviour within these mixtures.

References

1. V.K. Reddy, K.S. Reddy and A. Krishnaiah, J. Chem. Eng. Data 39, 615-617 (1994).
2. T.M. Aminabhavi and B. Gopalakrishna, J. Chem. Eng. Data 40, 856-861 (1995).
3. M.I. Aralaguppi, C.V. Jadar, and T.M. Aminabhavi, J. Chem. Eng. Data 41, 1307-1310 (1996).
4. S. Magazu, P. Migliardo, A.M. Musolino, and M.T. Sciortino, J. Phys. Chem. B, 101, 2348-2351 (1997).
5. A. Eliassi and H. Modarress, J. Chem. Eng. Data 43, 719-721 (1998).
6. K. Tamura, S. Tabata, and S. Murakami, J. Chem. Eng. Thermodyn. 30, 1319-1332 (1998).
7. A. Ali, S. Hyder and A.K. Nain, J. Mol. Liq. 79, 89-99 (1999).
8. M.T. Zafarani-Moattar and A. Mehrdad, J. Chem. Eng. Data 45, 386-390 (2000).
9. K. Tamura, A. Osaki, S. Murakami, B. Laurent and J.P.E. Grolier, Fluid Phase Equilib. 173, 285-296 (2000).
10. S. Baluja and S. Oza, Fluid Phase Equilib. 178, 233-238 (2001).
11. F. Ebner, A. Heller, F. Rippke, and I. Tausch, Ameri. J. Clinical Dermatology 3, 427-433 (2002).
12. T.A. Graber, H. Galleguillos, J.A. Asenjo and B.A. Andrews, J. Chem. Eng. Data 47, 174-178 (2002).
13. E.C. Sorenson, J.L. Price, B.R. McRae and E.M. Woolley, J. Chem. Eng. Thermodyn. 35, 529-553 (2003).
14. J. George and N.V.J. Sastry, J. Chem. Eng. Data 48, 977-989 (2003).
15. N.V. Sastry and M.C. Patel J. Chem. Eng. Data. 48, 1019-1027 (2003).
16. C.E.H. Schmelzer, W. Zwirbla, E. Rosenfeld and B.B.J. Linde, J. Mol. Struct. 699, 47-51 (2004).
17. V.K. Syal, A. Chauhan and S. Chauhan, J. Pure Appl. Ultrason. 27, 61-69 (2005).
18. W. Zwirbla, A. Sikorska and B.B.J. Linde, J. Mol. Struc. 743, 49-52 (2005).
19. M.B. Blodgett, S.P. Ziemer, B.R. Brown, T.L. Niederhauser and E.M. Woolley, J. Chem. Eng. Thermodyn. 39, 627-644 (2007).
20. M.N. Roy, B.K. Sarkar and R. Chanda, J. Chem. Eng. Data. 52, 1630-1637 (2007).
21. E. Ayraanci and M. Sahin, J. Chem. Thermodyn. 40, 1200-1207 (2008).

22. R. Palani and A. Geetha, *Phys. Chem. Liq.* 47, 542–552 (2008).
23. Z. JianBin, Z. PengYan, M. Kai, H. Fang, C. GuoHua and W. XiongHui, *Sci. China, Ser. B: Chem.* 51, 420-426 (2008).
24. C.M. Romero, M.S. Paez and D. Perez, *J. Chem. Thermodyn.* 40, 1645-1653 (2008).
25. C.M. Kinart, M. Maj, A. Ćwiklińska and W.J. Kinart, *J. Mol. Liq.* 139, 1-7 (2008).
26. Q. Zhao, Z.J. Sun, Q. Zhang, S.K. Xing, M. Liu, D.Z. Sun and L.W. Li, *Thermochimi. Acta* 487, 1-7 (2009).
27. S.S. Dhondge, C.P. Pandhurnekar and D.V. Parwate, *J. Chem. Thermodyn.* 41, 577-585 (2009).
28. R. Sadeghi and B. Jamehbozorg, *Fluid Phase Equilib.* 284, 86-98 (2009).
29. S.R. Patil, *Rasayan J. Chem.* 1, 66-73 (2010).
30. M.S. Raman, V. Ponnoswamy, P. Kolandaivel and K. Perumal, *J. Mol. Liq.* 151, 97-106 (2010).
31. E. Zorebski, M.G. Rybczynska, and B. Maciej, *J. Chem. Eng. Data* 55, 1025-1029 (2010).
32. H.P. Pan, T.C. Bai and X.D. Wang, *J. Chem. Eng. Data* 15, 2257-2262 (2010).
33. C. Zhu, Y. Ma and C. Zhou, *J. Chem. Eng. Data* 55, 3882-3885 (2010).
34. B. Sinha, A. Sarkar, and P.K. Roy, D. Brahman, *Inter. J. Thermophys.* 32, 2062-2078 (2011).
35. X.X. Li, M. Zhang, X.X. Wu, Y.W. Wang, G.C. Fan and X.X. Ma, *J. Mol. Liq.* 158, 92-96 (2011).
36. A. Pal and N. Chauhan, *J. Chem. Eng. Data* 56, 1687-1694 (2011).
37. R. Sadeghi and S. Azizpour, *J. Chem. Eng. Data* 56, 240-250 (2011).
38. Y. Yang, T.C. Bai and Y.L. Li, *J. Chem. Eng. Data* 56, 412-420 (2011).
39. A. Awasthi and A. Awasthi, *J. Chem. Thermodyn.* 53, 144-151 (2012).
40. S.S. Dhondge, S.P. Zodape and D.V. Parwate, *J. Chem. Thermodyn.* 48, 207-212 (2012).
41. X. Jiang, C. Zhu and Y. Ma, *J. Chem. Eng. Data* 58, 2970-2978 (2013).
42. A. Pal, H. Kumar, B. Kumar, P. Sharma, and K. Kaur *J. Chem. Thermodyn.* 57, 182-188 (2013).

43. C.P. Pandhurnekar, D.V. Parwate and S.S. Dhondge, *J. Mol. Liq.* 183, 94-101 (2013).
44. S.A. Shah, S.M. Gadegone and R.B. Lanjewar, *Int. J. Res. Biosci. Agricult. Tech.* 1, (2014).
45. A. Dixit, K.C. Juglan and A. Sharma, *J. Chem. Pharm. Res.* 6, 93-104 (2014).
46. S. Kumari, K.C. Juglan and A. Sharma, *J. Chem. Pharm. Res.* 6, 782-794 (2014).
47. P.K. Banipal, S. Arti, and T.S. Banipal, *J. Chem. Eng. Data* 60, 1023-1047 (2015).
48. S.P. Jengathe, S.S. Dhondge, L.J. Paliwal, V.M. Tangde and S. Mondal, *J. Chem. Thermodyn.* 87, 78-87 (2015).
49. V. Singh, G. Sharma and R.L. Gardas, *PLoS One*, 10, e0126091, (2015).
50. C.M. Romero, M.S. Pérez and M.J. Puchana, *J. Mol. Liq.* 223, 1192-1196 (2016).
51. M.S. Reddy, K.T.S. Raju, A.S. Rao, N. Sharmila and B.H. Babu, *J. Chem. Thermodyn.* 101, 139-149 (2016).
52. S. Reddy, M.N. Sk and K.T.S.S. Raju, *J. Mol. Liq.* 218, 83-94 (2016).
53. B. Naseem, M. Khan and M.A. Jamal, *J. Mol. Liq.* 220, 581-591 (2016).
54. M.S. Reddy, K.T.S. Raju, S. M. Nayeem, I. Khan, K.B.M. Krishana and B.H. Babu, *J. Sol. Chem.* 45, 675-701 (2016).
55. H. Kumar, Sheetal and S.K. Sharma, *J. Sol. Chem.* 45, 1-27 (2016).
56. H. Kumar, K. Kaur, S. Arti, and M. Singla, *J. Mol. Liq.* 221, 526-534 (2016).
57. T.S. Krishna, K. Narendra, M. Gowrisankar, A.K. Nain and B. Munibhadrayya, *J. Mol. Liq.* 227, 333-350 (2017).
58. J. Zhang, T. Fu, C. Zhu and Y. Ma, *J. Mol. Liq.* 242, 190-203 (2017).
59. P. Ghanta, M.R. Kalimi, P. Reniguntla, M.M. Tadavarthi and V.K. Tadekoru, *J. Chem. Eng. Data* 62, 3903-3914 (2017).
60. S.P. Jengathe, S.S. Dhondge, L.J. Paliwal and V.M. Tangde, *J. Chem. Thermodyn.* 115, 221-232 (2017).
61. J.V. Srinivasu, K. Narendra, C. Kavitha and B. Subba Rao, *J. Sol. Chem.* 46, 2066-2090 (2017).
62. K. Kaur, K.C. Juglan and H. Kumar, *J. Chem. Eng. Data* 62, 3769-3782 (2017).
63. R. Sharma and R.C. Thakur, *AIP Conference Proce.* 1860, (2017).
64. F. Bergua, M. Nuez, J. Muñoz-Embid, C. Lafuente and M. Artal, *J. Mol. Liq.* 258, 106-113 (2018).

65. G. Prasad, K.M. Reddy, R. Padamasuvarna, T.M. Mohan, T.V. Krishna and S.G. Rao, *J. Sol. Chem.* 47, 1980-2006 (2018).
66. K. Kaur, K.C. Juglan and H. Kumar, *J. Mol. Liq.* 268, 700-706 (2018).
67. Q.M. Omar, J.N. Jaubert and J.A. Awan, *Int. J Chem. Eng.* 2018, 8689534 (2018).
68. P. Bernal, S. Brown, M. Mera and Y. Bouchibti, *Food Chem.* 280, 164-174 (2019).
69. A. Shakila, R. Raju, T. Srinivasa Krishna, R. Dey and V. Pandiyan, *Phy. Chem. Liq.* 58, 263-279 (2019).
70. A.K. Nain, *J. Chem. Thermodyn.* 133, 123-134 (2019).
71. A. Thakur, K.C. Juglan, H. Kumar and K. Kaur, *J. Mol. Liq.* 288 (2019) 111014.
72. Z. Yan, L. Liu, X. Chen and Y. Niu, *J. Mol. Liq.* 274, 115-124 (2019).
73. R. Rani, A. Kumar, T. Sharma, T. Sharma and R.K. Banezai, *J. Chem. Thermodyn.* 135, 260-277 (2019).
74. J.S. Abella and C.M. Romero, *J. Sol. Chem.* 48, 1591-1602 (2019).
75. H. Makhoulouf, N. Muñoz-Rujas, F. Aguilar, B. Belhachemi, E.A. Montero and I. Bahadur, L. Negadi, *J. Chem. Thermodyn.* 128, 394-405 (2019).
76. H. Kumar and R. Sharma, *J. Mol. Liq.* 304, 112666 (2020).
77. Y. Shi, C. Zhu, T. Fu, X. Gao and Y. Ma, *J. Chem. Eng. Data* 66, 360-367 (2020).
78. A.K. Nain, *J. Mol. Liq.* 298, 112006 (2020).
79. A.K. Nain, *J. Mol. Liq.* 315, 113736 (2020).
80. D. Chand and A.K. Nain, *J. Chem. Thermodyn.* 146, 106106 (2020).
81. P. Kaur, N. Chakraborty, K.C. Juglan and H. Kumar, *J. Mol. Liq.* 315, 113763 (2020).
82. N. Chakraborty, K.C. Juglan and H. Kumar, *J. Chem. Thermodyn.* 154, 106326 (2021).
83. P. Rajput, T. Sharma and A. Kumar, *J. Mol. Liq.* 326, 115210 (2021).
84. J. Asghar, G. Sridhar and C. Sivakumar, *J. Adv. Sci. Res.* 12, 190-194 (2021).
85. H.P. Vankar and V.A. Rana, *Materials Today: Proceed.* (2021).
86. A. Sharma, M. Rani and S. Maken, *J. Mol. Liq.* 321 (2021) 114366.
87. P. Dhivya, R. Padmanaban and A. Gayathri, *Adv. Materi. Manufactu. Eng.* 7 (2021).
88. G.P. Dubey and L. Dhingra, *J. Chem. Thermodyn.* 157, 106388 (2021).
89. D.G. Diaz and J. M. Navaza, *J. Chem. Eng. Data* 66, 2160-2166 (2021).

90. K.D. Amirchand, S. Kaur, T.S. Banipal and V. Singh, J. Mol. Liq. 334, 116077 (2021).
91. P. Kaur, N. Chakraborty, H. Kumar, M. Singla and K.C. Juglan, J. Sol. Chem. 51, 1268-1291 (2022).
92. N. Chakraborty, K.C. Juglan, H. Kumar and M. Singla, J. Chem. Eng. Data 67, 2292-2306 (2022).
93. A. Bandral, H. Singh, Q. Majid and A. Kumar, J. Mol. Liq. (2022) 119350.
94. A. Bandral and A. Kumar, J. Mol. Liq. 348 (2022) 118081.
95. U. Shahazidy, M.A. Jamal, M. Muneer, B. Naseem and A.K. Qureshi, J. Mol. Liq. 350, 118543 (2022).
96. K. Bhakri, N. Chakraborty, K. C. Juglan, H. Kumar, and R. Sharma, J. Therm. Anal. Calorim. 148, 7185-7205 (2023).
97. V. Pathania, S. Sharma, B.K. Vermani, H. Kaur and R.C. Thakur, J. Mol. Liq. 371 (2023) 121067.
98. K.D. Amirchand, T.S. Banipal, Y.L. Yang and V. Singh, J. Mol. Liq. 370 (2023) 120839.
99. R. Gaba, N. Kaur, A. Pal and D. Sharma, J. Mol. Liq. 380, 121766 (2023).
100. M. Lamba, K. Bhakri, N. Chakraborty and K.C. Juglan, Physica Scripta 99, 105027 (2024).
101. M. Monira, M.N.H. Liton, M.Al Helal, M. Kamruzzaman, A.K.M.F.U. Islam and S. Kojima, Open Ceramics, 17, 100546 (2024).
102. R. Panda, S. Panda and S.K. Biswal, J. Therm. Anal. Calorim. 1-15 (2024).
103. D.R. Godhani, U.P. Mehta, A.H. Saiyad, K.P. Parmar and J.P. Mehta, J. Sol. Chem. 1-23 (2024).

CHAPTER 3

OBJECTIVES AND EXPERIMENTAL PROCEDURES

3.1. Research Objectives

To identify various chemicals that are utilized in different products and in different industries, hold beneficial properties. So, with the goal of enhancing these properties for desirable outcomes, the main focus of this research will be to explore the characteristics of different liquid combinations and their potential applications across different industries, such as pharmaceuticals, leather, chemicals, and cosmetics. The following steps will be undertaken in the research process:

1. To calculate density and speed of sound for the glycol ethers in aqueous solutions of inositol, erythritol and maltitol (sugar alcohols) at different temperatures and concentrations.
2. To calculate the various acoustic and thermodynamic parameters from experimental data.
3. To examine and to understand various types of intermolecular interactions occurring in liquid mixtures.

3.2. Research Methodology

3.2.1 Preparation of samples

In this investigation, sugar alcohols named as inositol, maltitol, and erythritol were used to make an aqueous solution and have molecular weights of 180.16, 344.31, and 122.12 g.mol⁻¹, respectively. After that, to make a ternary mixtures glycol ether were used. To prepare solvent mixture, a 100 ml volumetric flask and triple-distilled water have been used. The water has specific conductance of not more than 10⁶ S.cm⁻¹. Triple distilled was used, and after vacuum drying, the chemicals were held in desiccators with P₂O₅. For accurate measurements of chemicals as per concentrations and molalities, to



Figure 3.1: Sartorius CPA-225 D electronic weighing balance

prepare samples, the Sartorius weighing balance (modal: CPA 225D) has been used that is shown in **Figure 3.1**. The precision of the weighing balance was ± 0.00001 g. After that, the prepared sample has been stored in glass vials. These vials are provided with PFE septa lids and are closed by parafilm in order to avoid the atmospheric moisture absorption and to prevent any type of ageing effect samples were prepared just before measurements. These vials are provided with PFE septa lids and are closed by parafilm in order to avoid the atmospheric moisture absorption. **Figure 3.2**. showing sample preparations method. The significance of preparing such controlled and accurate mixtures lies in generating reliable data that reflects the true thermophysical behavior of these complex liquid systems, which can ultimately guide industrial formulation strategies and material development.

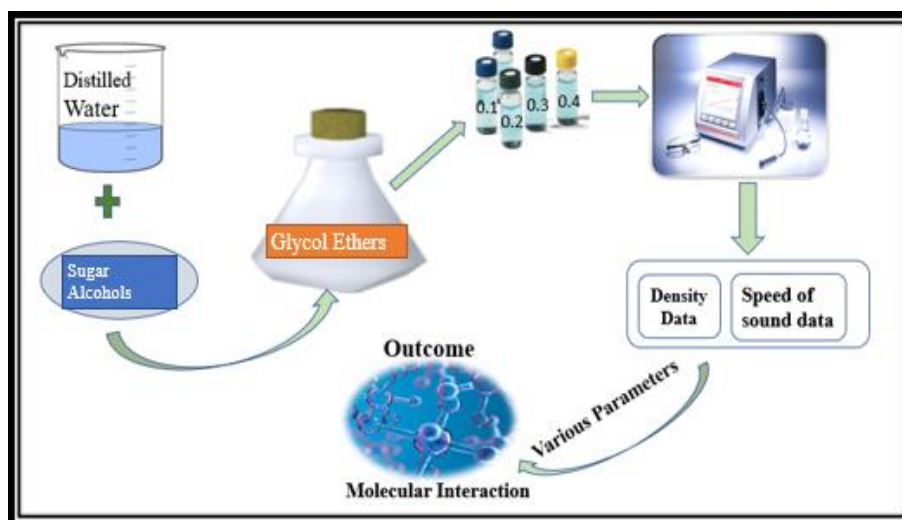


Figure 3.2. Preparation of samples

3.2.2 Measurements of experimental densities and sound speeds

In a water-based solution of sugar alcohols (inositol, maltitol and erythritol), two independent physical properties i.e., densities and ultrasonic velocity for six different glycol ethers, have been measured experimentally with the help of a density sound analyser, shown in **Figure 3.3**. Measurements of density values and sound speed values have been done in a temperature range from 288.15K to 318.15K. This range covers typical ambient and operational conditions encountered in many real-world industrial and laboratory settings. It allows for the investigation of temperature-dependent behaviors such as solubility, viscosity, and molecular interactions. Moreover, this range also closely aligns with naturally occurring environmental temperatures, ensuring the

relevance and practical applicability of the findings. In DSA, 5000 M samples were inserted by means of a syringe. The instrument works based on the vibrating U-tube principle as well as the propagation method for the estimation of these values.



Figure 3.3 Density and sound velocity analyser

3.2.3. Theory of measurement of density and speed of sound

The measurement of ρ for the samples is dependent on the frequency. The sample holder, which is in U-shape, can vibrate, and its fundamental frequency is affected by the mass of the sample, and by this means the sample's density can be obtained. The vibrational direction is at right angles to the plane of the U-tube (**Figure 3.4**). The measurement of density (ρ) using the Anton Paar DSA 5000 M depends on the vibration frequency of a U-shaped borosilicate glass tube, which is influenced by the mass of the sample. The U-tube vibrates perpendicular to its plane, and the sample's density is determined by analyzing its oscillation. A piezoelectric crystal converts electrical signals into ultrasonic waves that pass through the sample. As the waves travel, they interact with the sample's internal structures, and their speed-affected by the sample's density, elasticity, and molecular structure is measured by a receiving transducer.

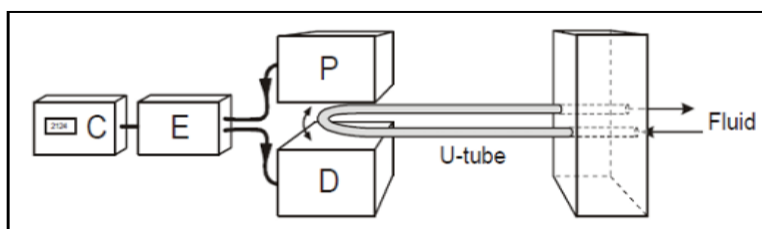


Figure 3.4. Schematic representation of Anton Paar DSA 5000 M

The DSA 5000 M includes two measuring cells: one for density and one for the speed of sound, allowing simultaneous measurement of both properties. It uses an oscillating U-tube technique, with temperature precisely controlled by a Peltier thermostat and monitored using integrated platinum thermometers. ThermoBalance™ technology

ensures long-term stability, requiring only one calibration at 20°C. The system supports both manual and automated sample filling and is suitable for various applications in pharmaceuticals, food, and chemical industries. Sound velocity is calculated based on the travel time of ultrasonic waves through the sample, corrected for temperature. The device offers high accuracy, detecting densities from 0 to 3 g/cm³ and sound velocities between 1000 and 2000 m/s. The system's molality measurements have a very low uncertainty of $\pm 2 \times 10^{-5}$ mol·kg⁻¹. Cells are cleaned with water and ethanol or acetone after each use, and the device is calibrated with distilled water before every measurement.

3.3. Fourier Transform Infrared Spectrometer

For FTIR measurements of the solution, the PerkinElmer Spectrum One FTIR spectrometer was used with a resolution of 0.5 cm⁻¹. This advanced system utilizes Fourier Transform Infrared (FT-IR) technology to analyze the molecular composition of samples by detecting electromagnetic fluctuations resulting from IR radiation interaction. The instrument is equipped with a diamond Attenuated Total Reflection (ATR) accessory, enabling direct analysis of both solids and liquids without extensive sample preparation. It offers a broad scan range of 8,300–350 cm⁻¹ and features high sensitivity (32,000:1) to ensure accurate results. The system is further supported by Spectrum 10 software and a real-time Atmospheric Vapour Compensation (AVC) function, which minimizes interference from water vapor and carbon dioxide. Additional features include an illuminated LCD screen, RS232C interface for efficient data management, and Procell software for smooth integration with external programs such as Excel. These capabilities make the system highly suitable for professional, GLP-compliant spectral analysis in diverse research environments.

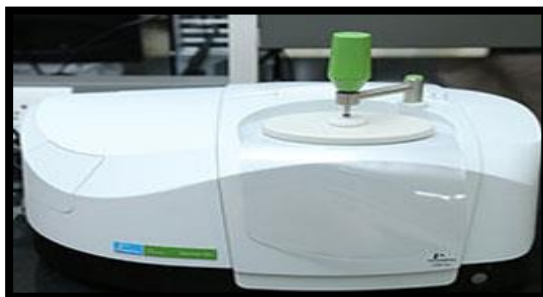
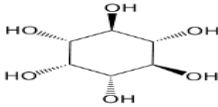
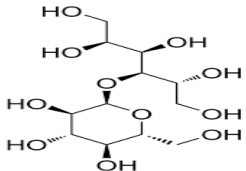
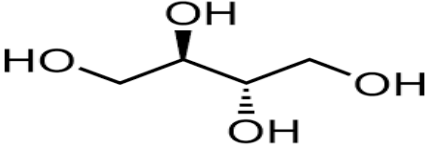
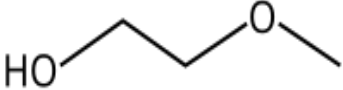
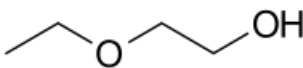
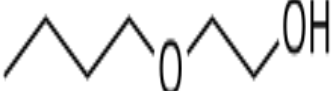
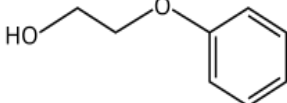

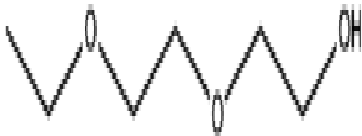


Figure 3.5. Fourier Transform Infrared Spectrometer

3.4. Chemical structures

The structures of the chemicals are provided in table below.

Table 3.1. List of chemical structures

Chemical Name	Chemical Structure
<i>myo</i> -Inositol	
Maltitol	
Erythritol	
EGMME	
EGMEE	
EGMBE	
EGMPE	
DEGMME	
DEGMEE	

3.5 Specifications of the Chemicals

Table. 3.2 Chemicals name along with their specifications

Sr. No.	Chemical	CAS No.	IUPAC name	Formula	Molar Mass g.mol⁻¹	Mass fraction Purity	Purification process
1.	Inositol	87-89-8	<i>myo</i> -Inositol	C ₆ H ₁₂ O ₆	180.16	≥0.99	Vacuum dried
2.	Maltitol	585-88-6	4-O- α -glucopyranosyl-D-sorbitol	C ₁₂ H ₂₄ O ₁₁	344.31	≥0.99	Vacuum dried
3.	Erythritol	149-32-6	Butane-1,2,3,4-tetrol	C ₄ H ₁₀ O ₄	122.12	≥0.99	Vacuum dried
4.	EGMME	109-86-4	2-Methoxyethan-1-ol	C ₃ H ₈ O ₂	76.09	≥0.99	Vacuum dried
5.	EGMEE	110-80-5	2-Ethoxyethanol	C ₄ H ₁₀ O ₂	92.12	≥0.99	Vacuum dried
6.	EGMBE	111-76-2	2-Butoxyethan-1-ol	C ₆ H ₁₄ O ₂	118.18	≥0.99	Vacuum dried
7.	EGMPE	122-99-6	2-Phenoxyethan-1-ol	C ₈ H ₁₀ O ₂	138.17	≥0.99	Vacuum dried
8.	DEGMME	111-77-3	2-(2-Methoxyethoxy) ethan-1-ol	C ₅ H ₁₂ O ₃	120.15	≥0.99	Vacuum dried
9.	DEGMEE	111-90-0	2-(2-Ethoxyethoxy) ethan-1-ol	C ₆ H ₁₄ O ₃	134.18	≥0.99	Vacuum dried

3.6. Calculation of Acoustics Parameters

In the present chapter the theoretical aspects of several acoustic and thermophysical properties are studied. The data of density and ultrasonic velocity is used to determine the following parameters.

3.6.1 Acoustic impedance

Acoustic impedance (Z) is a physical property that represents the resistance that a material provides to the transmission of sound. It is calculated as:

$$Z = \rho \times c \quad (3.1)$$

This value helps to determine how sound waves will behave when they encounter different mediums.

3.6.2 Adiabatic compressibility

It is a physical property that describes the compressibility of a substance under adiabatic conditions, where no heat is exchanged. It is mathematically expressed as:

$$\beta = 1/[\rho(c^2)] \quad (3.2)$$

where ρ = density of the material and c = speed of sound within the substance.

3.6.3 Wada's constant

is used to relate adiabatic compressibility to molecular characteristics of a material. It is defined by the formula:

$$W = (\beta)^{\frac{1}{7}} \left(\frac{M}{\rho} \right) \quad (3.3)$$

where M = molar mass of the material.

3.6.4 Rao's Constant

This parameter is used to assess the acoustic properties of liquids. It is calculated by using the formula given below

$$R = [(c^{\frac{1}{3}})M] / \rho \quad (3.4)$$

This constant provides insight into the relationship between the molecular structure of a liquid and its ability to transmit sound, helping in the understanding of molecular interactions.

3.6.5 Intermolecular free length

Intermolecular free length represents the average separation between molecules, influencing sound transmission in liquids. It is expressed as;

$$L_f = K_T (\beta)^{1/2} \quad (3.5)$$

where K is constant and β is the adiabatic compressibility. The greater free length implies the smaller intermolecular forces, together with a slower velocity of sound, so its measurement is of great importance for judging the fluid compressibility as well as the intermolecular distance.

3.6.6 Vander Waal's constant

Van der Waals' constant reflects the finite volume occupied by gas molecules, adjusting the ideal gas law to account for real gas behavior. It is determined using the equation;

$$b = \left(\frac{M}{\rho}\right) \left[1 - (RT/Mc^2) \sqrt{1 + (Mc^2/3RT)} - 1\right] \quad (3.6)$$

where R = gas constant, T = temperature, and M is the molar mass. This is critical in describing non-ideal gas behavior under different conditions.

3.7. Several Properties

3.7.1 Apparent molar volume

This is referring to the volume change that occurs when a small quantity of solute is added to a solvent and divided by the amount of solute added. It reflects the contribution of the solute to the overall solution volume and is important for studying solute-solvent interactions. It is obtained by utilising by equation given below:

$$V_\phi = (M/\rho) - \{(\rho - \rho_0)/(m_A \rho \rho_0)\} \quad (3.7)$$

In the above equation, M = molar mass of solutes (glycol ethers). ρ and ρ_0 = densities of solutions and solvent, respectively.

3.7.2 Partial molar volume

It mainly states the upsurge in the total volume of a solution due to the addition of a small amount of one component, other components being the same. It indicates how much that particular component contributes to the total volume of solution and informs about the behavior of mixtures. It is obtained by utilised the equation given below:

$$V_\phi = V_\phi^0 + S_V^* m_A \quad (3.8)$$

3.7.3 Partial molar volume of transfer

This parameter measures how the partial molar volume of a solute changes when it moves from one solvent to another. It is useful for investigating solvation dynamics and

how different solvents affect the solute's behavior. It is calculated by following equation;

$$\Delta V_{\phi}^0 = \Delta V_{\phi}^0 (\text{in aqueous sugar alcohol's solution}) - V_{\phi}^0 (\text{in water}) \quad (3.9)$$

3.7.4 Temperature-dependent partial molar volume

This describes how the partial molar volume of a solute varies with temperature change. It provides important information about how solutes and solvents interact thermally, particularly regarding expansion or contraction due to temperature shifts. It is calculated by the following equation:

$$V_{\phi}^0 = a + b(T - T_{ref}) + c(T - T_{ref})^2 \quad (3.10)$$

3.7.5 Apparent molar isentropic compression

This quantity refers to the contribution of a solute to the compressibility of a solution when entropy remains constant. It is useful for understanding how solutes influence the elasticity or compressibility of solutions under specific thermodynamic conditions. It is calculated by following equation:

$$K_{\phi,S} = (MK_S/\rho) - \{(K_{S,0}\rho - K_{S,\rho_0})/m_A\rho\rho_0\} \quad (3.11)$$

Additionally, to calculate K_S following equation is employed;

$$K_S = 1/c^2\rho \quad (3.12)$$

3.7.6 Partial molar isentropic compression

It represents how the isentropic compressibility of a solution changes with the addition of a small amount of solute. This value provides insights into solute-solvent interactions, particularly how they affect the mechanical properties of the solution under constant entropy. It is calculated by following equation:

$$K_{\phi,S} = K_{\phi,S}^0 + S_K^* m_A \quad (3.13)$$

3.7.7 Partial molar isentropic compression of transfer

This parameter information about how the isentropic compressibility of a solute shifts when moved from one solvent to another. It gives clues about how solute-solvent interactions differ between environments in terms of their compressibility effects. It is calculated by following equation:

$$\Delta K_{\phi}^0 = K_{\phi,S}^0 (\text{in aqueous sugar alcohol's solution}) - K_{\phi,S}^0 (\text{in water}) \quad (3.14)$$

3.7.8. Pair and triplet interaction coefficients

These coefficients assess the associations among pair or triplet of molecules in a solution. They help in examining the complexity of molecular interactions within non-ideal mixtures, offering a deeper understanding beyond simple binary collisions. It is calculated by following equation;

$$V_{\phi}^0 (H_2O - \text{sugar alcohol's}_{(aq)}) = 2V_{AB}m_B + 3V_{ABB}m_B^2 \quad (3.15)$$

$$\Delta K_{\phi,s}^0 (H_2O - \text{sugar alcohol's}_{(aq)}) = 2K_{AB}m_B + 3K_{ABB}m_B^2 \quad (3.16)$$

In above equations, *A* stands for glycol ethers, and *B* stands for co-solvent (sugar alcohol's).

3.7.9. Apparent specific volume

It is the volume taken by a definite mass of solute in a solution. It enables one to obtain the contribution of the solute towards the total volume and its density and also guides the association of the solute and the solvent. It is calculated as:

$$ASV = \frac{V_{\phi}}{M} \quad (3.17)$$

3.8. Isobaric thermal expansion coefficients

This coefficient measures how much an element expands or shrinks with temperature under pressure changes. The same is quite fundamental and decides how the substances would expand when their temperatures change with respect to volume change. It can be calculated from the following equation:

$$\alpha_p = \frac{1}{V_{\phi}^0} \left(\frac{\partial V_{\phi}^0}{\partial T} \right) \quad (3.18)$$

3.9. FTIR spectroscopy

FTIR spectroscopy is a valuable tool for identifying and analyzing molecular compounds through their vibrational transitions. In binary mixtures, it can reveal interactions between two components via peak shifts or broadening, while peak area ratios help determine composition. Ternary mixtures require more complex analysis due to overlapping peaks, with new bands possibly indicating complex formation. Chemometric methods assist in separating spectral contributions. FTIR is widely used in pharmaceuticals, food, environment, and materials science for quality control and understanding molecular interactions.

CHAPTER 4

RESULTS AND DISCUSSION

Section I

Problem 1

Volumetric and Ultrasonic Studies on Interactions of 2-Methoxyethanol/ 2-Ethoxyethanol in Aqueous Solutions of Inositol at Different Temperatures

In this problem, densities and speed of sound values of 2-methoxyethanol or 2-ethoxyethanol in (0.01, 0.03, and 0.05 mol. kg⁻¹) Inositol (aq) mixtures, were obtained at T= (288.15-318.15) K.

Density and Speed of Sound

The data of density demonstrate that values increase as inositol concentration increases and decrease as temperature increases [1,2]. However, as both the concentration and the temperature of the binary mixture (water and inositol) rise, the sound speeds (c) values are also rise. The values of density and sound speeds that were obtained experimentally, as well as estimated parameters are presented in **Tables 4.1** and **4.2** respectively. A comparison of density [3-7], and sound speeds [7,8] for experimental values of a binary mixture (inositol and water) with literature at 0.1 MPa pressure is shown in **Figure 4.2(a)** and **4.2(b)**. **Figure 4.2** clearly shows that the experimental data correlate well with literature data. Additionally, comparison of densities for (water + 2-ME) [9-12], (water + 2-EE) [10,11] shown in **Figure 4.3** and comparison of experimental values of sound speed of a binary mixture of (water + 2-ME), [9-12] (water + 2-EE) [10,11] with literature is shown in **Figure 4.4** respectively. Based on the observation, there is an increase in density with molality, which can be attributed to the increase in solute chain length [13]. The linear relationship of sound speeds with temperature is suggested that intermolecular as well as intramolecular H-bond exist in the solute-solvent interactions. Moreover, the way the sound speed of the ternary mixture varies with temperature is almost the same as that found in pure water. This similarity arises from the dynamics of monomeric water molecules forming and breaking hydrogen bonds within the water structure. Furthermore, the formation of bonds among inositol and water molecules is destroyed when simultaneously new hydrogen bonds are formed among 2-ME, 2-EE, and inositol molecules [14].

Table 4.1 Density measurements of 2-ME and 2-EE in inositol (aq) at 0.1 MPa pressure and different thermal conditions.

$^a m_A / (\text{mol} \cdot \text{kg}^{-1})$	$\rho \times 10^{-3} / (\text{kg} \cdot \text{m}^{-3})$				$^a m_A / (\text{mol} \cdot \text{kg}^{-1})$	$\rho \times 10^{-3} / (\text{kg} \cdot \text{m}^{-3})$			
	T=288.15K	T=298.15K	T=308.15K	T=318.15K		T=288.15K	T=298.15K	T=308.15K	T=318.15K
2-Methoxyethanol + 0.00 mol · kg ⁻¹ Inositol					2-Ethoxyethanol + 0.00 mol · kg ⁻¹ Inositol				
0.00000	0.99926	0.99705	0.99406	0.99036	0.00000	0.99926	0.99705	0.99406	0.99036
0.11039	0.99935	0.99715	0.99415	0.99049	0.11029	0.99927	0.99707	0.99408	0.99040
0.21052	0.99946	0.99726	0.99427	0.99063	0.21002	0.99928	0.99709	0.99410	0.99044
0.31655	0.99958	0.99739	0.99442	0.99079	0.30655	0.99930	0.99711	0.99413	0.99048
0.39717	0.99970	0.99752	0.99455	0.99094	0.39917	0.99936	0.99714	0.99415	0.99051
0.49763	0.99986	0.99768	0.99473	0.99113	0.49989	0.99941	0.99716	0.99414	0.99055
2-Methoxyethanol + 0.01 mol · kg ⁻¹ Inositol					2-Ethoxyethanol + 0.01 mol · kg ⁻¹ Inositol				
0.00000	0.99964	0.99759	0.99456	0.99074	0.00000	0.99964	0.99759	0.99456	0.99074
0.11209	0.99971	0.99766	0.99465	0.99085	0.10098	0.99965	0.99760	0.99457	0.99077
0.19967	0.99978	0.99774	0.99474	0.99095	0.19868	0.99966	0.99761	0.99458	0.99080
0.30462	0.99988	0.99785	0.99486	0.99109	0.29879	0.99967	0.99762	0.99459	0.99083
0.41720	1.00001	0.99798	0.99500	0.99126	0.39986	0.99968	0.99763	0.99461	0.99087
0.49969	1.00013	0.99810	0.99513	0.99140	0.50160	0.99969	0.99764	0.99462	0.99090
2-Methoxyethanol + 0.03 mol · kg ⁻¹ Inositol					2-Ethoxyethanol + 0.03 mol · kg ⁻¹ Inositol				

0.00000	1.00122	0.99911	0.99605	0.99218	0.00000	1.00122	0.99911	0.99605	0.99218
0.09854	1.00125	0.99915	0.99610	0.99225	0.09950	1.00128	0.99917	0.99611	0.99233
0.19952	1.00130	0.99920	0.99616	0.99233	0.19608	1.00136	0.99924	0.99618	0.99242
0.30013	1.00137	0.99928	0.99625	0.99244	0.31671	1.00147	0.99935	0.99628	0.99255
0.39901	1.00145	0.99937	0.99635	0.99256	0.40076	1.00156	0.99944	0.99638	0.99265
0.49901	1.00156	0.99948	0.99647	0.99270	0.50702	1.00168	0.99957	0.99651	0.99282
2-Methoxyethanol + 0.05 mol · kg ⁻¹ Inositol					2-Ethoxyethanol + 0.05 mol · kg ⁻¹ Inositol				
0.00000	1.00301	1.00088	0.99781	0.99396	0.00000	1.00301	1.00088	0.99781	0.99396
0.10520	1.00301	1.00088	0.99783	0.99400	0.10061	1.00306	1.00093	0.99787	0.99404
0.20180	1.00302	1.00090	0.99786	0.99405	0.19980	1.00312	1.00100	0.99794	0.99414
0.30091	1.00306	1.00095	0.99791	0.99412	0.30196	1.00320	1.00108	0.99804	0.99425
0.39624	1.00311	1.00100	0.99799	0.99421	0.40376	1.00330	1.00118	0.99815	0.99438
0.49912	1.00319	1.00108	0.99808	0.99432	0.50022	1.00339	1.00129	0.99826	0.99452

Table 4.2 Speed of sound measurements of 2-ME and 2-EE in inositol (aq) at 0.1 MPa pressure and at different thermal conditions.

^a m _A /(mol · kg ⁻¹)	c/(m · s ⁻¹)				^a m _A /(mol · kg ⁻¹)	c/(m · s ⁻¹)			
	T=288.15	T=298.15	T=308.15	T=318.15		T=288.15	T=298.15	T=308.15	T=318.15
2-Methoxyethanol + 0.00 mol · kg ⁻¹ Inositol					2-Ethoxyethanol + 0.00 mol · kg ⁻¹ Inositol				
0.00000	1466.5	1495.8	1519.8	1536.0	0.00000	1466.5	1495.8	1519.8	1536.0
0.11039	1472.4	1501.1	1523.7	1538.9	0.11029	1491.9	1510.1	1530.2	1547.1

0.21052	1478.1	1505.5	1527.6	1542.1	0.21002	1498.6	1518.9	1538.1	1555.2
0.31655	1483.9	1510.1	1531.5	1545.8	0.30655	1502.7	1527.9	1546.4	1563.4
0.39717	1488.5	1513.9	1534.8	1548.8	0.39917	1505.9	1532.9	1551.5	1568.2
0.49763	1493.9	1518.1	1538.9	1552.4	0.49989	1510.4	1537.9	1555.8	1572.8
2-Methoxyethanol + 0.01 mol · kg ⁻¹ Inositol					2-Ethoxyethanol + 0.01 mol · kg ⁻¹ Inositol				
0.00000	1467.8	1497.3	1521.2	1536.9	0.00000	1467.8	1497.3	1521.2	1536.7
0.11209	1474.4	1503.1	1525.5	1540.5	0.10098	1492.4	1511.2	1531.1	1548.2
0.19967	1479.5	1507.2	1529.1	1543.6	0.19868	1499.5	1519.9	1538.8	1556.1
0.30462	1485.4	1512.1	1532.9	1547.4	0.29879	1503.1	1528.9	1546.5	1564.2
0.41720	1491.8	1517.5	1537.4	1551.2	0.39986	1507.2	1535.5	1552.9	1570.1
0.49969	1496.5	1521.0	1540.7	1554.5	0.50160	1512.4	1540.4	1558.1	1574.4
2-Methoxyethanol + 0.03 mol · kg ⁻¹ Inositol					2-Ethoxyethanol + 0.03 mol · kg ⁻¹ Inositol				
0.00000	1468.9	1499.4	1522.7	1538.1	0.00000	1468.9	1499.4	1522.7	1538.1
0.09854	1475.2	1504.5	1526.9	1541.5	0.09950	1494.4	1513.3	1532.6	1549.7
0.19952	1481.2	1509.4	1531.1	1545.4	0.19608	1501.2	1521.9	1540.5	1557.6
0.30013	1487.5	1514.4	1534.9	1549.1	0.31671	1505.1	1532.7	1549.3	1566.9
0.39901	1493.1	1518.8	1539.1	1552.4	0.40076	1509.1	1537.6	1554.7	1571.8
0.49901	1499.1	1523.9	1543.0	1556.5	0.50702	1514.5	1543.6	1560.1	1575.9
2-Methoxyethanol + 0.05 mol · kg ⁻¹ Inositol					2-Ethoxyethanol + 0.05 mol · kg ⁻¹ Inositol				

0.00000	1469.9	1501.9	1524.1	1539.7	0.00000	1469.9	1501.9	1524.1	1539.7
0.10520	1477.1	1507.4	1528.9	1543.4	0.10061	1496.4	1515.4	1534.7	1550.7
0.20180	1483.4	1512.1	1532.7	1547.1	0.19980	1503.2	1524.9	1542.4	1559.4
0.30091	1489.8	1517.1	1536.8	1550.6	0.30196	1506.1	1533.9	1550.5	1567.4
0.39624	1495.5	1521.4	1540.9	1554.2	0.40376	1511.2	1539.9	1556.8	1573.4
0.49912	1501.9	1526.5	1544.9	1557.9	0.50022	1515.9	1545.9	1562.5	1577.8

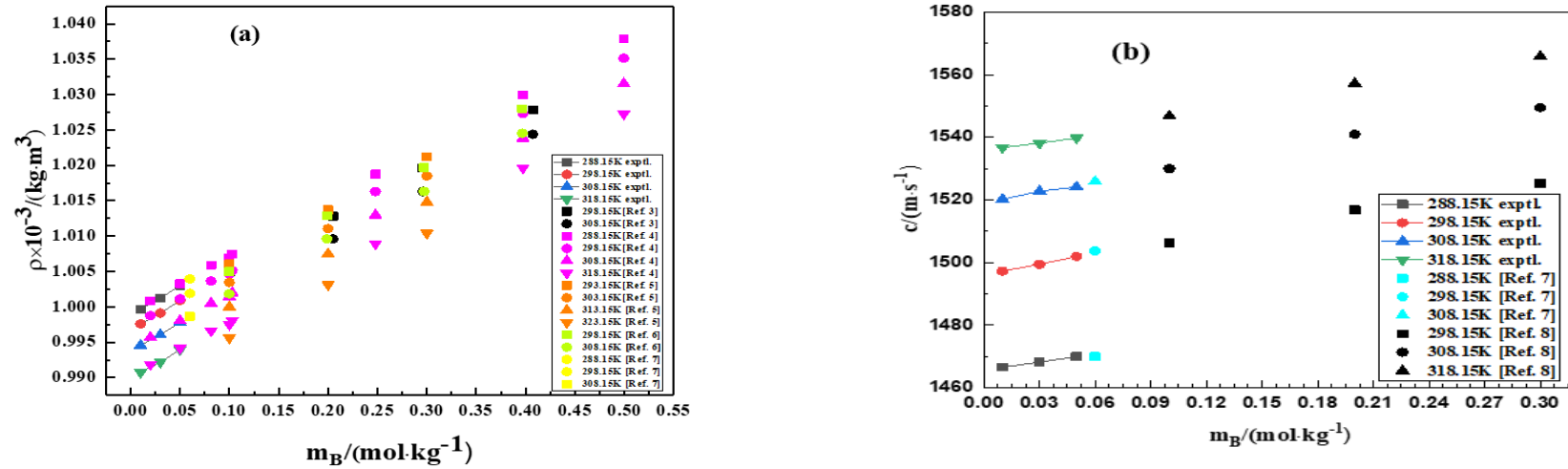


Figure 4.2 Comparison graph of (a) density [3-7] and (b) speed of sound [7,8] for a binary mixture (Inositol + water) at different temperatures.

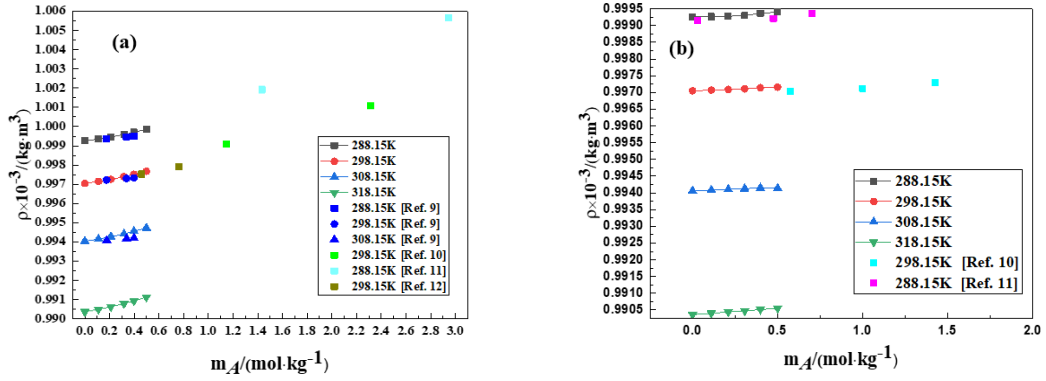


Figure 4.3 Comparison graph of density (a) Water + 2-ME [9-12] and (b) Water + 2-EE [10,11] at different temperatures.

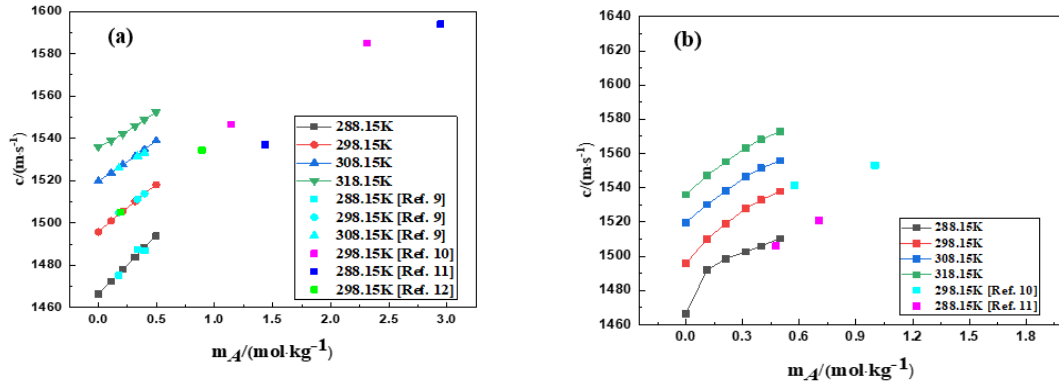


Figure 4.4 Comparison graph of speed of sound (a) Water + 2-ME [9-12] and (b) Water + 2-EE [10,11] at different temperatures.

Apparent molar volume

To calculate the V_ϕ , density value is needed. A solution's hydrated molecules are actually measured in order to provide a description of the overall volume of the molecules [15]. By utilising the densities of solutions (ρ) and solvents (ρ_0) for binary and ternary mixtures at four different temperatures and concentrations, given equation [16] is used to calculate V_ϕ ,

$$V_\phi = (M/\rho) - \{(\rho - \rho_0)/(m_A \rho \rho_0)\} \quad (4.1)$$

Calculated V_ϕ values of solutes (2-ME, 2-EE) in binary and ternary mixtures are given in **Table 4.3**, along with values of density. The volume increases with concentrations, it is due to the associations among molecules of solute and solvent. Certain solutes,

such as glycol ethers (such as 2-ME and 2-EE), can change the characteristics of water and disrupt its structure when they are introduced to it. These solutes have hydrocarbon chains, an oxygen atom (from the ether group), and polar properties. As a result, they can connect with and solvate water molecules through hydrogen bonds. **Figure 4.5** illustrates the variation in apparent molar volume through a two-dimensional plot. 2-EE has greater values than 2-ME. These changes occur due to the solvent (inositol). 2-EE has greater values than 2-ME. These changes occur due to the solvent (inositol). All positive 2-ME/2-EE and inositol values indicate strong solute-solvent interactions. Additionally, **Figure 4.1** indicates the combination of liquids and depicts that 2-EE has higher molecular interactions as compared to 2-ME [17,18]. V_ϕ is significantly influenced by interactions in solutions between the solute and solvent. The result is attributed to the phenomenon of solvation and the solvent's pronounced affinity. This relationship elucidates the different type of molecular associations within the arrangement. The presence of water promotes several types of interactions including intermolecular and intramolecular H-bonds, hydrophobic dynamics, hydrophobic solvation, dipole-2 associations and dipole-induced dipole associations.

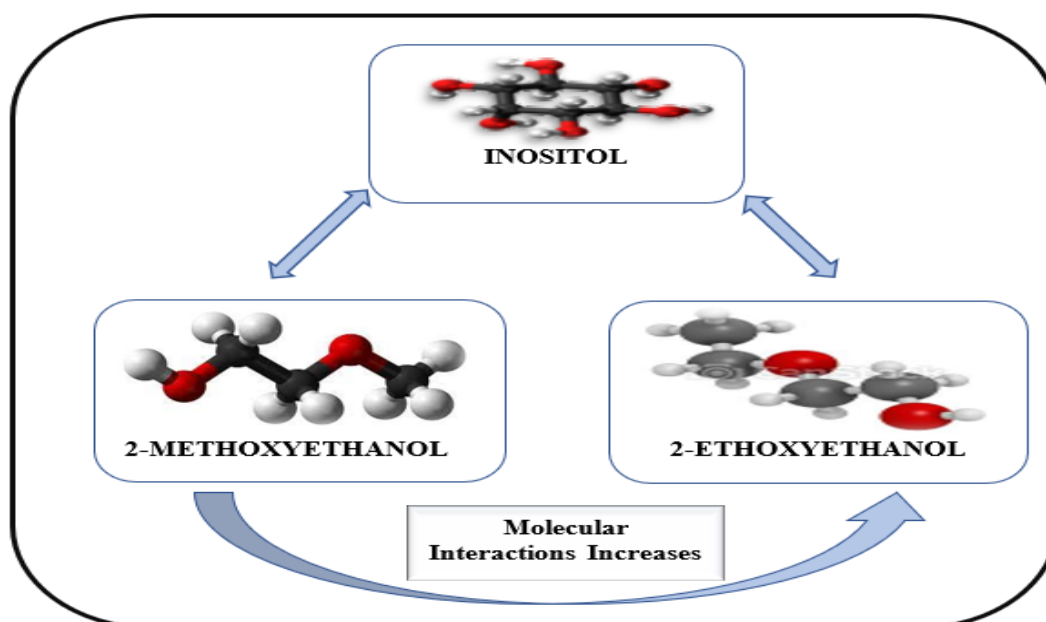


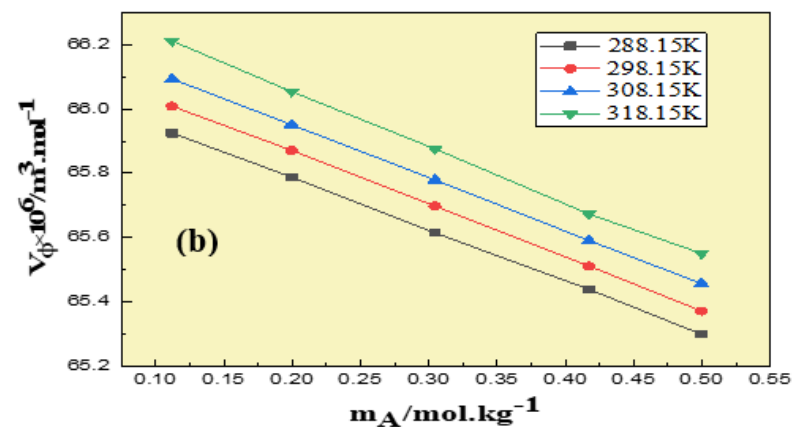
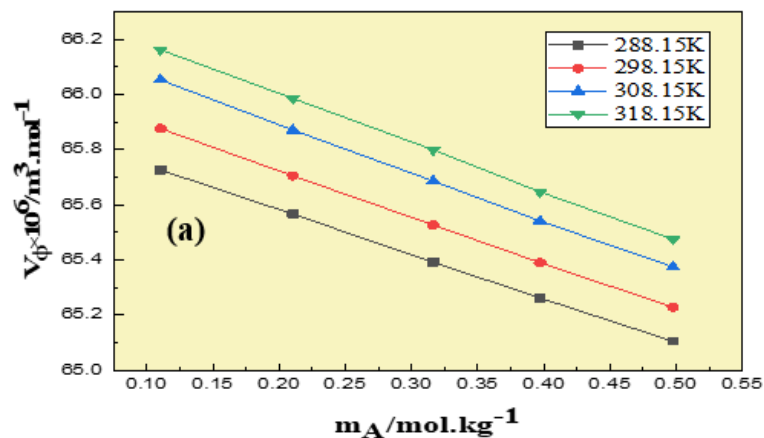
Figure 4.1 2-ME/ 2-EE and Inositol interactions

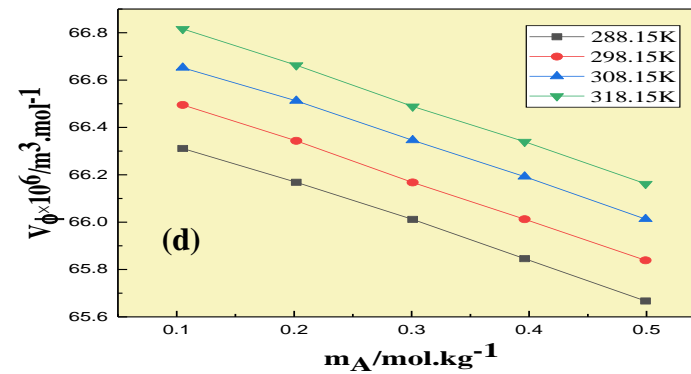
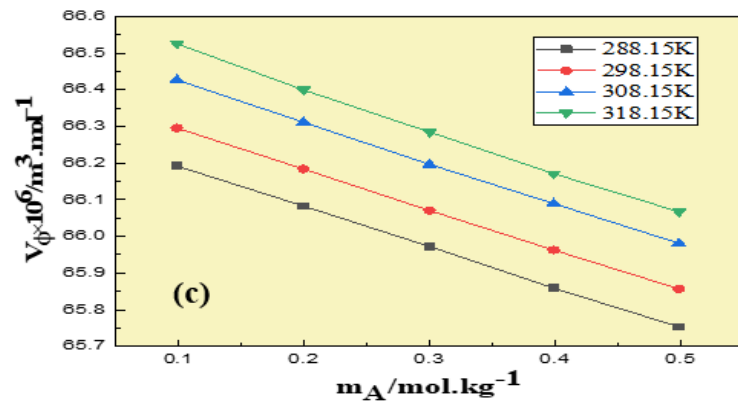
Table 4.3 Values of V_ϕ , for 2-ME /2-EE in inositol (aq) mixtures at constant frequency and different temperatures.

$^a m_A / (\text{mol} \cdot \text{kg}^{-1})$	$V_\phi \times 10^6 / (\text{m}^3 \cdot \text{mol}^{-1})$				$^a m_A / (\text{mol} \cdot \text{kg}^{-1})$	$V_\phi \times 10^6 / (\text{m}^3 \cdot \text{mol}^{-1})$			
	T/K=288.15	T/K=298.15	T/K=308.15	T/K=318.15		T/K=288.15	T/K=298.15	T/K=308.15	T/K=318.15
2-Methoxyethanol + 0.00 mol · kg ⁻¹ Inositol					2-Ethoxyethanol + 0.00 mol · kg ⁻¹ Inositol				
0.11039	65.73	65.88	66.05	66.16	0.11039	79.72	79.80	79.87	79.94
0.21052	65.57	65.71	65.87	65.99	0.21052	79.61	79.69	79.76	79.82
0.31655	65.39	65.53	65.69	65.80	0.31655	79.50	79.57	79.64	79.70
0.39717	65.26	65.39	65.54	65.65	0.39717	79.41	79.48	79.55	79.61
0.49763	65.11	65.23	65.38	65.48	0.49763	79.30	79.36	79.44	79.50
2-Methoxyethanol + 0.01 mol · kg ⁻¹ Inositol					2-Ethoxyethanol + 0.01 mol · kg ⁻¹ Inositol				
0.11209	65.93	66.01	66.09	66.21	0.10098	80.61	80.70	80.82	80.94
0.19967	65.79	65.87	65.95	66.05	0.19868	80.35	80.46	80.58	80.70
0.30462	65.61	65.70	65.78	65.88	0.29879	80.11	80.20	80.32	80.43
0.41720	65.44	65.51	65.59	65.67	0.39986	79.84	79.95	80.05	80.17
0.49969	65.30	65.37	65.46	65.55	0.50160	79.58	79.67	79.79	79.90
2-Methoxyethanol + 0.03 mol · kg ⁻¹ Inositol					2-Ethoxyethanol + 0.03 mol · kg ⁻¹ Inositol				
0.09854	66.19	66.30	66.43	66.53	0.09950	81.30	81.46	81.63	81.76
0.19952	66.08	66.18	66.31	66.40	0.19608	81.10	81.26	81.42	81.56
0.30013	65.97	66.07	66.20	66.28	0.31671	80.86	81.00	81.16	81.30

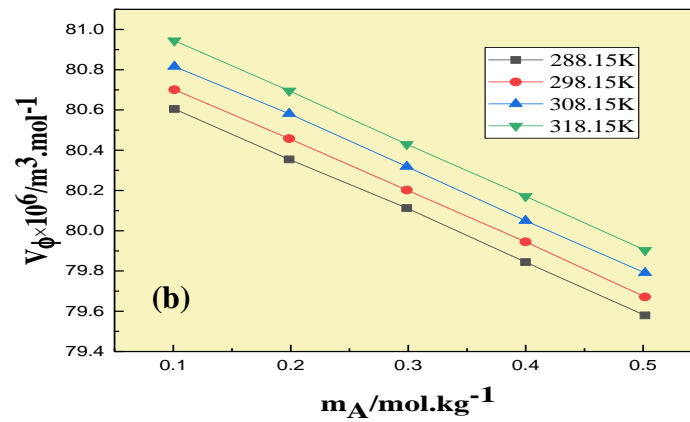
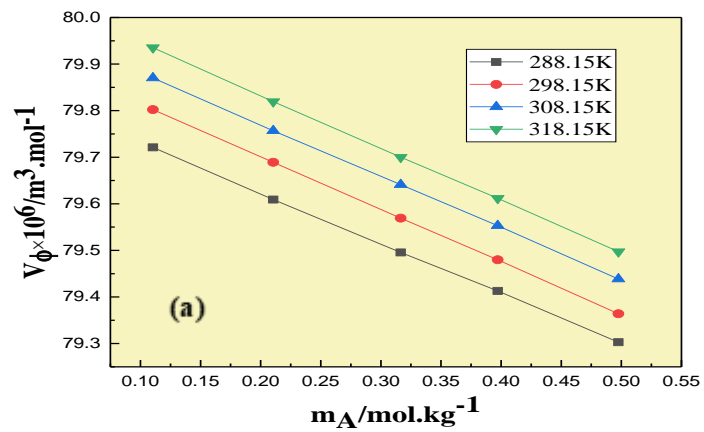
0.39901	65.86	65.96	66.09	66.17	0.40076	80.69	80.83	80.97	81.11
0.49901	65.75	65.86	65.98	66.07	0.50702	80.48	80.61	80.75	80.89
2-Methoxyethanol + 0.05 mol · kg ⁻¹ Inositol					2-Ethoxyethanol + 0.05 mol · kg ⁻¹ Inositol				
0.10520	66.31	66.49	66.65	66.82	0.10061	81.65	81.81	81.97	82.12
0.20180	66.17	66.34	66.51	66.66	0.19980	81.44	81.59	81.74	81.90
0.30091	66.01	66.17	66.35	66.49	0.30196	81.22	81.36	81.52	81.67
0.39624	65.85	66.01	66.19	66.34	0.40376	81.00	81.13	81.28	81.43
0.49912	65.67	65.84	66.01	66.16	0.50022	80.79	80.91	81.06	81.22

(I)





(II)



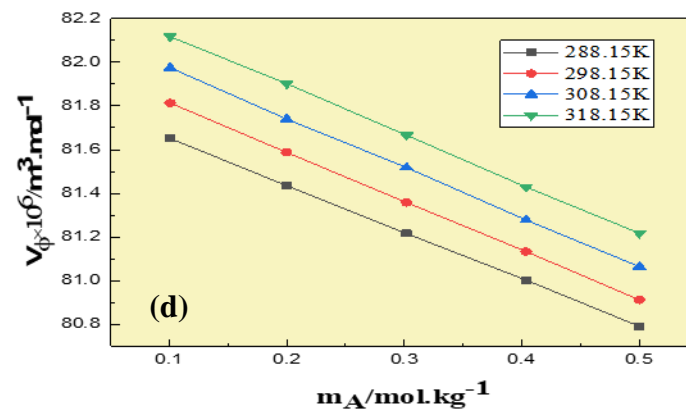
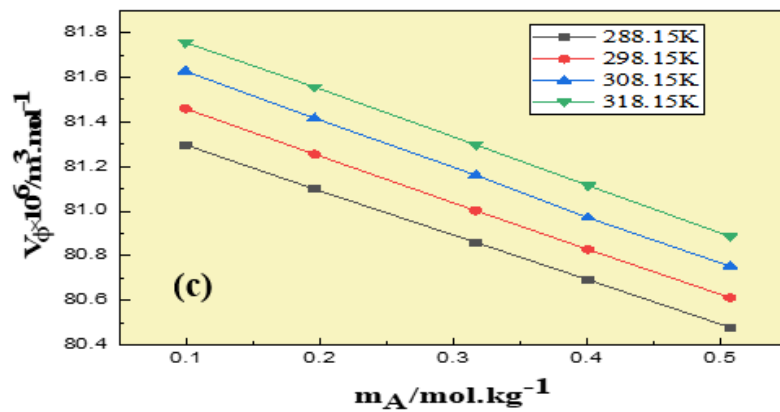


Figure 4.5 Variations in V_ϕ of 2-ME (I) and 2-EE (II) in (a) 0.00 inositol, (b) 0.01 inositol, (c) 0.03 inositol and (d) 0.05 $\text{mol} \cdot \text{kg}^{-1}$ inositol.

Partial molar volume

Values for V_{ϕ}^0 were determined using the following equation [16],

$$V_{\phi} = V_{\phi}^0 + S_V^* m_A \quad (4.2)$$

The values in this polynomial equation were fitted using the least squares approach to get the extrapolation of the V_{ϕ} at infinite dilution. At infinite dilution, the value of V_{ϕ}^0 is considered to be equal to the value of V_{ϕ} [19,20]. **Table 4.4** shows computed V_{ϕ}^0 values for different concentrations and temperatures, along with their respective standard errors. Additionally, S_V^* values along with errors are also given in the same table. The temperature effect is less, and the values for each solute are rising gradually with rise in temperature. The positive value of V_{ϕ}^0 in aqueous inositol solutions and water indicates strong solute-solvent interactions. **Figure. 4.6** depicts that the value of V_{ϕ}^0 gradually increases with temperature and inositol concentration. According to the co-sphere overlap model, volume changes depend on the interactions between hydration shells. When the hydration layers of two ions come close and overlap, this results in an expansion of volume. However, when overlaps occur between ionic and hydrophobic regions or between two hydrophobic regions, the volume decreases. Positive V_{ϕ}^0 values are indicative of hydrophobic interactions and highlight the presence of strong H-bonding. The temperature-dependent shifts in V_{ϕ}^0 point to effects such as the creation of H-bonds, and the release of gas molecules previously trapped within solvent layers. As the temperature increases, molecules that were part of the solvation layers around the solute may detach and mix into the solution, influencing these observed changes [21,22]. The partial molar property has been found to be temperature-dependent and is influenced by solvent-solvent interactions, with increasing molar mass resulting in higher values of V_{ϕ}^0 . Furthermore, S_V^* values are small and negative, which suggests that the mixtures have weak solute-solute interactions. The comparatively low S_V^* values relative to V_{ϕ}^0 suggest that solute-solvent interactions. Values reveals that associations within the mixture are largely governed by interactions between solute and solvent molecules, rather than between solute molecules alone [23,24]. In the system under investigation, the solute-solvent associations occur, including hydrophobic interactions between the hydrocarbon parts

Table 4.4 Values of V_{ϕ}^0 and S_V^* for 2-ME and 2-EE in inositol (aq) mixes at pressure of 0.1 MPa.

$^a m_B / (\text{mol} \cdot \text{kg}^{-1})$	$V_{\phi}^0 \times 10^6 (\text{m}^3 \cdot \text{mol}^{-1})$				$S_V^* \times 10^6 (\text{m}^3 \cdot \text{kg} \cdot \text{mol}^{-2})$			
	T = 288.15K	T = 298.15K	T = 308.15K	T = 398.15K	T = 288.15K	T = 298.15K	T = 308.15K	T = 38.15K
2-Methoxyethanol								
0.00	65.9(±0.003)	66.0(±0.004)	66.2(±0.005)	66.3(±0.004)	-1.6(±0.008)	-1.6(±0.011)	-1.7(±0.016)	-1.7(±0.013)
0.01	66.1(±0.004)	66.2(±0.004)	66.2(±0.002)	66.4(±0.009)	-1.6(±0.011)	-1.6(±0.012)	-1.6(±0.005)	-1.7(±0.026)
0.03	66.3(±0.002)	66.4(±0.002)	66.5(±0.003)	66.6(±0.007)	-1.1(±0.007)	-1.1(±0.007)	-1.1(±0.010)	-1.1(±0.021)
0.05	66.4(±0.011)	66.6(±0.005)	66.8(±0.009)	66.9(±0.005)	-1.6(±0.034)	-1.6(±0.016)	-1.6(±0.029)	-1.6(±0.016)
2-Ethoxyethanol								
0.00	79.8(±0.003)	79.9(±0.001)	79.9(±0.002)	80.0(±0.002)	-1.0(±0.008)	-1.1(±0.003)	-1.1(±0.005)	-1.1(±0.005)
0.01	80.8(±0.007)	80.9(±0.007)	81.0(±0.008)	81.2(±0.003)	-2.5(±0.022)	-2.5(±0.021)	-2.5(±0.025)	-2.6(±0.008)
0.03	81.4(±0.002)	81.6(±0.003)	81.8(±0.005)	81.9(±0.004)	-2.0(±0.006)	-2.0(±0.010)	-2.1(±0.016)	-2.1(±0.011)
0.05	81.8(±0.003)	82.0(±0.003)	82.2(±0.006)	82.3(±0.005)	-2.1(±0.009)	-2.2(±0.009)	-2.2(±0.017)	-2.2(±0.016)

of glycol ethers (2-ME, 2-EE) and water molecules. These interactions play a pivotal role in shaping the partial molar volume V_{ϕ}^0 , values, indicating strong solvation effects and the presence of hydrophobic effects. Additionally, hydrophilic interactions occur among the CH_3 and $-\text{OH}$ groups of the glycol ethers and inositol molecules, contributing to solvation effects and the overall stability of the ternary liquid mixture. These interactions collectively influence the system's structural dynamics and volumetric properties, providing valuable insights into its behaviour.

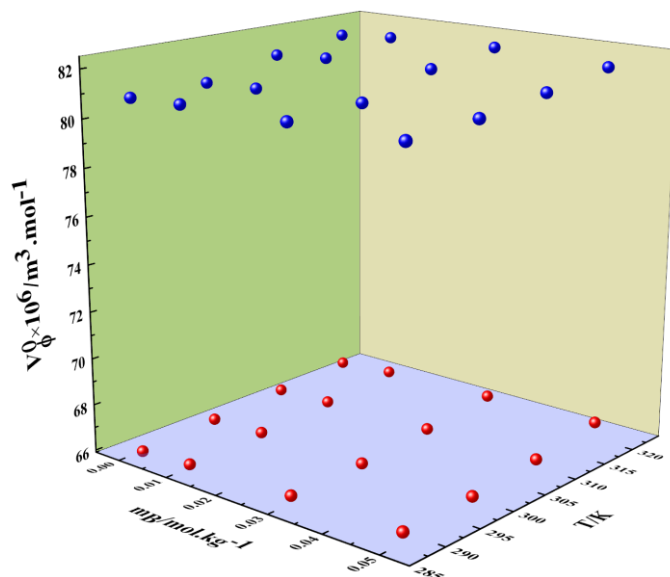


Figure. 4.6 Plots of the variations in partial molar volume, V_{ϕ}^0 , of 2-ME (red) and 2-EE (blue) in an inositol aqueous solution at various temperatures.

Partial molar volume of Transfer

The microscopic structure of the liquid and the solute-cosolute ratio in the mixture are both represented by transfer properties [25,26]. By equation (4.3) [16], ΔV_{ϕ}^0 for 2-ME and 2-EE in inositol (aq) solutions at thermal condition was calculated:

$$\Delta V_{\phi}^0 = \Delta V_{\phi}^0 (\text{in aqueous inositol solution}) - V_{\phi}^0 (\text{in water}) \quad (4.3)$$

Table 4.5 contains the computed value of ΔV_{ϕ}^0 . All the ΔV_{ϕ}^0 values are increasing in the ternary solution. As per co-sphere overlap hypothesis, solvation in the presence of non-solvents' interactions and structural aspects tend to enhance the structure of these

solutes due to their nature. The ΔV_{ϕ}^0 data are consistent with the theory which states that the contribution solute-2 association are negligible. Therefore, the cited values provide useful information on solute-solvent association. Following are the interactions that take place in the liquid mixture.

1. Hydrophobic-hydrophobic interactions occur among the hydrocarbon parts of glycol ethers (2-ME, 2-EE) and the hydrocarbon parts of inositol molecules.

Table 4.5 Values of ΔV_{ϕ}^0 of 2-ME and 2-EE in inositol (aq) solutions at pressure, $p=0.1$ MPa.

$m_B/(\text{mol} \cdot \text{kg}^{-1})$	$\Delta V_{\phi}^0 \times 10^6 (\text{m}^3 \cdot \text{mol}^{-1})$			
	T = 288.15K	T = 298.15K	T = 308.15K	T = 318.15K
2-Methoxyethanol				
0.01	0.20	0.14	0.04	0.04
0.03	0.40	0.34	0.29	0.27
0.05	0.59	0.61	0.59	0.63
2-Ethoxyethanol				
0.01	1.03	1.04	1.09	1.15
0.03	1.66	1.74	1.85	1.92
0.05	2.03	2.11	2.21	2.29

2. Hydrophilic-2 associations occur among the CH_3 and $-\text{OH}$ groups of the glycol ethers and inositol, respectively.
3. Hydrophobic-2 associations occur between the hydrocarbon part of glycol ethers (2-ME, 2-EE) and the inositol-OH group.

The interactions involving ions and hydrophobic groups, as well as between two hydrophobic groups, result in negative volume contributions. On the other hand, interactions between ions and hydrophilic groups or between two hydrophilic groups produce positive volume contributions. The positive ΔV_{ϕ}^0 values found in this study indicate that hydrophilic associations are more prominent than hydrophobic interactions in this context.

Temperature dependent partial molar volume

The variation of V_{ϕ}^0 with temperature can be represented using the below [16]:

Table 4.6 Values a, b, and c of 2-ME and 2-EE in inositol (aq) solutions along with R² and ARD (deviations).

$m_B/(\text{mol. kg}^{-1})$	$a \times 10^6(\text{m}^3. \text{mol}^{-1})$	$b \times 10^6(\text{m}^3. \text{mol}^{-1}. \text{K}^{-1})$	$c \times 10^6(\text{m}^3. \text{mol}^{-1}. \text{K}^{-2})$	R ²	ARD
2-Methoxyethanol					
0.01	66.1909	0.0088	0.0001	0.9999	0.0001
0.03	66.4120	0.0113	0.0000	0.9999	0.0001
0.05	66.6707	0.0171	0.0000	0.9999	0.0000
2-Ethoxyethanol					
0.01	80.9672	0.0109	0.0001	0.9999	0.0000
0.03	81.6721	0.0170	-0.0001	0.9999	0.0001
0.05	82.0390	0.0167	-0.0001	0.9999	0.0000

$$V_{\phi}^0 = a + b(T - T_{\text{ref}}) + c(T - T_{\text{ref}})^2 \quad (4.4)$$

In the relationship mentioned above, T stands for temperature, T_{ref} for reference temperature, or 298.15K. The obtained values of a , b , and c for glycol ethers in an aqueous solution of inositol are mentioned in **Table 4.6**. At infinite dilution, the E_{ϕ}^0 are given as $E_{\phi}^0 = (\partial E_{\phi}^0 / \partial T)_p$, which is considered an important indicator of the interactions between the solute and solvent in the solutions [28]. This is determined using the following formula [16]:

$$E_{\phi}^0 = (\partial E_{\phi}^0 / \partial T)_p = b + 2c(T - T_{\text{ref}}) \quad (4.5)$$

The E_{ϕ}^0 values are all positive and are presented in **Table 4.7**. This positivity is attributed to the packing or caging effect, resulting in all E_{ϕ}^0 values being positive [29-31]. The following equation [16] describes the extent to which a solute can both create and disrupt structures:

$$(\partial E_{\phi}^0 / \partial T)_p = (\partial^2 V_{\phi}^0 / \partial T^2)_p = 2c \quad (4.6)$$

Table 4.7 Values of E_{ϕ}^0 for 2-ME and 2-EE in inositol (aq) solutions at different thermal conditions.

^a m _B (mol · kg ⁻¹)	$E_{\phi}^0 \times 10^6(\text{m}^3 \cdot \text{mol}^{-1} \cdot \text{K}^{-1})$				$(\partial E_{\phi}^0/\partial T)_p/(\text{m}^3 \cdot \text{mol}^{-1} \cdot \text{K}^{-2})$
	T=288.15	T=298.15	T=308.15	T=318.15	
2-Methoxyethanol					
0.01	0.0073	0.0088	0.0104	0.0119	0.0002
0.03	0.0114	0.0113	0.0112	0.0110	0.0000
0.05	0.0180	0.0171	0.0161	0.0151	-0.0001
2-Ethoxyethanol					
0.01	0.0096	0.0109	0.0121	0.0134	0.0001
0.03	0.0189	0.0170	0.0152	0.0133	-0.0002
0.05	0.0179	0.0167	0.0155	0.0143	-0.0001

The sign $(\partial E_{\phi}^0 / \partial T)_p$ serves as an indicator of the solute's ability to either disrupt or reinforce the structure of the surrounding solvent. The calculated values of $(\partial E_{\phi}^0 / \partial T)_p$ presented in **Table 4.7**, along with E_{ϕ}^0 values. All E_{ϕ}^0 values, positive at every thermal condition and it indicates that there are solute-solvent associations exist

[32,33]. Furthermore, it was observed that the E_{ϕ}^0 values show no trend with rise in concentration and temperature.

Apparent molar isentropic compression

The given equation [16] used to calculate the K_S ,

$$K_S = 1 / c^2 \rho \quad (4.7)$$

After $\kappa_{\phi,s}$ determine the by the following equation [16];

$$K_{\phi,s} = (MK_S/\rho) - \{(K_{S_{s,o}}\rho - K_S\rho_o)/m_A\rho\rho_o\} \quad (4.8)$$

The symbol, K_S , $K_{\phi,s}$ in the preceding equation represents the solution and solvent isentropic compressibility, respectively. K_S is mainly made up of two contributions: (I) the compressibility of the pure solvent without any solute present, and (II) the compressibility of the solute without the solvent. The first component stems from a compression of solvent molecules, whereas the second component is associated with the region surrounding the glycol ethers. **Table 4.8** shows the observed value of sound speed as well as the computed $K_{\phi,s}$ values. At all temperatures and solvent concentrations, all values of $K_{\phi,s}$ are negative. Additionally, as the temperature rises, the magnitude declines. With rise in temperature and solvent concentration, the negativity of $K_{\phi,s}$ decreases, but the negativity of $K_{\phi,s}$ increases with the molality of glycol ethers. The thermal motion of solute molecules being released into the solvent, which causes an increase in volume and an increase in compressibility, could explain these negative values. Also, the mobility of the solvent molecules and the hydration sphere surrounding the solute active centres play a role in the $K_{\phi,s}$ behavior as well. The negative values also suggest that water molecules exhibit lower compressibility compared to bulk water around the glycol ether's ionic charge groups. Furthermore, the structural compressibility of water decreases as the solute with solvent interact more strongly, which is reflected in the negative $K_{\phi,s}$ values [34,35]. **Figure. 4.7** depicts a linear plot of $K_{\phi,s}$ versus molality.

Table 4.8 Values of $K_{\phi,S}$, 2-ME and 2-EE in inositol (aq) solution at, $p = 0.1$ MPa.

$^a m_A / (\text{mol} \cdot \text{kg}^{-1})$	$K_{\phi,S} \times 10^6 / (\text{m}^3 \cdot \text{mol}^{-1} \cdot \text{GPa}^{-1})$				$^a m_A / (\text{mol} \cdot \text{kg}^{-1})$	$K_{\phi,S} \times 10^6 / (\text{m}^3 \cdot \text{mol}^{-1} \cdot \text{GPa}^{-1})$			
	T=288.15	T=298.15	T=308.15	T=318.15		T=288.15	T=298.15	T=308.15	T=318.15
2-Methoxyethanol + 0.00 mol \cdot kg $^{-1}$ Inositol					2-Ethoxyethanol + 0.00 mol \cdot kg $^{-1}$ Inositol				
0.11039	-46.26	-44.39	-43.01	-42.10	0.11039	-46.26	-44.39	-43.01	-42.11
0.21052	-46.51	-44.63	-43.24	-42.34	0.21052	-46.51	-44.63	-43.25	-42.34
0.31655	-46.64	-44.76	-43.36	-42.46	0.31655	-46.64	-44.76	-43.37	-42.46
0.39717	-46.71	-44.82	-43.43	-42.52	0.39717	-46.71	-44.82	-43.43	-42.52
0.49763	-46.79	-44.90	-43.50	-42.59	0.49763	-46.78	-44.89	-43.50	-42.59
2-Methoxyethanol + 0.01 mol \cdot kg $^{-1}$ Inositol					2-Ethoxyethanol + 0.01 mol \cdot kg $^{-1}$ Inositol				
0.11209	-46.14	-44.26	-42.93	-42.01	0.10098	-46.09	-44.21	-42.88	-41.96
0.19967	-46.36	-44.48	-43.14	-42.22	0.19868	-46.36	-44.47	-43.14	-42.21
0.30462	-46.50	-44.60	-43.27	-42.34	0.29879	-46.48	-44.59	-43.26	-42.33
0.41720	-46.59	-44.70	-43.36	-42.43	0.39986	-46.57	-44.68	-43.34	-42.41
0.49969	-46.65	-44.75	-43.42	-42.49	0.50160	-46.65	-44.75	-43.41	-42.48
2-Methoxyethanol + 0.03 mol \cdot kg $^{-1}$ Inositol					2-Ethoxyethanol + 0.03 mol \cdot kg $^{-1}$ Inositol				
0.09854	-45.97	-44.07	-42.73	-41.88	0.09950	-45.97	-44.07	-42.73	-41.88
0.19952	-46.25	-44.35	-43.00	-42.14	0.19608	-46.24	-44.33	-42.98	-42.13
0.30013	-46.38	-44.47	-43.11	-42.26	0.31671	-46.38	-44.47	-43.11	-42.26

0.39901	-46.46	-44.55	-43.19	-42.34	0.40076	-46.45	-44.53	-43.18	-42.32
0.49901	-46.53	-44.61	-43.26	-42.40	0.50702	-46.52	-44.60	-43.25	-42.39
2-Methoxyethanol + 0.05 mol · kg ⁻¹ Inositol					2-Ethoxyethanol + 0.05 mol · kg ⁻¹ Inositol				
0.10520	-45.89	-43.96	-42.69	-41.82	0.10061	-45.86	-43.93	-42.66	-41.79
0.20180	-46.15	-44.20	-42.92	-42.05	0.19980	-46.13	-44.19	-42.91	-42.04
0.30091	-46.27	-44.32	-43.03	-42.16	0.30196	-46.25	-44.30	-43.02	-42.15
0.39624	-46.35	-44.39	-43.11	-42.24	0.40376	-46.33	-44.38	-43.10	-42.23
0.49912	-46.42	-44.46	-43.18	-42.31	0.50022	-46.39	-44.44	-43.16	-42.29

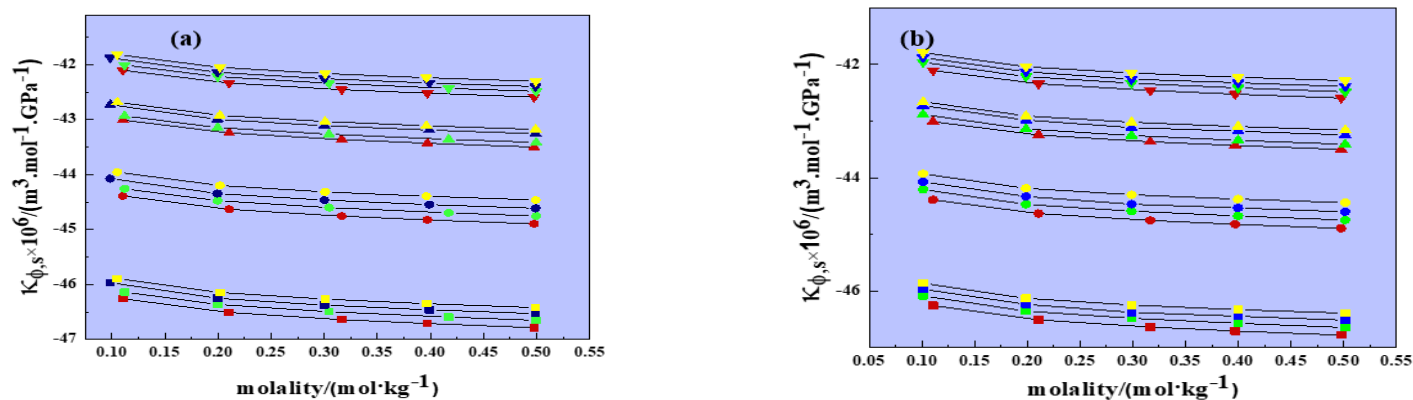


Figure. 4.7 Plots of the variations of $K_{\phi,s}$, of (a) 2-ME and (b) 2-EE in an Inositol (aq) solutions. (Symbol: red = 288.15K, green = 298.15K, blue = 308.15K, and yellow = 318.15K).

Partial molar isentropic compression

The values of $K_{\phi,s}^0$, was determined by using equation [16];

$$K_{\phi,s} = K_{\phi,s}^0 + S_K^* m_A \quad (4.9)$$

Table 4.9 lists the values of $K_{\phi,s}^0$, together with associated standard errors. $K_{\phi,s}^0$ and S_K^* were determined using the least-squares fitting approach. Because of the small size of S_K^* , solute-solute associations are very less [36,37]. All the $K_{\phi,s}^0$ values are negative. The $K_{\phi,s}^0$ values get less negative with increasing temperature and solvent concentration (water + inositol); this implies that some water molecules around the glycol ether (2-ME/2-EE) are less compressible. The $K_{\phi,s}^0$ values tend to become less negative as the temperature is increased. This trend indicates that molecules from the hydration layers surrounding solute molecules migrate and disperse into the bulk solution. The negative value suggests that the extent to which the solvent can be compressed is reduced, following rationalization that the compression is due to the presence of electrostrictive solvation of the ions around which strong compression occurs [38,39]. The values of S_K^* are near about zero as compared to the $K_{\phi,s}^0$ values. The values of $K_{\phi,s}^0$ represent the degree of interaction between the solute and the solvent. The values give great insight into solute-2 associations. **Figure 4.8** shows a linear plot of $K_{\phi,s}^0$ with molality. In the liquid mixture, solute-2 associations are insignificant, which suggests that solute-solvent associations predominate in the solution.

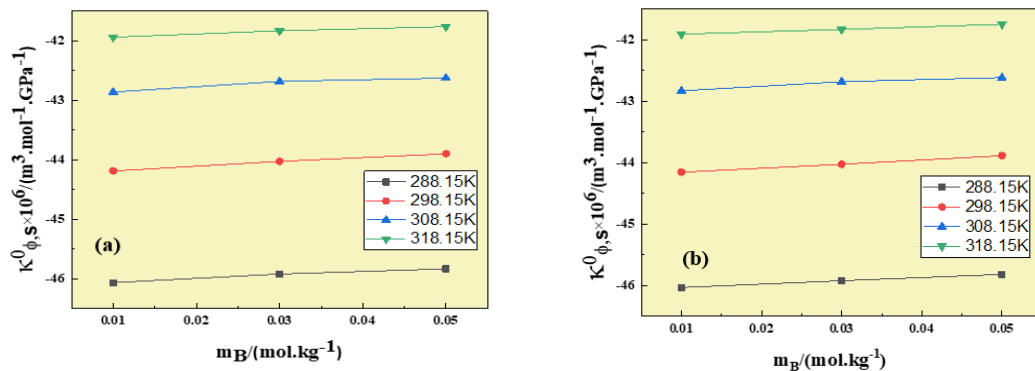


Figure 4.8 Variations of $K_{\phi,s}^0$ versus molality ($\text{mol} \cdot \text{kg}^{-1}$) of (a) 2-ME and (b) 2-EE in aqueous Inositol solutions at different temperatures.

Table 4.9 Values of, $K_{\phi,s}^0$ and S_K^* , with errors of 2-ME and 2-EE in water and inositol (aq) mixes pressure, $p=0.1$ MPa.

$^a m_B /$ (mol · kg ⁻¹	$K_{\phi,s}^0 \times 10^6 / (\text{m}^3 \cdot \text{mol}^{-1} \cdot \text{GPa}^{-1})$				$S_K^* \times 10^6 (\text{kg} \cdot \text{m}^3 \cdot \text{mol}^{-2} \cdot \text{GPa}^{-1})$			
	T = 288.15K	T = 298.15K	T = 308.15K	T = 318.15K	T = 288.15K	T = 298.15K	T = 308.15K	T = 318.15K
2-Methoxyethanol								
0.00	-46.18(±0.06)	-44.31(±0.06)	-42.93(±0.06)	-42.03(±0.06)	-1.31(±0.20)	-1.26(±0.19)	-1.23(±0.18)	-1.21(±0.18)
0.01	-46.06(±0.06)	-44.19(±0.06)	-42.86(±0.05)	-41.94(±0.05)	-1.26(±0.18)	-1.21(±0.18)	-1.19(±0.17)	-1.17(±0.17)
0.03	-45.92(±0.07)	-44.03(±0.07)	-42.68(±0.07)	-41.83(±0.07)	-1.33(±0.24)	-1.28(±0.23)	-1.25(±0.22)	-1.24(±0.22)
0.05	-45.83(±0.07)	-43.90(±0.06)	-42.63(±0.06)	-41.76(±0.06)	-1.28(±0.21)	-1.23(±0.20)	-1.20(±0.20)	-1.18(±0.20)
2-Ethoxyethanol								
0.00	-46.18(±0.06)	-44.32(±0.06)	-42.94(±0.06)	-42.03(±0.06)	-1.30(±0.20)	-1.25(±0.19)	-1.22(±0.19)	-1.21(±0.18)
0.01	-46.03(±0.07)	-44.15(±0.07)	-42.83(±0.07)	-41.91(±0.07)	-1.33(±0.22)	-1.28(±0.22)	-1.25(±0.21)	-1.24(±0.21)
0.03	-45.92(±0.08)	-44.03(±0.07)	-42.68(±0.07)	-41.83(±0.07)	-1.30(±0.24)	-1.25(±0.23)	-1.22(±0.23)	-1.21(±0.22)
0.05	-45.82(±0.07)	-43.89(±0.07)	-42.61(±0.07)	-41.75(±0.07)	-1.25(±0.23)	-1.21(±0.22)	-1.18(±0.22)	-1.17(±0.21)

Partial molar isentropic compression of transfer

The ΔK_{ϕ}^0 for 2-ME and 2-EE in aqueous inositol obtained by using the equation [16] given below:

$$\Delta K_{\phi}^0 = K_{\phi,s}^0 \text{ (in aqueous Inositol solution)} - K_{\phi,s}^0 \text{ (in water)} \quad (4.10)$$

Table 4.10 contains the values for ΔK_{ϕ}^0 . All values of ΔK_{ϕ}^0 are found to be greater than zero (positives), and with an increase in the solvent (inositol + water) concentration, ΔK_{ϕ}^0 model proposed by Friedman and Krishnan which considers both the expansion and shrinkage distortion that occurs when solute molecules are present. The model explains that, a positive value of ΔK_{ϕ}^0 suggests an increase in volume with the displacement of water that is otherwise bound at the hydrophilic centres. This means that such positive numbers suggest that the solute and solvent are strongly associated. For instance, it suggests that for low temperatures and low inositol concentrations, more water molecules are clustered around the solute, in particular ions. The interaction between solute and solvent is quite strong and is characterized by low ΔK_{ϕ}^0 values and high ΔK_{ϕ}^0 values; therefore, at low temperature and low concentration of inositol, more water molecules are interacting with the solute, specifically the ions [40].

Table 4.10 Values of $\Delta K_{\phi,s}^0$ for 2-ME and 2-EE in inositol (aq) solutions.

^a m _B (mol · kg ⁻¹)	$\Delta K_{\phi,s}^0 \times 10^6 (\text{m}^3 \cdot \text{mol}^{-1} \text{GPa}^{-1})$			
	T = 288.15K	T = 298.15K	T = 308.15K	T = 318.15K
2-Methoxyethanol				
0.01	0.12	0.13	0.07	0.09
0.03	0.26	0.29	0.25	0.20
0.05	0.35	0.42	0.31	0.27
2-Ethoxyethanol				
0.01	0.15	0.16	0.11	0.12
0.03	0.26	0.29	0.25	0.20
0.05	0.36	0.43	0.32	0.28

Pair and Triplet Coefficients

Friedman and Krishnan [41] updated McMillian and Mayer's [42] hypothesis to describe the properties of a solute's transfer from water to an aqueous solution. They

Table 4.11 Interaction coefficients of 2-ME and 2-EE in inositol (aq)solutions at different thermal conditions.

T/K	$V_{AB} \times 10^6 (\text{m}^3 \cdot \text{mol}^{-2} \cdot \text{kg})$	$V_{ABB} \times 10^6 (\text{m}^3 \cdot \text{mol}^{-3} \cdot \text{kg}^2)$	$K_{AB} \times 10^6 (\text{m}^3 \cdot \text{mol}^{-2} \cdot \text{kg} \cdot \text{GPa}^{-1})$	$K_{ABB} \times 10^6 (\text{m}^3 \cdot \text{mol}^{-3} \cdot \text{kg}^2 \cdot \text{GPa}^{-1})$
2-Methoxyethanol				
288.15	8.90	-41.05	5.91	-32.54
298.15	5.73	4.94	6.16	-27.04
308.15	2.45	46.57	5.19	-27.72
318.15	1.54	64.14	4.52	-24.53
2-Ethoxyethanol				
288.15	45.44	-341.33	6.50	-39.03
298.15	46.99	-350.45	6.73	-33.48
308.15	50.13	-379.37	5.79	-34.37
318.15	52.32	-398.09	5.09	-30.77

T/K is the temperatures.

provided a method to obtain the solute and co-solute interaction coefficients. The relationship between ΔV_{ϕ}^0 and $\Delta K_{\phi,s}^0$, is depicted as follows using their method [16]:

$$\Delta V_{\phi}^0(\text{water to aqueous Inositol solution}) = 2V_{AB}m_B + 3V_{ABB}m_B^2 \quad (4.11)$$

$$\Delta K_{\phi,s}^0(\text{water to aqueous Inositol solution}) = 2K_{AB}m_B + 3K_{ABB}m_B^2 \quad (4.12)$$

where A stands for glycol ethers (2-ME, 2-EE) and B stands for co-solvent (inositol). Additionally, m_B , is the molality of the solvent. To attain the values for these coefficients, the values of ΔV_{ϕ}^0 and $\Delta K_{\phi,s}^0$ must be fitted into the above two equations. The values of interaction coefficients are shown in **Table 4.11**. The pair coefficients for both volume and compressibility are all positive. In addition, triplet coefficients for volume have both negative and positive values but K_{ABB} are all negative. **Table 4.11** shows that the values for V_{AB} , and K_{AB} are all positive with temperature, which illustrates the pairwise association among 2-ME, 2-EE, and inositol. The interactions among the solute and co-solute arise because of overlapping hydration spheres. Furthermore, values of the triplet coefficient (V_{ABB} , K_{ABB}) are negative except at three temperatures (298.15, 308.15, and 318.15)K for 2-Methoxyethanol [43,25].

Isobaric thermal expansion coefficients

It is mainly quantifying the way a material's volume responds to temperature fluctuations while maintaining a constant pressure. It represents the proportional alteration in volume per unit temperature change under conditions of unchanging pressure. The equation [44] for calculating the isobaric thermal expansion coefficient is articulated as follows:

$$\alpha_p = \frac{1}{V_{\phi}^0} \left(\frac{\partial V_{\phi}^0}{\partial T} \right) \quad (4.13)$$

incorporates the variable α_p , representing the isobaric thermal expansion coefficient, while T signifies temperature. Understanding the significance of the coefficient of thermal expansion is vital in elucidating solute-solvent interactions [45]. Hepler's theory introduces the concept of Hepler's constant, denoted as $\left(\frac{\partial V_{\phi}^0}{\partial T} \right)$, which serves to categorise a solute into two distinct roles: as a builder or a breaker of structure. When the value of $\frac{\partial V_{\phi}^0}{\partial T}$ is positive, it indicates that the solute promotes the formation or enhancement of structure. **Table 4.12** computes the coefficient of thermal expansion

values at various temperatures. Especially the α_p , values for 2-methoxyethanol (2-ME) and 2-ethoxyethanol (2-EE) exhibit positive values with rising temperatures, Values of α_p , suggest volumetric expansion and reduction compression in inositol aqueous solutions upon the introduction of glycol ethers, emphasising the role of the isobaric thermal expansion coefficient in characterising these interactions.

Table 4.12 Isothermal expansion coefficients for 2-ME and 2-EE in Inositol (aq) solutions at different temperatures.

$^a m_B / (\text{mol} \cdot \text{kg}^{-1})$	$\alpha_p \times 10 / (\text{K}^{-1})$			
	T=288.15K	T=298.15K	T=308.15K	T=318.15K
2-Methoxyethanol				
0.01	0.110	0.133	0.156	0.179
0.03	0.173	0.170	0.168	0.166
0.05	0.271	0.256	0.240	0.225
2-Ethoxyethanol				
0.01	0.119	0.134	0.150	0.165
0.03	0.232	0.209	0.185	0.163
0.05	0.219	0.204	0.189	0.174

FTIR Spectroscopic Study

The ATR technique was used to record the spectra of the binary mixture (inositol and water) at three concentrations in the wavelength range $400\text{--}4000 \text{ cm}^{-1}$. It is essential because it makes it easier to understand how strong the molecular interactions are and whether hydrogen bonds are present in the mixture. The FTIR spectra for three concentrations are given in **Figure 4.9**. At various analyte concentrations, FTIR spectroscopy can determine the type of interaction that is taking place during the IR measurements. Even NMR spectroscopy cannot easily obtain information at this level. A sugar alcohol's infrared spectrum contains a prosperity of data. When a band associated with H-bond associations weakens or disappears, it suggests that the contact is intramolecular. Conversely, if the intensity of the band increases, it indicates that the interaction is intermolecular [46,47]. There is an intermolecular hydrogen bond between water and inositol in the present mixes. In **Figure 4.9** the spectra for inositol

between 4000-400 cm^{-1} obtained with water are shown. In the presence of water, a strong bond at 3259, 3288, and 3303 appeared. It also shows intermolecular bonding and O-H stretching. Additionally, two weaker bands on the low frequency occurred at 1610, 1625, 1640, and 560, 570, and 585 for inositol, respectively. It shows absorption due to -OH groups. and strength is increasing due to CH groups [48]. The FT-IR results thus provide strong support for the insights gained from physicochemical data on the ion-dipole and hydrogen bonds. **Figure 4.9** indicates the presence of an intermolecular H-bond in a binary mixture.

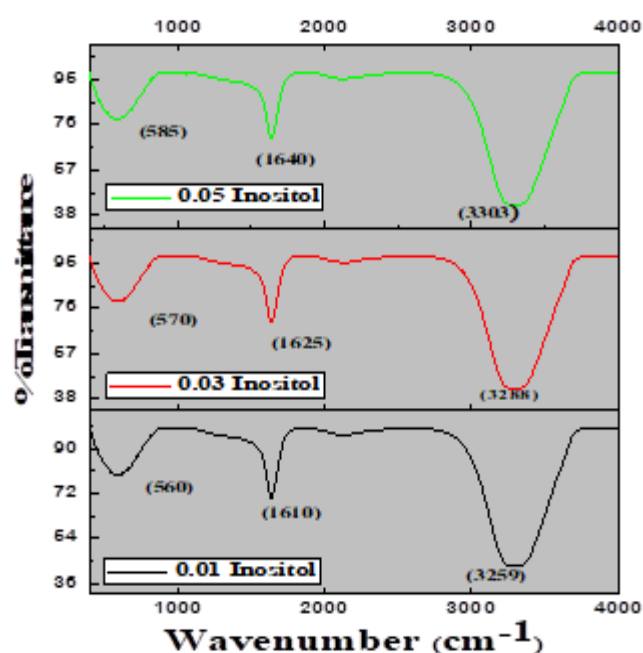


Figure 4.9 FTIR spectra for a binary mixture (Inositol + water).(black: 0.01, red: 0.03, and green: 0.05 $\text{mol} \cdot \text{kg}^{-1}$ inositol).

References

1. K. Klimaszewski, E. Stronka-Lewkowska, K. Abramczyk and A. Bald, *J. Chem. Thermodyn.* 89, 212–222 (2015).
2. A. Thakur, K.C. Juglan, H. Kumar and K. Kaur, *J. Mol. Liq.* 288, 111014 (2019).
3. C.M. Romero, M.S. Páez and M.J. Puchana, *J. Mol. Liq.* 223, 1192–1196 (2016).
4. M.B. Blodgett, S.P. Ziemer, B.R. Brown, T.L. Niederhauser and E.M. Woolley, *J. Chem. Thermodyn.* 39, 627–644 (2007).
5. J. Zhang, T. Fu, C. Zhu and Y. Ma, *J. Mol. Liq.* 242, 190–203 (2017).
6. Q. Zhao, Z.J. Sun, Q. Zhang, S.K. Xing, M. Liu, D.Z. Sun and L.W. Li, *Thermochim. Acta* 487, 1–7 (2009).
7. S.P. Jengathe, S.S. Dhondge, L.J. Paliwal, V.M. Tangde and S. Mondal, *J. Chem. Thermodyn.* 87, 78–87 (2015).
8. P. Rajput, T. Sharma, T. Sharma and A. Kumar, *J. Mol. Liq.* 326, 115210 (2021).
9. A. Pal, H. Kumar, B. Kumar, P. Sharma and K. Kaur, *J. Chem. Thermodyn.* 57, 182–188 (2013).
10. S.S. Dhondge, C.P. Pandhurnekar and D.V. Parwate, *J. Chem. Thermodyn.* 41, 577–585 (2009).
11. C.P. Pandhurnekar, D.V. Parwate and S.S. Dhondge, *J. Mol. Liq.* 183, 94–101 (2013).
12. M. Page, J.Y. Huot and C.A. Jolicœur, *J. Chem. Thermodyn.* 25, 139–154 (1993).
13. P. Kaur, N. Chakraborty, H. Kumar, M. Singla and K.C. Juglan, *J. Sol. Chem.* 51, 1268–1291 (2022).
14. Ankita, D. Chand and A.K. Nain, *J. Chem. Thermodyn.* 146, 106106 (2020).
15. X. Wang, R. Fu, Y. Guo, and R. Lin, *J. Mol. Liq.* 197, 73–76 (2014).
16. N. Chakraborty, K. Kaur, K.C. Juglan and H. Kumar, *J. Chem. Eng. Data* 65, 1435–1446 (2020).
17. N. Chakraborty, K.C. Juglan and H. Kumar, *J. Chem. Thermodyn.* 163, 106584 (2021).
18. H. Kaur, N. Chakraborty, K.C. Juglan and H. Kumar, *J. Sol. Chem.* 50, 1079–1102 (2021).
19. C. Jolicœur and G. Lacroix, *Can. J. Chem.* 54, 624–631 (1976).

20. N. Chakraborty, K.C. Juglan and H. Kumar, *J. Chem. Thermodyn.* 154, 106326 (2021).
21. A. Pal and Y. P. Singh, *J. Chem. Eng. Data* 41, 425–427 (1996).
22. K.B. Belibagli and E. Ayrançi, *J. Sol. Chem.* 19, 867–882 (1990).
23. P. Kaur, N. Chakraborty, K.C. Juglan and H. Kumar, *J. Mol. Liq.* 315, 113763 (2020).
24. N. Chakraborty, K.C. Juglan and H. Kumar, *J. Mol. Liq.* 337, 116605 (2021).
25. M.J. Iqbal and M.A. Chaudhry, *J. Chem. Thermodyn.* 42, 951-956 (2010).
26. A.K. Mishra and J.C. Ahluwalia, *J. Phys. Chem.* 88, 86-92 (1984).
27. T. Sharma, R. Rani, A. Kumar and R.K. Bamezai, *J. Mol. Liq.* 300, 111985 (2020).
28. R. Rani, A. Kumar and R.K. Bamezai, *J. Mol. Liq.* 224, 1142-1153 (2016).
29. L.G. Hepler, *Canadi. J. Chem.* 47, 4613-4617 (1969).
30. B. Sinha, A. Sarkar, P.K. Roy and D. Brahman, *Inter. J. Thermophys.* 32, 2062-2078 (2011).
31. M.N. Roy, V.K. Dakua and B. Sinha, *Inter. J. Thermophys.* 28, 1275-1284 (2007).
32. K.C. Juglan and H. Kumar, *J. Chem. Thermodyn.* 140, 105916 (2020).
33. H. Kumar, M. Singla and R. Jindal, *Monatshe. Für Chemie-Chem. Mont.* 145, 1063-1082 (2014).
34. H.S. Frank and M.W. Evans, *J. Chem. Phys.* 13, 507–532 (1945).
35. H. Kumar, K. Kaur, S. Arti and M. Singla, *J. Mol. Liq.* 221, 526–534 (2016).
36. N. Chakraborty, H. Kumar, K. Kaur, and K.C. Juglan, *J. Chem. Thermodyn.* 126, 137– 146 (2018).
37. K. Kaur, K.C. Juglan and H. Kumar, *J. Mol. Liq.* 268, 700–706 (2018).
38. J.G. Kirkwood, *Chem. Rev.* 24, 233–251 (1939).
39. P. Ramasami and R. Kakkar, *J. Chem. Thermodyn.* 38, 1385–1395 (2006).
40. U. Gazal, *Ameri. J. Analy. Chem.* 14, 72-94 (2023).
41. C.V. Krishnan and H.L. Friedman, *J. Sol. Chem.* 2, 37-51 (1973).
42. W.G. McMillan Jr and J.E. Mayer, *J. Chem. Phys.* 13, 276-305 (1945).
43. A. Pal, H. Kumar, R. Maan and H.K. Sharma, *J. Sol. Chem.* 42, 1988-2011 (2013).
44. R. Gaba, A. Pal, D. Sharma and D.A. Khajuria, *J. Mol. Liq.* 234, 187–193 (2017).
45. Q.M. Omar, J.N. Jaubert and J.A. Awan, *Int. J. Chem. Eng.* 1–10 (2018).
46. P.K. Pandey, A. Awasthi and A. Awasthi, *Chem. Phys.* 423, 119–126 (2013).

47. H. Kumar and R. Sharma, J. Mol. Liq. 304, 112666 (2020).

48. IR Spectrum Table.

<https://www.sigmaaldrich.com/IN/en/technical-documents/technical-article/analytical-chemistry/photometry-and-reflectometry/irspectrum-table>

accessed on 23/08/ 2023

Section II

Problem 2

Thermodynamic and physicochemical characteristics of 2-Butoxyethanol/ 2-Phenoxyethanol in aqueous Maltitol solutions

In this problem, densities and speed of sound values, of 2-BE or 2-PhE in (0.01, 0.02, and 0.03 mol. kg⁻¹) maltitol (aq) mixtures, were obtained at T= (288.15-308.15) K.

Density

The solution densities of 2-butoxyethanol (2-BE) and 2-phenoxyethanol (2-PhE) were experimentally determined for aqueous solutions containing maltitol. To validate the accuracy of the experimental results, the obtained densities of the aqueous maltitol solutions were compared with existing literature data [1]. The similarity between the experimental and literature densities is visually presented in **Figure 4.10**. The graphical representation indicates a notable agreement values, thus affirming the reliability of the experimental data. The values of densities decline with a rise in temperature; it typically indicates that the volume of the substance has increased due to thermal expansion. As temperature increases, the particles in the substance gain kinetic energy and move more rapidly, which causes them to take up more space and spread out, resulting in a decrease in density. This relationship between temperature and density is typically observed in most materials, including liquids and gases [2-4]. The experimental measurements of density (ρ) for 2-butoxyethanol (2-BE) and 2-phenoxyethanol (2-PhE) within aqueous maltitol solutions have been employed to assess their volumetric characteristics. The experimental values for density are given in **Table 4.13**. To assess the impact of maltitol concentration on solution density, it is important to consider the role of maltitol's molecular structure in comparison to organic compounds. These hydroxyl groups contribute to its ability to form H-bonds with water molecules. Such interactions can result in an increase in the effective volume of the solution, leading to a higher density. The rise in density with increasing concentration seen in our study is likely due to the stronger formation of H-bonds between maltitol and water as its concentration increases. In comparison, 2-butoxyethanol and 2-phenoxyethanol, which have distinct molecular structures with fewer hydroxyl groups and different functional groups, exhibit a less significant density increases with concentration [5,6].

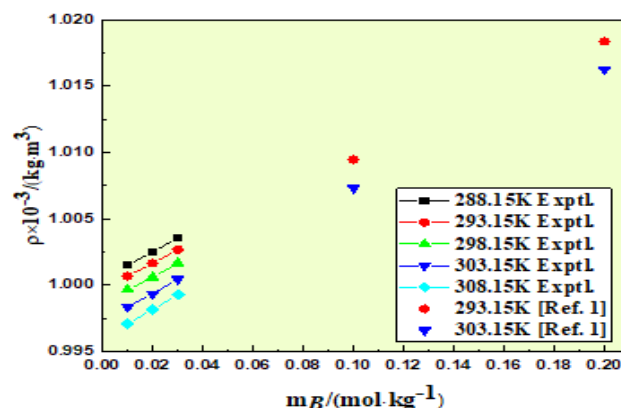


Figure 4.10 The density of a binary mixture (Maltitol + water) was plotted at various temperatures using both experimental and literature values [1].

Apparent molar volumes

The apparent molar volume provides a quantitative measure of the volume change that occurs when one mole of a solute is added to a solution. It is specifically defined as the difference between the molar volume of the solution and the sum of the molar volumes of the individual components present in the solution [7,8]. In **Table 4.13**, recorded densities values and V_ϕ are provided for solutions of 2-butoxyethanol (2-BE) and 2-phenoxyethanol (2-PhE) at various molalities in maltitol solutions. **Table 4.13** also includes the corresponding density values for each set of measurements and **Table 4.14** indicates the values of V_ϕ for maltitol (aq) solutions of different concentrations. The V_ϕ were calculated by **4.1** equation. The determination of apparent molar volume can provide valuable insights into the interactions between the solute and solvent within a mixture [9]. The findings indicate that the V_ϕ values are positive. Furthermore, with increasing temperature and concentration of maltitol, the apparent molar volume consistently rises across all three concentrations. This trend is visually represented in **Figure. 4.11**, which suggests that solute molecules are more closely packed in the solution than in the pure state, indicating favourable solute-solvent interactions. These associations lead to reduce electrostriction of water molecules into the majority of the solution, increasing the V_ϕ values [10]. The observed difference in V_ϕ values between 2-phenoxyethanol (2-PhE) and 2-butoxyethanol (2-BE) can be explained by considering their respective molecular structures and the various parameters that influence molecular interactions in solutions. 2-phenoxyethanol contains a phenyl ring

(aromatic ring) in its structure, which introduces additional π -electron delocalization and electron-rich regions compared to the linear alkyl chain of 2-Butoxyethanol. The presence of the aromatic ring in 2-PhE enhances its ability to engage in π - π interactions with other aromatic compounds in the solution, including the phenyl ring of other 2-PhE molecules and potentially aromatic components in maltitol. These π - π interactions can lead to stronger solute-solvent interactions and, consequently, a higher apparent molar volume. The aromatic ring in 2-PhE may allow for more diverse and stronger hydrogen bonding interactions due to its unique electron distribution. This increased hydrogen bonding capacity can contribute to greater solute-solvent interactions. Van der Waals forces, including London dispersion forces, can also affect solute-solvent interactions [11]. The aromatic ring in 2-PhE can induce stronger van der Waals interactions compared to the linear alkyl chain in 2-BE. **Figure 4.12** illustrates the major findings. The associations among the solute- solvent are primarily responsible for the increase in volume as the concentration rises.

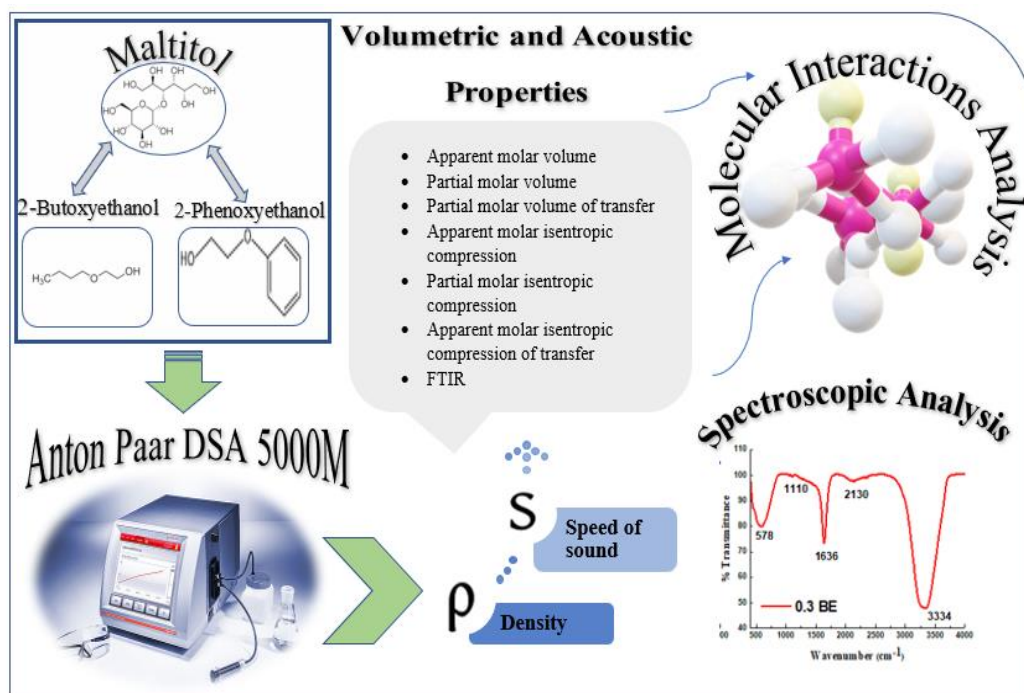


Figure 4.12 2-BE/ 2-PhE and Maltitol interactions

Table 4.13 Densities (ρ) values and apparent molar volumes (V_ϕ) values were measured for solutions of 2-BE/2-PhE in maltitol aqueous solutions at pressure, $p = 0.1$ MPa

$^a m_A / (mol \cdot kg^{-1})$	$\rho \times 10^{-3} / (kg \cdot m^{-3})$					$V_\phi \times 10^6 / (m^3 \cdot mol^{-1})$				
	288.15 K	293.15 K	298.15 K	303.15 K	308.15 K	288.15 K	293.15 K	298.15 K	303.15 K	308.15 K
2-Butoxyethanol + 0.00 $mol \cdot kg^{-1}$ Maltitol										
0.00000	0.99996	0.99871	0.99725	0.99586	0.99415					
0.10016	0.99755	0.99555	0.99302	0.99112	0.98912	116.14	116.27	116.43	116.53	116.64
0.20147	0.99386	0.99115	0.98885	0.98598	0.98315	116.21	116.34	116.50	116.61	116.71
0.29196	0.98982	0.98755	0.98475	0.98175	0.97851	116.27	116.40	116.56	116.67	116.78
0.39510	0.98498	0.98196	0.97917	0.97596	0.97356	116.35	116.48	116.64	116.76	116.87
0.49928	0.98012	0.97754	0.97414	0.97054	0.96854	116.45	116.58	116.75	116.87	116.98
2-Butoxyethanol + 0.01 $mol \cdot kg^{-1}$ Maltitol										
0.00000	1.00152	1.00069	0.99965	0.99835	0.99709					
0.09936	1.00169	1.00086	0.99982	0.99852	0.99726	116.24	116.37	116.53	116.63	116.74
0.19784	1.00185	1.00101	0.99996	0.99867	0.99742	116.31	116.44	116.61	116.71	116.81
0.29997	1.00199	1.00115	1.00010	0.99881	0.99756	116.37	116.51	116.66	116.77	116.88
0.39999	1.00211	1.00127	1.00022	0.99893	0.99768	116.45	116.58	116.74	116.86	116.97
0.49999	1.00221	1.00136	1.00030	0.99901	0.99777	116.55	116.68	116.85	116.97	117.08
2-Butoxyethanol + 0.02 $mol \cdot kg^{-1}$ Maltitol										

0.00000	1.00250	1.00166	1.00058	0.99935	0.99818					
0.09649	1.00265	1.00184	1.00072	0.99950	0.99833	116.34	116.47	116.63	116.73	116.84
0.19649	1.00278	1.00202	1.00085	0.99963	0.99846	116.41	116.54	116.71	116.81	116.91
0.29964	1.00291	1.00219	1.00097	0.99975	0.99859	116.48	116.62	116.78	116.89	116.99
0.39620	1.00300	1.00233	1.00106	0.99984	0.99868	116.56	116.69	116.85	116.96	117.07
0.49690	1.00308	1.00247	1.00113	0.99991	0.99875	116.65	116.78	116.95	117.07	117.18

2-Butoxyethanol + 0.03 $\text{mol} \cdot \text{kg}^{-1}$ Maltitol

0.00000	1.00358	1.00268	1.00166	1.00045	0.99929					
0.09833	1.00371	1.00285	1.00178	1.00058	0.99942	116.44	116.57	116.73	116.83	116.94
0.19730	1.00382	1.00301	1.00189	1.00068	0.99953	116.51	116.64	116.81	116.91	117.01
0.29999	1.00392	1.00316	1.00198	1.00078	0.99963	116.58	116.72	116.89	116.99	117.09
0.39556	1.00400	1.00329	1.00205	1.00085	0.99970	116.66	116.79	116.95	117.06	117.17
0.50009	1.00406	1.00342	1.00210	1.00090	0.99975	116.75	116.88	117.05	117.17	117.28

2-Phenoxyethanol + 0.00 $\text{mol} \cdot \text{kg}^{-1}$ Maltitol

0.00000	0.99996	0.99871	0.99725	0.99586	0.99415					
0.09102	0.99969	0.99865	0.99748	0.99610	0.99455	133.48	133.57	133.69	133.79	133.87
0.20047	1.00017	0.99913	0.99798	0.99660	0.99507	133.59	133.68	133.78	133.88	133.97
0.29106	1.00055	0.99951	0.99836	0.99699	0.99546	133.66	133.76	133.86	133.97	134.06
0.39951	1.00097	0.99994	0.99879	0.99742	0.99591	133.75	133.86	133.96	134.07	134.17
0.49928	1.00132	1.00028	0.99914	0.99778	0.99628	133.86	133.97	134.07	134.19	134.28

2-Phenoxyethanol + 0.01 mol · kg ⁻¹ Maltitol										
0.00000	1.00152	1.00069	0.99965	0.99835	0.99709					
0.10160	1.00195	1.00113	1.00009	0.99880	0.99755	133.66	133.73	133.79	133.85	133.91
0.20047	1.00235	1.00153	1.00050	0.99922	0.99799	133.70	133.77	133.84	133.90	133.96
0.30106	1.00275	1.00193	1.00090	0.99963	0.99841	133.74	133.81	133.88	133.95	134.00
0.39111	1.00308	1.00226	1.00125	0.99999	0.99877	133.78	133.85	133.92	133.98	134.03
0.50061	1.00346	1.00265	1.00164	1.00039	0.99919	133.83	133.90	133.97	134.03	134.08
2-Phenoxyethanol + 0.02 mol · kg ⁻¹ Maltitol										
0.00000	1.00290	1.00207	1.00099	0.99977	0.99861					
0.09965	1.00328	1.00245	1.00139	1.00018	0.99902	133.76	133.83	133.89	133.95	134.01
0.19973	1.00367	1.00285	1.00179	1.00059	0.99944	133.82	133.88	133.95	134.01	134.07
0.30870	1.00398	1.00316	1.00211	1.00092	0.99978	133.89	133.95	134.00	134.07	134.14
0.40020	1.00430	1.00348	1.00244	1.00125	1.00012	133.94	134.01	134.06	134.13	134.20
0.49992	1.00290	1.00207	1.00099	0.99977	0.99861	134.01	134.07	134.13	134.20	134.27
2-Phenoxyethanol + 0.03 mol · kg ⁻¹ Maltitol										
0.00000	1.00396	1.00307	1.00206	1.00086	0.99971					
0.10110	1.00432	1.00343	1.00243	1.00124	1.00010	133.86	133.91	133.96	134.03	134.08
0.20067	1.00466	1.00378	1.00278	1.00160	1.00047	133.92	133.98	134.03	134.09	134.14
0.30178	1.00498	1.00411	1.00312	1.00195	1.00083	133.99	134.04	134.10	134.15	134.20

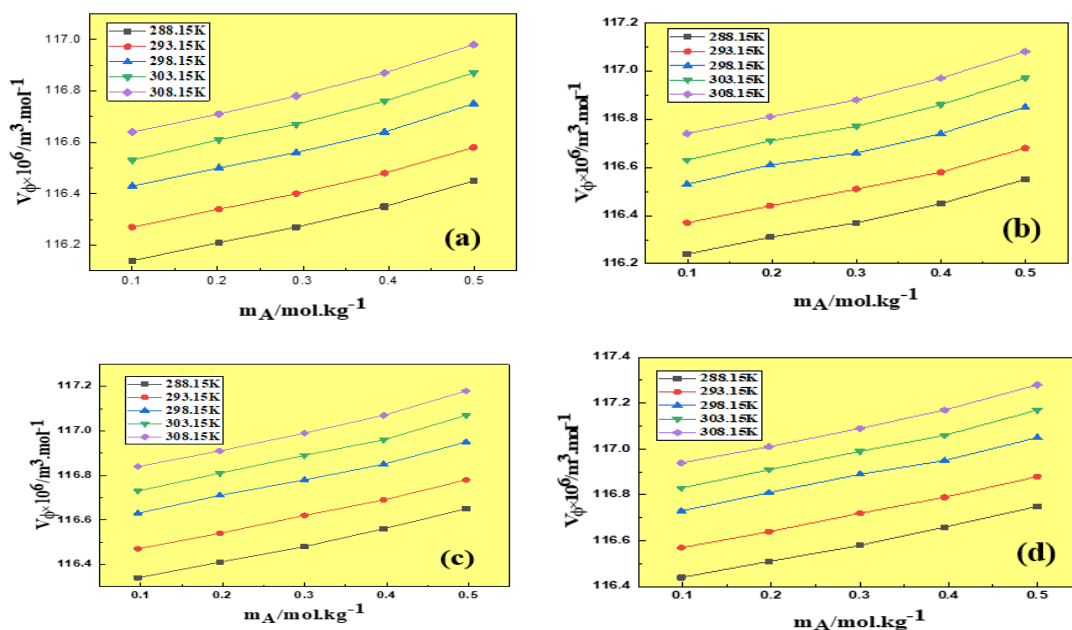
0.40480	1.00527	1.00440	1.00342	1.00225	1.00114	134.05	134.11	134.16	134.21	134.26
0.50173	1.00396	1.00307	1.00206	1.00086	0.99971	134.11	134.17	134.22	134.27	134.32

Table 4.14 Values of V_ϕ for aqueous maltitol solutions of different concentrations.

$^a m_B / (\text{mol} \cdot \text{kg}^{-1})$	$V_\phi \times 10^6 / (\text{m}^3 \cdot \text{mol}^{-1})$				
	288.15 K	293.15 K	298.15 K	303.15 K	308.15 K
0.01	188.1178	146.0535	103.5837	94.32948	49.22578
0.02	216.8628	196.3935	177.348	169.093	141.9827
0.03	222.9404	211.3393	196.6446	190.6881	172.1907

$^a m_B$ is the molality of aqueous Maltitol.

(I)



(II)

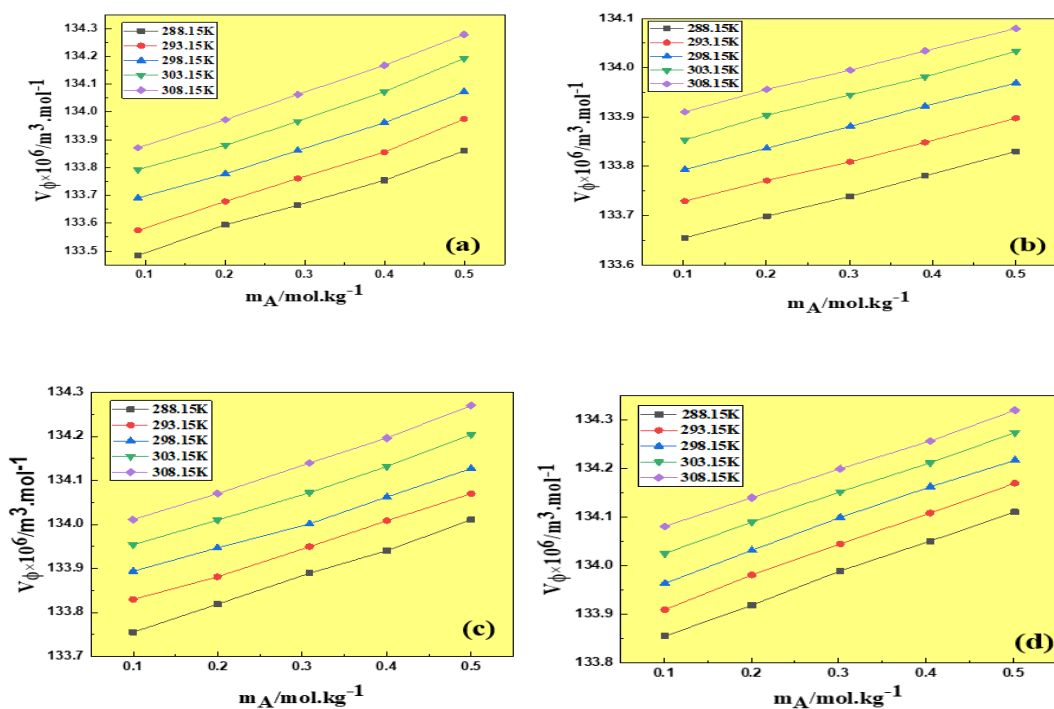


Figure 4.11 Plots depicting the changes in apparent molar volumes of (I) 2-BE and (II)-PhE when transitioning from water to an aqueous Maltitol solution at varying temperatures, specifically for (a) 0.00 Maltitol, (b) 0.01 Maltitol, (c) 0.02 Maltitol, and (d) 0.03 Maltitol ($\text{mol} \cdot \text{kg}^{-1}$).

Partial molar volume

The concept of V_{ϕ}^0 pertains to alterations in the volume of a solution that occur when a small quantity of solute is introduced or extracted, all under the condition of constant temperature and pressure [12]. It represents the change in volume per mole of solute added or removed from the solution, and is denoted by the symbol V_{ϕ}^0 and it is calculated by the equation 4.2. The partial molar volume is a valuable parameter for understanding the behaviour of solutions and their components. **Table 4.15** presents data on the V_{ϕ}^0 and the experimental slope (S_V^*) for different temperatures and maltitol concentrations with standard errors. The values of (V_{ϕ}^0) and (S_V^*) are determined using the method of least squares fitting. It is noteworthy that all the (V_{ϕ}^0) values are demonstrate an increasing trend with both the concentration of maltitol and the temperatures. This relationship is visually depicted in **Figure 4.13**. **Table 4.15** depicts that the values of partial molar volume are all positive. It means that the addition of more solute to the solution will cause an increase in volume. By understanding the partial molar volume, it can be better predicted how solutions will behave under different conditions and how to design processes that take these behaviours into account. Moreover, the experimental slope values (S_V^*) provide insights into the solute-2 associations between mixture and are also referred to as semiempirical solute-2 associations parameters. These values do not exhibit a consistent pattern concerning the experimental temperatures and solvent concentrations [13-15]. However, it is important to note that the S_V^* values are relatively small when compared to the magnitudes of V_{ϕ}^0 values. This observation implies that the associations between solute molecules in the solution are primarily governed by the influence of solute-solvent associations rather than solute-2 associations.

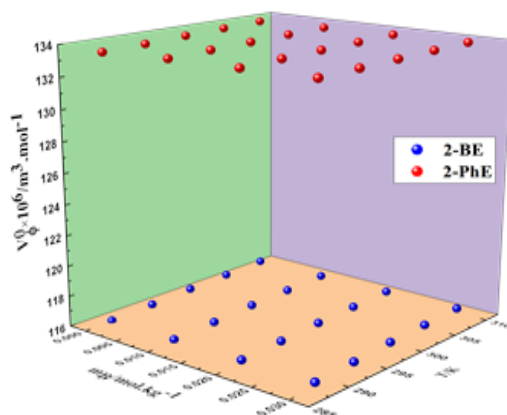


Figure 4.13 Plots illustrating the changes in partial molar volume, V_{ϕ}^0 , for 2-BE (blue) and 2-PhE (red) within an Maltitol aqueous solution at various temperatures.

Partial molar volume of Transfer

It is also known as the excess molar volume, and it is thermodynamic property that describes the variation in volume when a solute molecule is transferred from one phase to another [16]. Mathematically, it can be expressed as equation 4.3. **Table 4.15** provides the computed values of ΔV_{ϕ}^0 , all of which are positive. The ΔV_{ϕ}^0 is an important property in the study of solutions as it provides insights into the associations among molecules of solute-solvent. This information is valuable in the design and optimisation of chemical processes, such as pharmaceutical production or natural gas purification. In the context of the present study involving the combination of [maltitol + water + 2-butoxyethanol (2-BE)/2-phenoxyethanol (2-PhE)], it's significant to know that the solute and solvent are non-electrolytes. Therefore, there are no ion-ion or ion-hydrophilic associations in the system. The values of ΔV_{ϕ}^0 can be attributed to the formation of a structured composition resulting from solvophobic solvation and structural interactions between the two components. The observed positive ΔV_{ϕ}^0 values play a significant role in characterising various associations within the mixes. As per co-sphere overlap model, ΔV_{ϕ}^0 positive's values are associated with hydrophilic-2 associations. Conversely, negative effects on the ΔV_{ϕ}^0 can be attributed to hydrophobic-hydrophobic interactions [17,18].

Table 4.15 Values of V_ϕ^0 , experimental slopes, S_V^* , with standard deviations of linear regression and partial molar volume of transfer, ΔV_ϕ^0 of 2-BE/ 2-PhE in water and Maltitol (aq) solutions.

Parameters	T/K				
	288.15	293.15	298.15	303.15	308.15
2-Butoxyethanol in water					
$V_\phi^0 \times 10^6 (m^3 \cdot mol^{-1})$	116.06 (± 0.011)	116.19 (± 0.012)	116.34 (± 0.015)	116.44 (± 0.011)	116.55 (± 0.013)
$S_V^* \times 10^6 (m^3 \cdot kg \cdot mol^{-2})$	0.75 (± 0.032)	0.76 (± 0.038)	0.80 (± 0.047)	0.84 (± 0.032)	0.84 (± 0.041)
2-Butoxyethanol + 0.01 $mol \cdot kg^{-1}$ Maltitol					
$V_\phi^0 \times 10^6 (m^3 \cdot mol^{-1})$	116.16 (± 0.014)	116.29 (± 0.012)	116.45 (± 0.019)	116.54 (± 0.017)	116.65 (± 0.017)
$S_V^* \times 10^6 (m^3 \cdot kg \cdot mol^{-2})$	0.76 (± 0.044)	0.76 (± 0.035)	0.77 (± 0.058)	0.83 (± 0.052)	0.84 (± 0.050)
$\Delta V_\phi^0 \times 10^6 (m^3 \cdot mol^{-1})$	0.096	0.102	0.112	0.104	0.097
2-Butoxyethanol + 0.02 $mol \cdot kg^{-1}$ Maltitol					
$V_\phi^0 \times 10^6 (m^3 \cdot mol^{-1})$	116.26 (± 0.009)	116.39 (± 0.006)	116.65 (± 0.012)	116.55 (± 0.010)	116.75 (± 0.014)
$S_V^* \times 10^6 (m^3 \cdot kg \cdot mol^{-2})$	0.77 (± 0.027)	0.77 (± 0.019)	0.83 (± 0.036)	0.78 (± 0.031)	0.84 (± 0.043)
$\Delta V_\phi^0 \times 10^6 (m^3 \cdot mol^{-1})$	0.199	0.204	0.216	0.209	0.200
2-Butoxyethanol + 0.03 $mol \cdot kg^{-1}$ Maltitol					
$V_\phi^0 \times 10^6 (m^3 \cdot mol^{-1})$	116.36 (± 0.003)	116.49 (± 0.001)	116.65 (± 0.001)	116.74 (± 0.002)	116.85 (± 0.000)
$S_V^* \times 10^6 (m^3 \cdot kg \cdot mol^{-2})$	0.77 (± 0.008)	0.77 (± 0.005)	0.78 (± 0.003)	0.83 (± 0.007)	0.84 (± 0.001)

$\Delta V_{\phi}^0 \times 10^6 (m^3 \cdot mol^{-1})$	0.298	0.303	0.317	0.308	0.299
2-Phenoxyethanol in water					
$V_{\phi}^0 \times 10^6 (m^3 \cdot mol^{-1})$	133.40 (± 0.009)	133.48 (± 0.010)	133.60 (± 0.011)	133.69 (± 0.014)	133.78 (± 0.006)
$S_V^* \times 10^6 (m^3 \cdot kg \cdot mol^{-2})$	0.90 (± 0.028)	0.96 (± 0.030)	0.93 (± 0.033)	0.98 (± 0.042)	0.99 (± 0.019)
2-Phenoxyethanol + 0.01 $mol \cdot kg^{-1}$ Maltitol					
$V_{\phi}^0 \times 10^6 (m^3 \cdot mol^{-1})$	133.61 (± 0.002)	133.69 (± 0.002)	133.75 (± 0.001)	133.81 (± 0.003)	133.87 (± 0.002)
$S_V^* \times 10^6 (m^3 \cdot kg \cdot mol^{-2})$	0.44 (± 0.006)	0.42 (± 0.007)	0.44 (± 0.002)	0.44 (± 0.010)	0.42 (± 0.006)
$\Delta V_{\phi}^0 \times 10^6 (m^3 \cdot mol^{-1})$	0.21	0.20	0.15	0.12	0.09
2-Phenoxyethanol + 0.02 $mol \cdot kg^{-1}$ Maltitol					
$V_{\phi}^0 \times 10^6 (m^3 \cdot mol^{-1})$	133.69 (± 0.003)	133.76 (± 0.004)	133.83 (± 0.007)	133.89 (± 0.007)	133.94 (± 0.005)
$S_V^* \times 10^6 (m^3 \cdot kg \cdot mol^{-2})$	0.63 (± 0.010)	0.61 (± 0.013)	0.58 (± 0.021)	0.62 (± 0.020)	0.64 (± 0.015)
$\Delta V_{\phi}^0 \times 10^6 (m^3 \cdot mol^{-1})$	0.29	0.28	0.23	0.20	0.17
2-Phenoxyethanol + 0.03 $mol \cdot kg^{-1}$ Maltitol					
$V_{\phi}^0 \times 10^6 (m^3 \cdot mol^{-1})$	133.79 (± 0.003)	133.85 (± 0.004)	133.90 (± 0.005)	133.96 (± 0.002)	134.02 (± 0.003)
$S_V^* \times 10^6 (m^3 \cdot kg \cdot mol^{-2})$	0.64 (± 0.009)	0.64 (± 0.011)	0.63 (± 0.014)	0.62 (± 0.007)	0.59 (± 0.008)
$\Delta V_{\phi}^0 \times 10^6 (m^3 \cdot mol^{-1})$	0.39	0.36	0.31	0.27	0.25

The outcomes of the current investigation suggest that the existence of robust interactions, notably hydrophilic-hydrophilic interactions, augments the solute's capacity to enhance the structural integrity of the solution. The positive transfer volume observed in the study can be rationalized by considering the partial molar volume as the summation of the inherent volume of the solutes and the volume alteration resulting from the associations among the solute- solvent, a concept consistent with previous research [19].

Temperature-dependent partial molar volume

It can be described by the expression **4.4**. In equation, T represents the temperature, T_{ref} denotes the reference temperature. The specific values of empirical constants for glycol ethers in an aqueous solution of maltitol can be found in **Table 4.16**. The primary objective of studying V_{ϕ}^0 is to determine molar expansibility [20]. The limiting apparent molar expansibility, can be calculated using the relationship **4.5**. The values of E_{ϕ}^0 are all positive and can be found in **Table 4.17**. The phenomenon known as the packing or caging effect contributes to the positive values observed for E_{ϕ}^0 [21,22]. This phenomenon indicates that the hydration spheres surrounding the solute molecules expand in volume as the solvent system (maltitol + water) undergoes changes. This expansion is primarily attributed to the increased hydrophilic-hydrophilic associations among the solute (glycol ethers) and maltitol molecules. The application of Helper's thermodynamic relation is a valuable tool for determining the structure-making or structure-breaking characteristics of a solute in a mixed solvent system [23]. This is calculated by using the equation **4.6**. The sign of the Helpers constant is highly informative for determining whether a solute exhibits a structure-making or structure-breaking characteristic. The calculated $(\partial E_{\phi}^0 / \partial T)_p$ values presented in **Table 4.17**, along with the corresponding E_{ϕ}^0 values, can provide great insights. A positive value suggests that the solute has a structure-forming characteristic, whereas a negative value indicates a structure-disrupting behavior. In these mixes, below zero values of the Helpers constant were obtained for 2-butoxyethanol (2-BE) and 2-phenoxyethanol (2-PhE) in an aqueous medium, except at a concentration of $0.03 \text{ mol} \cdot \text{kg}^{-1}$. This indicates the structure-breaking behaviour of these solutes in water.

Table 4.16 Empirical parameters of Eq. 4.4, for 2-BE and 2-PhE in Maltitol (aq) solutions at different temperatures along with R^2 and ARD (deviations)

$^a m_B / (\text{mol} \cdot \text{kg}^{-1})$	$a \times 10^6 (\text{m}^3 \cdot \text{mol}^{-1})$	$b \times 10^6 (\text{m}^3 \cdot \text{mol}^{-1} \cdot \text{K}^{-1})$	$c \times 10^6 (\text{m}^3 \cdot \text{mol}^{-1} \cdot \text{K}^{-2})$	R^2	ARD
2-Butoxyethanol					
0.01	116.4334	0.0245	-0.0003	0.9999	0.00009
0.02	116.5374	0.0247	-0.0004	0.9999	0.00009
0.03	116.6376	0.0246	-0.0004	0.9999	0.00009
2-Phenoxyethanol					
0.01	133.7502	0.0129	-0.0001	0.9999	0.00044
0.02	133.8298	0.0125	-0.0001	0.9999	0.00001
0.03	133.9050	0.0115	0.0000	0.9999	0.00002

Table 4.17 Values of E_{ϕ}^0 , for 2-BE and 2-PhE in Maltitol (aq) solutions at different temperatures.

$^a m_B$ (mol · kg ⁻¹)	$E_{\phi}^0 \times 10^6 (m^3 \cdot mol^{-1} \cdot K^{-1})$					$(\partial E_{\phi}^0 / \partial T)_p / ($ $m^3 \cdot mol^{-1} \cdot K^{-2})$
	T =	T =	T =	T =	T =	
	288.15	293.15	298.15	303.15	308.15	
	K	K	K	K	K	
2-Butoxyethanol						
0.01	0.0315	0.0280	0.0245	0.0211	0.0176	-0.00069
0.02	0.0318	0.0282	0.0247	0.0211	0.0175	-0.00072
0.03	0.0321	0.0283	0.0246	0.0209	0.0172	0.06410
2-Phenoxyethanol						
0.01	0.0149	0.0139	0.0129	0.0118	0.0108	-0.0002
0.02	0.0149	0.0137	0.0125	0.0113	0.0101	-0.0002
0.03	0.0111	0.0113	0.0115	0.0117	0.0118	0.0000

Isobaric thermal expansion coefficients

It symbolised as α_p , it characterises how the volume of a material changes in response to temperature variations while keeping pressure constant. It measures the proportionate change in volume per unit change in temperature under constant pressure conditions [24]. The isobaric thermal expansion coefficient is calculated by equation **4.13**. The formula presented includes the variable α_p , which represents the isobaric thermal expansion coefficient, while T denotes the temperature. The coefficient of thermal expansion plays a crucial role in understanding solute-solvent interactions [25]. **Table 4.18** lists the documented values of the coefficients of thermal expansion for different temperatures. It is observed that the α_p values for 2-butoxyethanol (2-BE) and 2-phenoxyethanol (2-PhE) decrease as the temperature increases, suggesting strong interactions between the (2-BE/2-PhE + maltitol) system at different temperatures. The α_p value indicates an expansion in volume and a lessening compression of maltitol (aq) mixes upon the addition of glycol ethers.

Table 4.18 Isothermal expansion coefficients for 2-BE and 2-PhE in Maltitol (aq) solutions at different temperatures.

$^a m_B / (\text{mol} \cdot \text{kg}^{-1})$	$\alpha_p \times 10^3 / (K^{-1})$				
¹⁾	T=288.15K	T=293.15K	T=298.15K	T=303.15K	T=308.15K
2-Butoxyethanol					
0.01	0.271	0.241	0.211	0.181	0.151
0.02	0.274	0.243	0.212	0.181	0.150
0.03	0.275	0.243	0.211	0.179	0.148
2-Phenoxyethanol					
0.01	0.112	0.104	0.096	0.088	0.081
0.02	0.112	0.102	0.093	0.084	0.075
0.03	0.083	0.085	0.086	0.087	0.088

Speed of sound

Experimental measurements were performed to determine sound speeds (*c*) in solutions of 2-butoxyethanol (2-BE) and 2-phenoxyethanol (2-PhE) at pressure 0.1 MPa. The findings, summarised in **Table 4.19**, indicate that the speed of sound increases as temperature and maltitol concentration rise. Several factors contribute to this observed increase, including the establishment of a 3-D network of H-bonds within the water structure as well as the presence of intra- and intermolecular H-bonds involving the solute and solute-solvent molecules. These hydrogen bond interactions lead to a higher speed of sound in the mixture, indicating stronger molecular association [26,27]. It is important to note that the formation of a H-bond network among the 2-BE/2-PhE and the maltitol aqueous molecules influences the observed enhancement in ‘*c*’ with increasing molality of glycol ethers.

Apparent molar isentropic compression

The K_S , was calculated using equation 4.7. The determined value of K_S was then used to solve the equation 4.8 to determine the $K_{\phi,S}$. The calculated values of $K_{\phi,S}$ and the

Table 4.19 Values of the c , and $K_{\phi,S}$, for 2-BE and 2-PhE in aqueous Maltitol solutions at different temperatures.

$^a m_A / (mol \cdot kg^{-1})$	$c / (m \cdot s^{-1})$		$K_{\phi,S} \times 10^6 / (m^3 \cdot mol^{-1} \cdot GPa^{-1})$							
	288.15 K	293.15 K	298.15 K	303.15 K	308.15 K	288.15 K	293.15 K	298.15 K	303.15 K	308.15 K
2-Butoxyethanol + 0.00 $mol \cdot kg^{-1}$ Maltitol										
0.00000	1466.59	1482.64	1495.95	1508.84	1519.84					
0.10016	1499.99	1522.00	1539.01	1549.99	1562.44	-46.04	-45.07	-44.27	-43.52	-42.89
0.20147	1539.55	1555.92	1574.19	1586.91	1598.92	-46.29	-45.30	-44.50	-43.74	-43.11
0.29196	1568.63	1587.54	1603.21	1615.83	16310.5	-46.37	-45.38	-44.58	-43.82	-43.32
0.39510	1599.95	1618.42	1634.55	1648.14	1659.92	-46.42	-45.43	-44.62	-43.86	-43.43
0.49928	1622.86	1643.45	1659.91	1672.01	1688.04	-46.45	-45.46	-44.65	-43.89	-43.56
2-Butoxyethanol + 0.01 $mol \cdot kg^{-1}$ Maltitol										
0.00000	1470.37	1486.31	1499.67	1511.93	1523.32					
0.09936	1471.78	1487.64	1501.10	1513.13	1524.33	-45.80	-44.82	-44.02	-43.31	-42.67
0.19784	1472.92	1488.77	1502.61	1514.29	1525.52	-46.04	-45.05	-44.25	-43.54	-42.89
0.29997	1474.39	1489.98	1504.08	1515.55	1526.79	-46.12	-45.14	-44.34	-43.62	-42.97
0.39999	1475.62	1491.24	1505.59	1516.61	1527.92	-46.17	-45.18	-44.38	-43.66	-43.01
0.49999	1476.93	1492.41	1507.17	1518.02	1529.12	-46.19	-45.21	-44.40	-43.69	-43.04
2-Butoxyethanol + 0.02 $mol \cdot kg^{-1}$ Maltitol										
0.00000	1472.53	1488.79	1501.97	1514.00	1525.44					

0.09649	1473.82	1489.99	1503.53	1515.49	1526.63	-45.65	-44.66	-43.88	-43.18	-42.53
0.19649	1475.27	1491.29	1505.12	1516.81	1527.81	-45.90	-44.90	-44.12	-43.42	-42.77
0.29964	1476.79	1492.52	1506.71	1518.32	1529.22	-45.98	-44.99	-44.20	-43.50	-42.85
0.39620	1478.33	1493.71	1508.48	1519.61	1530.34	-46.03	-45.03	-44.24	-43.54	-42.89
0.49690	1479.71	1494.96	1509.98	1521.01	1531.55	-46.05	-45.06	-44.26	-43.56	-42.91
2-Butoxyethanol + 0.03 $mol \cdot kg^{-1}$ Maltitol										
0.00000	1474.42	1490.65	1503.99	1515.91	1527.22					
0.09833	1476.13	1492.11	1505.77	1517.31	1528.58	-45.54	-44.56	-43.77	-43.08	-42.44
0.19730	1477.54	1493.41	1507.56	1518.83	1529.85	-45.78	-44.79	-44.00	-43.31	-42.67
0.29999	1479.18	1494.78	1509.29	1520.24	1531.32	-45.86	-44.88	-44.08	-43.39	-42.75
0.39556	1480.64	1495.97	1510.77	1521.83	1532.49	-45.90	-44.92	-44.12	-43.42	-42.78
0.50009	1482.26	1497.31	1512.56	1523.19	1533.67	-45.93	-44.95	-44.14	-43.45	-42.81
2-Phenoxyethanol + 0.00 $mol \cdot kg^{-1}$ Maltitol										
0.00000	1466.59	1482.64	1495.95	1508.84	1519.84					
0.09102	1468.35	1484.22	1497.53	1510.52	1520.93	-46.00	-45.01	-44.21	-43.46	-42.87
0.20047	1470.33	1486.33	1499.53	1512.66	1522.97	-46.30	-45.31	-44.50	-43.75	-43.15
0.29106	1472.25	1488.23	1501.22	1514.40	1524.76	-46.39	-45.40	-44.59	-43.83	-43.24
0.39951	1474.66	1490.33	1503.36	1516.50	1526.98	-46.46	-45.46	-44.65	-43.89	-43.30
0.49928	1476.55	1492.22	1505.41	1518.59	1528.66	-46.50	-45.50	-44.69	-43.93	-43.34

2-Phenoxyethanol + 0.01 $\text{mol} \cdot \text{kg}^{-1}$ Maltitol										
0.00000	1470.37	1486.31	1499.67	1511.93	1523.32					
0.10160	1473.38	1488.89	1502.14	1514.51	1525.38	-45.82	-44.84	-44.05	-43.34	-42.69
0.20047	1476.13	1491.77	1504.72	1517.07	1527.34	-46.06	-45.08	-44.28	-43.57	-42.92
0.30106	1478.79	1494.57	1507.38	1519.21	1529.33	-46.16	-45.17	-44.37	-43.66	-43.01
0.39111	1481.24	1497.13	1509.91	1521.18	1530.94	-46.21	-45.22	-44.42	-43.71	-43.06
0.50061	1484.11	1500.07	1513.25	1524.07	1533.47	-46.25	-45.27	-44.47	-43.75	-43.10
2-Phenoxyethanol + 0.02 $\text{mol} \cdot \text{kg}^{-1}$ Maltitol										
0.00000	1472.53	1488.79	1501.97	1514.00	1525.44					
0.09965	1476.17	1492.41	1505.51	1517.14	1527.55	-45.68	-44.69	-43.90	-43.21	-42.56
0.19973	1479.29	1496.13	1509.21	1520.12	1529.94	-45.93	-44.93	-44.14	-43.45	-42.80
0.30870	1482.42	1499.92	1512.89	1523.52	1532.74	-46.03	-45.03	-44.24	-43.54	-42.89
0.40020	1485.44	1503.04	1516.20	1525.97	1534.77	-46.07	-45.07	-44.29	-43.59	-42.94
0.49992	1488.05	1505.99	1519.73	1528.74	1537.04	-46.11	-45.11	-44.32	-43.62	-42.97
2-Phenoxyethanol + 0.03 $\text{mol} \cdot \text{kg}^{-1}$ Maltitol										
0.00000	1474.42	1490.65	1503.99	1515.91	1527.22					
0.10110	1477.76	1494.98	1508.21	1519.55	1529.73	-45.57	-44.58	-43.79	-43.11	-42.47
0.20067	1481.21	1498.99	1512.73	1522.92	1532.47	-45.81	-44.82	-44.03	-43.34	-42.70
0.30178	1484.56	1502.92	1517.16	1526.15	1535.12	-45.90	-44.91	-44.12	-43.42	-42.78

0.40480	1487.69	1507.19	1521.52	1529.76	1538.11	-45.95	-44.96	-44.17	-43.48	-42.84
0.50173	1490.67	1510.88	1525.26	1532.79	1540.22	-45.99	-44.99	-44.20	-43.51	-42.87

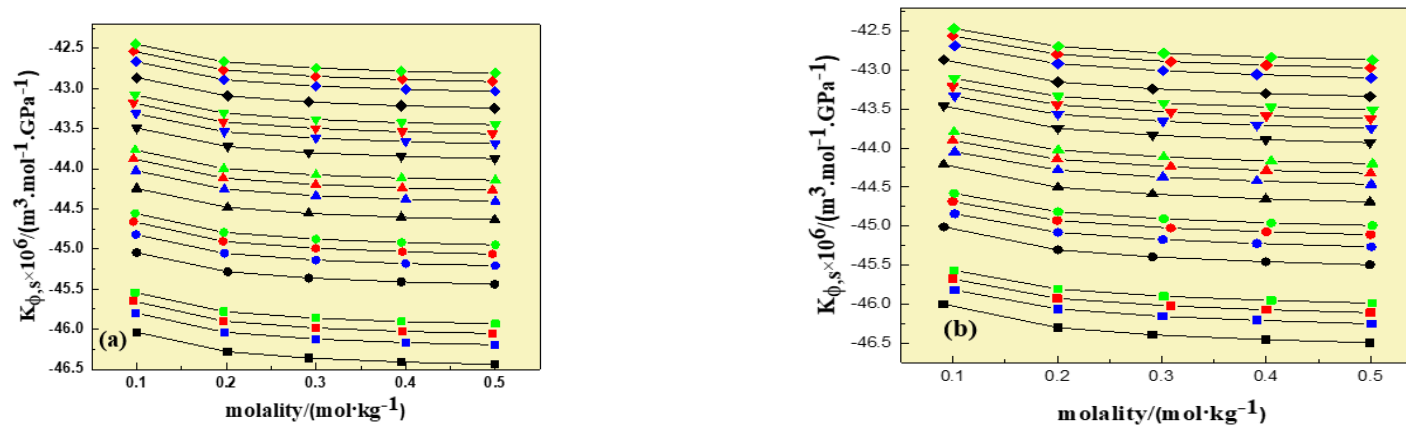


Figure 4.14 Plots illustrating the changes in $K_{\phi,s}$, of (a) 2-BE and (b) 2-PhE within an aqueous Maltitol solution, for concentrations of 0.00 Maltitol (in black), 0.01 Maltitol (in blue), 0.02 Maltitol (in red), and 0.03 Maltitol (in green), at various temperatures. (squares: 288.15K, circles: 293.15K, upward triangles: 298.15K, downward triangles: 303.15K, and diamonds: 308.15K).

ultrasonic velocity is presented in **Table 4.19**. The results are graphically illustrated in **Figure 4.14**. The experimental data indicates that the values of glycol ethers (2-BE and 2-PhE) in aqueous maltitol solution increase with temperature. The calculated $K_{\phi,s}$ data is consistently negative across all conditions. Furthermore, the negativity of $K_{\phi,s}$ becomes more pronounced as the concentration of glycol ethers increases, while it diminishes with rising temperature. The negative values of $K_{\phi,s}$ signify that molecules of water surrounding the ionic charge groups of solutes are not as much compressible than those in the bulk solution [28,29]. The structure of water around the hydrophilic cluster of maltitol and zwitter ions of glycol ethers may undergo disruption at higher temperatures, leading to a specific organization of H₂O molecules around both solutes. This phenomenon suggests that the compressibility of H₂O is expressively affected by both solutes, resulting in a greater aligning effect [30,31]. **Figure 4.14** illustrates a linear relationship between $K_{\phi,s}$ and molality.

Partial Molar Isentropic Compression

The $K_{\phi,s}^0$ data was determined by equation 4.9. The values of $K_{\phi,s}^0$ and S_K^* were obtained through the least squares fitting method and are accompanied by standard errors. The all values of $K_{\phi,s}^0$ and S_K^* are provided in **Table 4.20**. **Figure 4.15** illustrates a linear relationship between $K_{\phi,s}^0$ and molality. It is evident from the calculated S_K^* values that solute-2 associations become negligible at infinite dilution due to their very small values [4]. With increasing temperature, the negative values of $K_{\phi,s}^0$ become less pronounced, indicating strong attractive interactions between water and glycol ethers. The negative $K_{\phi,s}^0$ value that results from the negative effect or the penetration into the intra-ionic free space outweighs the positive effect (solvent intrinsic compressibility) [32]. Furthermore, the decrease in negative $K_{\phi,s}^0$ values with temperature suggests attractive associations among the ions of maltitol and H₂O molecules, resulting in the glycol ether's dehydration. Consequently, the water molecules surrounding glycol ethers exhibit lower compressibility at lower concentrations compared to higher concentrations [33]. The calculation of the ΔK_{ϕ}^0 in maltitol (aq) mixes is performed using the equation 4.10. The ΔK_{ϕ}^0 values are reported in **Table 4.20**. Importantly, all the calculated ΔK_{ϕ}^0 esteems are positive and exhibit an increasing trend with higher

Table 4.20 Values of $K_{\phi,s}^0$, experimental slopes, S_K^* , and $\Delta K_{\phi,s}^0$, for 2-BE and 2-PhE in aqueous Maltitol solutions at different temperatures.

Property	T/K				
	288.15	293.15	298.15	303.15	308.15
2-Butoxyethanol in water					
$K_{\phi,s}^0 \times 10^6 / (m^3 \cdot mol^{-1} \cdot Gpa^{-1})$	-46.03 (± 0.08)	-45.04 (± 0.08)	-44.24 (± 0.08)	-43.48 (± 0.08)	-42.85 (± 0.08)
$S_K^* \times 10^6 (kg \cdot m^3 \cdot mol^{-2} \cdot Gpa^{-1})$	-0.94 (± 0.25)	-0.92 (± 0.24)	-0.90 (± 0.24)	-0.89 (± 0.23)	-0.88 (± 0.23)
2-Butoxyethanol + 0.01 Maltitol					
$K_{\phi,s}^0 \times 10^6 / (m^3 \cdot mol^{-1} \cdot Gpa^{-1})$	-45.79 (± 0.08)	-44.81 (± 0.08)	-44.02 (± 0.08)	-43.30 (± 0.08)	-42.66 (± 0.07)
$S_K^* \times 10^6 (kg \cdot m^3 \cdot mol^{-2} \cdot Gpa^{-1})$	-0.92 (± 0.24)	-0.90 (± 0.24)	-0.88 (± 0.23)	-0.87 (± 0.23)	-0.86 (± 0.23)
$\Delta K_{\phi,s}^0 \times 10^6 (m^3 \cdot mol^{-1} \cdot Gpa^{-1})$	0.24	0.22	0.22	0.18	0.20
2-Butoxyethanol + 0.02 Maltitol					
$K_{\phi,s}^0 \times 10^6 / (m^3 \cdot mol^{-1} \cdot Gpa^{-1})$	-45.64 (± 0.08)	-44.65 (± 0.08)	-43.87 (± 0.08)	-43.18 (± 0.08)	-42.53 (± 0.08)
$S_K^* \times 10^6 (kg \cdot m^3 \cdot mol^{-2} \cdot Gpa^{-1})$	-0.94 (± 0.25)	-0.94 (± 0.25)	-0.90 (± 0.24)	-0.89 (± 0.24)	-0.88 (± 0.24)
$\Delta K_{\phi,s}^0 \times 10^6 (m^3 \cdot mol^{-1} \cdot Gpa^{-1})$	0.38	0.38	0.37	0.31	0.32
2-Butoxyethanol + 0.03 Maltitol					
$K_{\phi,s}^0 \times 10^6 / (m^3 \cdot mol^{-1} \cdot Gpa^{-1})$	-45.54 (± 0.08)	-44.55 (± 0.08)	-43.76 (± 0.08)	-43.08 (± 0.08)	-42.44 (± 0.08)
$S_K^* \times 10^6 (kg \cdot m^3 \cdot mol^{-2} \cdot Gpa^{-1})$	-0.90 (± 0.24)	-0.91 (± 0.24)	-0.86 (± 0.23)	-0.85 (± 0.23)	-0.84 (± 0.23)
$\Delta K_{\phi,s}^0 \times 10^6 (m^3 \cdot mol^{-1} \cdot Gpa^{-1})$	0.49	0.49	0.47	0.41	0.42

2-Phenoxyethanol in water					
$K_{\phi,s}^0 \times 10^6 / (m^3 \cdot mol^{-1} \cdot GPa^{-1})$	-46.00 (± 0.09)	-45.01 (± 0.09)	-44.21 (± 0.09)	-43.45 (± 0.09)	-42.86 (± 0.09)
$S_K^* \times 10^6 (kg \cdot m^3 \cdot mol^{-2} \cdot GPa^{-1})$	-1.13 (± 0.28)	-1.11 (± 0.28)	-1.09 (± 0.27)	-1.08 (± 0.27)	-1.07 (± 0.27)
2- Phenoxyethanol + 0.01 Maltitol					
$K_{\phi,s}^0 \times 10^6 / (m^3 \cdot mol^{-1} \cdot GPa^{-1})$	-45.80 (± 0.08)	-44.82 (± 0.08)	-44.02 (± 0.08)	-43.31 (± 0.07)	-42.66 (± 0.07)
$S_K^* \times 10^6 (kg \cdot m^3 \cdot mol^{-2} \cdot GPa^{-1})$	-1.02 (± 0.24)	-1.00 (± 0.23)	-0.99 (± 0.23)	-0.98 (± 0.22)	-0.97 (± 0.22)
$\Delta K_{\phi,s}^0 \times 10^6 (m^3 \cdot mol^{-1} GPa^{-1})$	0.20	0.19	0.18	0.14	0.20
2- Phenoxyethanol + 0.02 Maltitol					
$K_{\phi,s}^0 \times 10^6 / (m^3 \cdot mol^{-1} \cdot GPa^{-1})$	-45.66 (± 0.08)	-44.66 (± 0.08)	-43.88 (± 0.08)	-43.19 (± 0.08)	-42.54 (± 0.07)
$S_K^* \times 10^6 (kg \cdot m^3 \cdot mol^{-2} \cdot GPa^{-1})$	-1.02 (± 0.24)	-1.00 (± 0.23)	-0.99 (± 0.23)	-0.98 (± 0.23)	-0.97 (± 0.22)
$\Delta K_{\phi,s}^0 \times 10^6 (m^3 \cdot mol^{-1} GPa^{-1})$	0.34	0.34	0.32	0.27	0.32
2- Phenoxyethanol + 0.03 Maltitol					
$K_{\phi,s}^0 \times 10^6 / (m^3 \cdot mol^{-1} \cdot GPa^{-1})$	-45.55 (± 0.08)	-44.56 (± 0.08)	-43.77 (± 0.07)	-43.09 (± 0.07)	-42.45 (± 0.07)
$S_K^* \times 10^6 (kg \cdot m^3 \cdot mol^{-2} \cdot GPa^{-1})$	-0.98 (± 0.23)	-0.96 (± 0.23)	-0.95 (± 0.22)	-0.94 (± 0.22)	-0.94 (± 0.22)
$\Delta K_{\phi,s}^0 \times 10^6 (m^3 \cdot mol^{-1} GPa^{-1})$	0.45	0.44	0.43	0.37	0.41

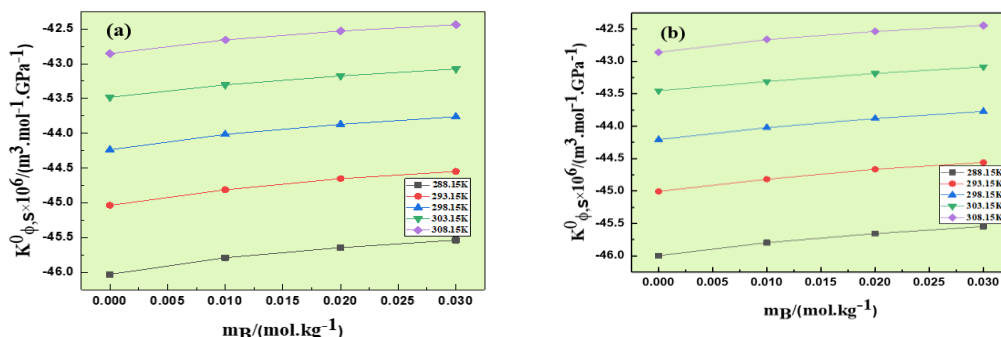


Figure 4.15 Plots showing the changes in $K_{\phi,s}^0$ with respect to the molality of (a) 2-BE and (b) 2-PhE in aqueous solutions of Maltitol at different temperatures.

maltitol concentrations. These positive values of ΔK_{ϕ}^0 suggest the solute's ability to enhance its structural properties. As the maltitol concentration increases, the interactions between the glycol ether molecules and maltitol become stronger, resulting in an amplified structure-making ability. As a consequence, the compressibility of maltitol decreases with increasing concentration, making the solution more compressible compared to the pure solvent. Consequently, the values of $K_{\phi,s}^0$ are negative while ΔK_{ϕ}^0 values are positive [34,35]. The significantly negative values of $K_{\phi,s}^0$ and positive values of ΔK_{ϕ}^0 indicate that the observed solute-solvent associations are attributed to the association of more H_2O molecules with the ion at lower temperatures as well as at lower concentrations of maltitol [36].

Pair and triplet interaction coefficient

The coefficients for volume and compressions are obtained by equation 4.11 and 4.12 respectively. In these equations, A indicates solutes i.e. 2-BE and 2-PhE and B indicates solvents, i.e. maltitol. The determination of interaction coefficients is based on the McMillan theory, which has been further refined by Friedman and Krishnan [37,38]. These coefficients provide insights into the splitting of effects resulting from the associations among solute molecules and solvents molecules. It is crucial to emphasise that the interaction coefficients reflect the strength of the interactions and may vary depending on the specific chemical characteristics of the solute molecules under consideration. Therefore, understanding the nature and magnitude of these interactions

Table 4.21 Interaction coefficients for 2-Butoxyethanol and 2-Phenoxyethanol in aqueous maltitol at different temperatures.

T/K	$V_{AB} \times 10^6 (m^3 \cdot mol^{-2} \cdot kg)$	$V_{ABB} \times 10^6 (m^3 \cdot mol^{-3} \cdot kg^2)$	$K_{AB} \times 10^6 (m^3 \cdot mol^{-2} \cdot kg \cdot GPa^{-1})$	$K_{ABB} \times 10^6 (m^3 \cdot mol^{-3} \cdot kg^2 \cdot GPa^{-1})$
2-Butoxyethanol				
288.15	4.848	2.782	13.16	-111.38
293.15	5.129	-1.686	12.67	-101.47
298.15	5.700	-9.223	12.16	-94.96
303.15	5.284	-3.235	9.79	-66.89
308.15	4.888	2.424	10.94	-89.40
2-Phenoxyethanol				
288.15	10.56	1.83	10.91	-76.56
293.15	10.69	1.68	10.51	-68.42
298.15	8.16	0.77	10.03	-62.38
303.15	6.20	0.60	7.70	-34.67
308.15	4.70	0.30	10.93	-90.36

T/K= Temperature in kelvin

is crucial for predicting and controlling the behaviour of solute molecules in solution. The volume pair and triplet coefficients, denoted as V_{AB} , and V_{ABB} , respectively, as well as the isentropic compression pair and triplet coefficients, represented by K_{AB} and K_{ABB} respectively, are reported in **Table 4.21** for the entire temperature range. **Table 4.21** illustrates that the pair-wise coefficients for volume (V_{AB}) and isentropic compression (K_{AB}) are consistently positive across all temperatures and for both glycol ethers, namely 2-butoxyethanol (2-BE) and 2-phenoxyethanol (2-PhE). On the other hand, triplet coefficients for volume are negative except at temperature 288.15, 308.15 K for 2-BE, but for 2-PhE, triplet coefficient V_{ABB} are all positive. Additionally, K_{ABB} are negative at all temperatures and for both glycol ethers (2-BE and 2-PhE).

FTIR Spectroscopic study

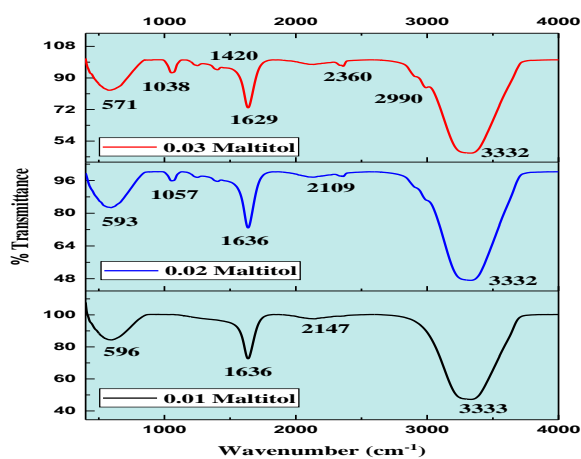
The functional groups that are present in a substance can be significantly learned about via FTIR spectroscopy. Wave number shift and band width are reported to change when the environment is marginally altered [39,40]. The structural integrity of FTIR spectroscopy is used to examine system modifications and intermolecular associations. To investigate the presence of hydrogen bonding and the strength of intermolecular interactions in mixes of 2-BE and 2-PhE with maltitol, the spectra of binary and ternary mixtures were obtained using the ATR technique. The recorded spectra covered the wavelength range of $400\text{--}4000\text{ cm}^{-1}$ with a resolution of 0.5 cm^{-1} . All the observed FT-IR spectra for the solution presented in **Figure 4.16** and **Table 4.22**. **Figure 4.16 (I)** depicts that the sharp bands appeared at 3333 and 3332 cm^{-1} for maltitol + water which shows strong O-H bonding and intermolecular bonding. Hydrogen bonding is often observed in the range of $3000\text{--}4000\text{ cm}^{-1}$ in FTIR spectra. The presence of bands at $3000\text{--}4000\text{ cm}^{-1}$ suggests that hydrogen bonding may be occurring in the mixture of butoxyethanol/ phenoxyethanol + water and 0.01 , 0.02 , and $0.03\text{ mol} \cdot \text{kg}^{-1}$ maltitol. Hydrogen bonds are created when a hydrogen atom is attracted to an electronegative atom, such as oxygen or nitrogen, present in another molecule. Therefore, it is possible that the hydrogen atoms in butoxyethanol, water, or maltitol are forming hydrogen bonds with other molecules in the mixture. The hydroxyl (O-H) functional group, which is present in both butoxyethanol and water, typically exhibits stretching vibrations between $3200\text{--}3600\text{ cm}^{-1}$ in FTIR spectra. The observed bands for butoxyethanol and

for phenoxyethanol in **Figure 4.16** (II, III, and IV) could be attributed to the stretching vibrations of the O-H groups in these molecules. As concentrations and molalities increase, the number of absorption bands also increases.

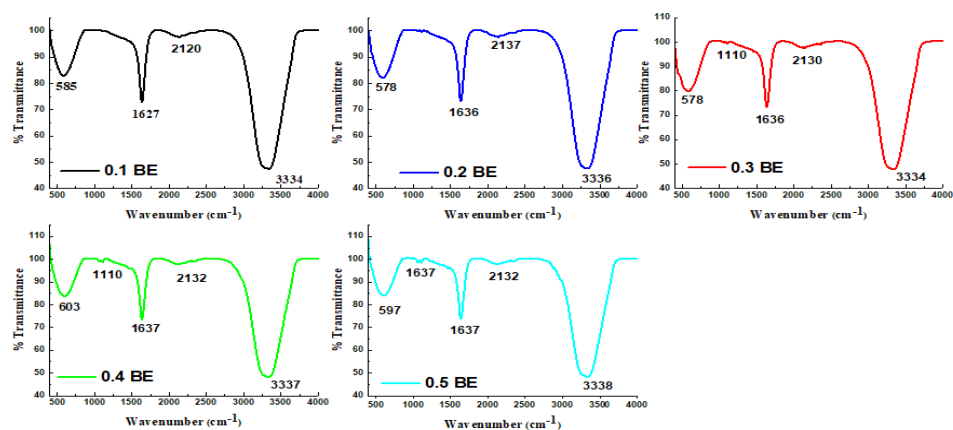
Table 4.22 Functional Group and its quantified frequencies from the FTIR data.

Wave Number	Functional Group (cm^{-1})
Alcohol, OH out-of-plane bend	570-720
Primary alcohol, C-O stretch	~ 1050
tertiary alcohol, OH bend	1410–1310
Normal “polymeric” OH stretch	3400–3200
O–H	3650 to 3590
Aromatic ethers	1270–1230
C-H stretch ($\text{CH}_3\text{-O-}$)	2820–2810
C-O stretch	1150–1050
C-O-O- stretch	890–820

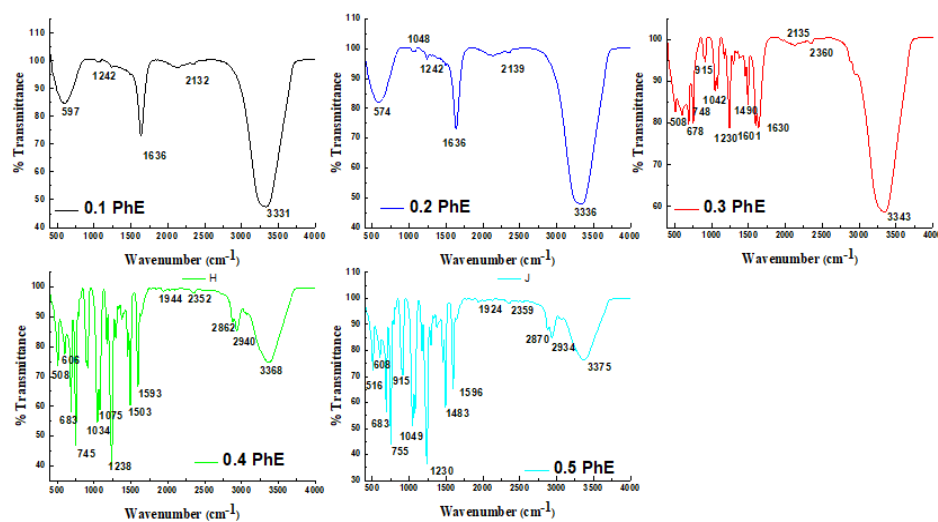
(I)



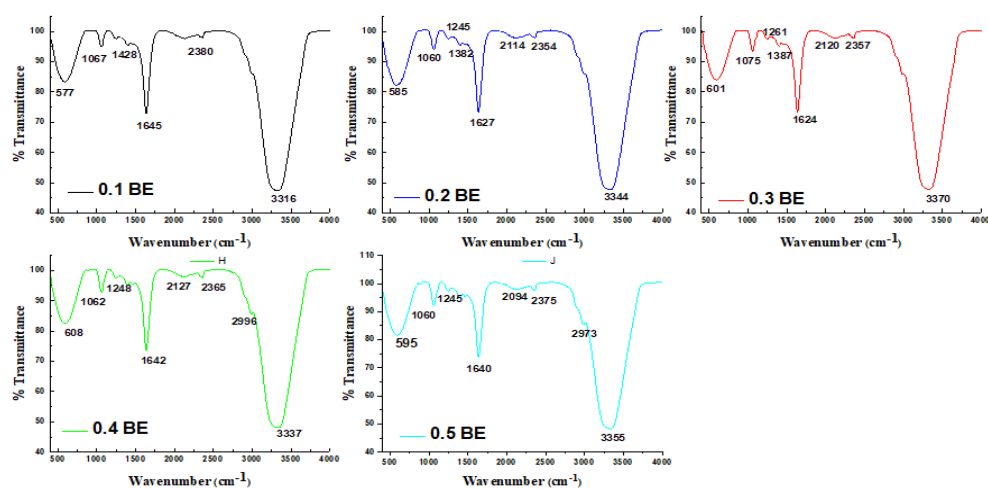
(II) (a)



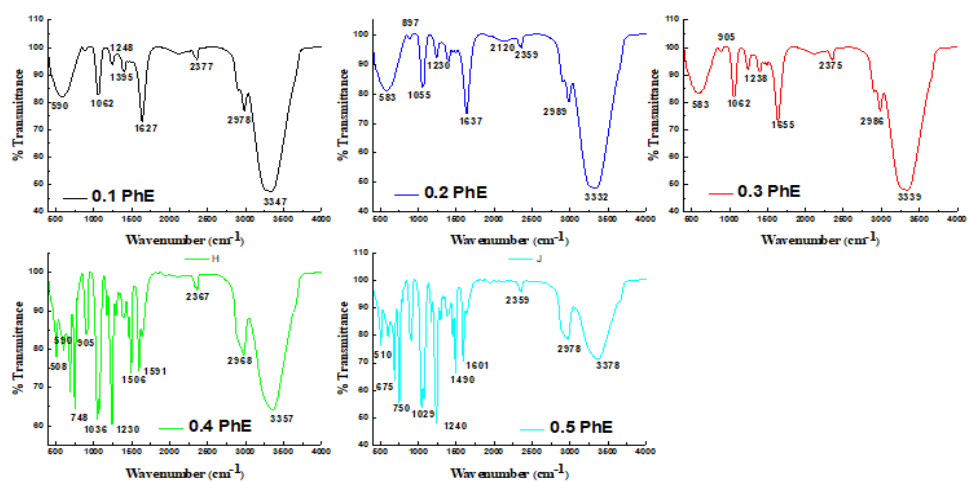
(b)



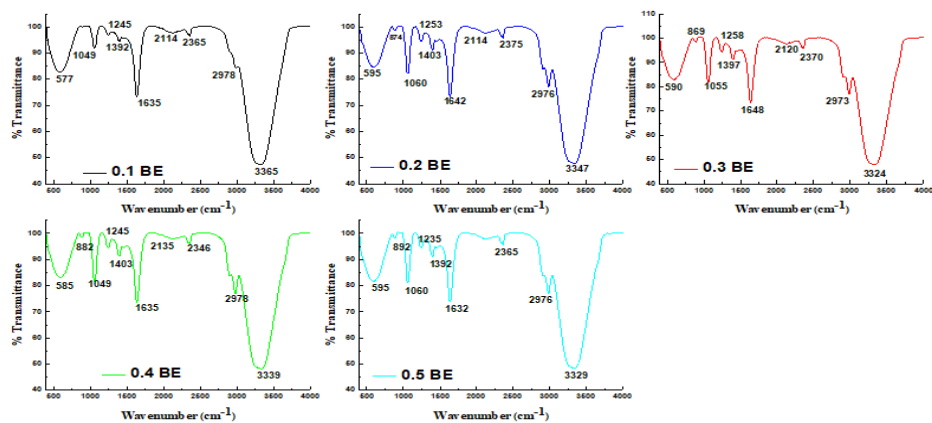
(III) (a)



(b)



(IV) (a)



(b)

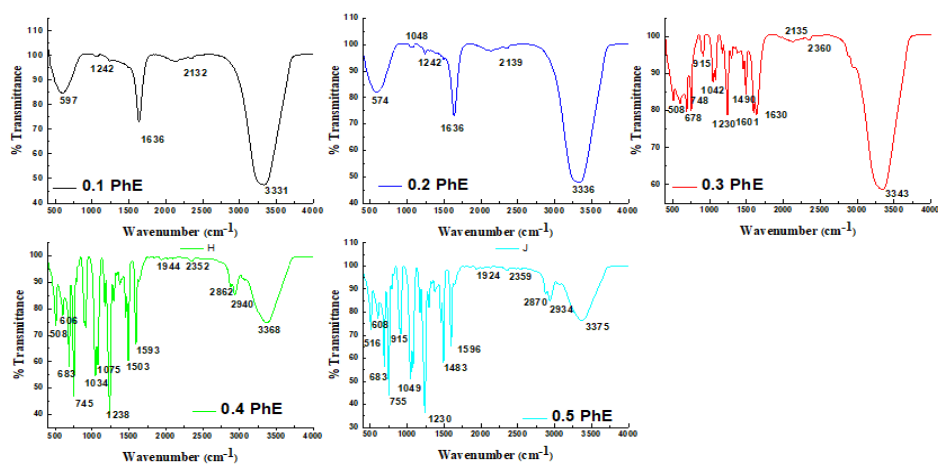


Figure 4.16 FTIR spectra for 2-Butoxyethanol (2-BE)/ 2-Phenoxyethanol (2-PhE) having molality (0.1-0.5) $\text{mol} \cdot \text{kg}^{-1}$ in (0.01, 0.02, and 0.03) $\text{mol} \cdot \text{kg}^{-1}$ maltitol solutions (I) Maltitol + Water (black: 0.01 maltitol, Blue: 0.02 Maltitol, red: 0.03 Maltitol) (II) (a) 2-BE in 0.1-0.5 $\text{mol} \cdot \text{kg}^{-1}$ (b) 2-PhE in 0.1-0.5 $\text{mol} \cdot \text{kg}^{-1}$ in 0.01 maltitol solution. (III) 2-BE in 0.1-0.5 $\text{mol} \cdot \text{kg}^{-1}$ (b) 2-PhE in 0.1-0.5 $\text{mol} \cdot \text{kg}^{-1}$ in 0.02 maltitol solution. (IV) 2-BE in 0.1-0.5 $\text{mol} \cdot \text{kg}^{-1}$ (b) 2-PhE in 0.1-0.5 $\text{mol} \cdot \text{kg}^{-1}$ in 0.03 maltitol solution. (Black: 0.1, blue: 0.2, red: 0.3, green: 0.4, sky blue: 0.5) $\text{mol} \cdot \text{kg}^{-1}$ of 2-BE/ 2-PhE.

Problem 3

Characteristics of a temperature dependent aqueous solution of Maltitol with DEGMME/ DEGMEE: An acoustic and volumetric approach

In this problem, densities values and speed of sound values, of DEGMME/DEGMEE in (0.04, 0.06 and 0.08 mol. kg⁻¹) maltitol (aq) mixes, were obtained at T= (288.15-318.15) K.

Apparent molar volume

Values of ρ of solution of aqueous maltitol with DEGMME/ DEGMEE obtained experimentally. By using the densities values and by using equation 4.1, values of V_ϕ have been estimated. Experimentally obtained values of densities and V_ϕ are given in Table 4.23. Furthermore Figure 4.17 represents the comparison between the literature and experimental values of binary mixture (maltitol + water), and shows the same trend [41,1]. Apparent molar volume provides great understanding about solute and the solvent. As Table 4.23 depicts that all the values of V_ϕ are positives, which indicates that solutes are causing the solution to occupy more volume than the pure solvent would alone [42]. Figure 4.18 represents the variation of V_ϕ with molality. Apparent molar volume also important to understand the properties of solutions, particularly in dilute solutions where the interaction among solute and solvent molecules can significantly affect the volume [43,44]. The V_ϕ data for DEGMME/ DEGMEE in aqueous maltitol at different temperature shows strong solute-solvent associations and the values also increasing. The upsurge in solute-solvent associations rise with rise in glycol ether's molar mass.

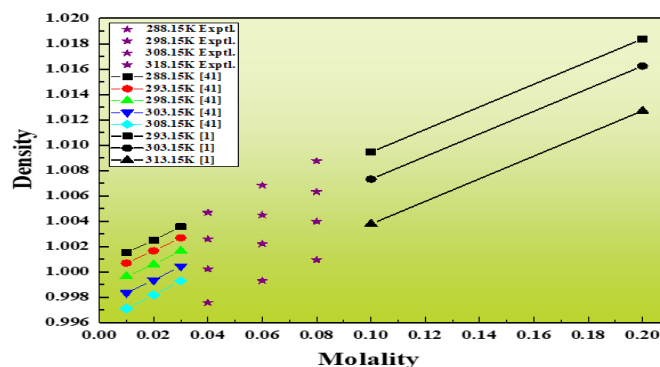


Figure 4.17 Comparison of density of maltitol + water at different temperatures with literature values [41,1].

Table 4.23 Density and calculated V_ϕ values for (DEGMME/ DEGMEE + maltitol) at 0.1 MPa pressure.

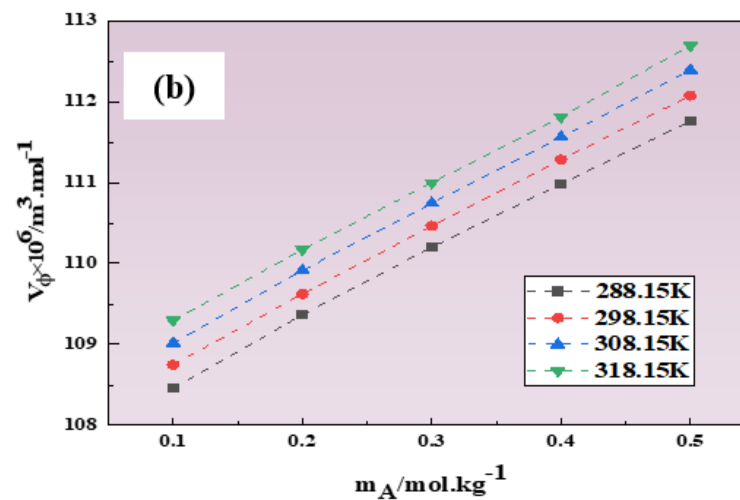
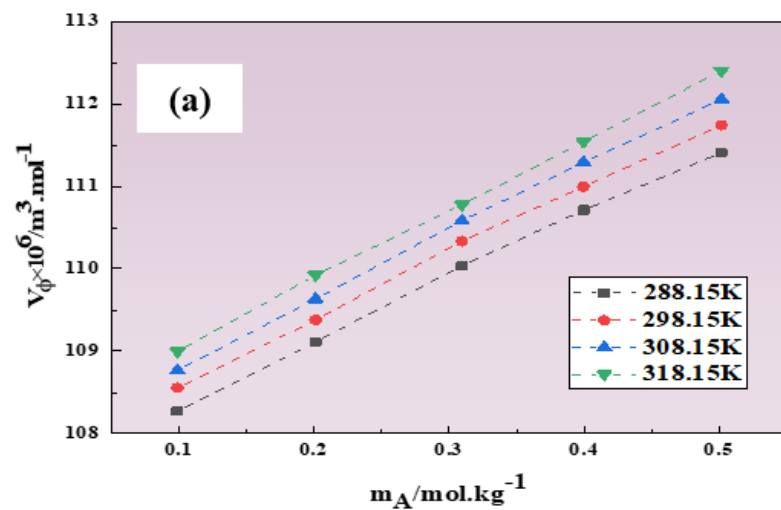
$^a m_A / (mol \cdot kg^{-1})$	$\rho \times 10^{-3} / (kg \cdot m^{-3})$				$V_\phi \times 10^6 / (m^3 \cdot mol^{-1})$			
	T = 288.15K	T = 298.15K	T = 308.15K	T = 318.15K	T = 288.15K	T = 298.15K	T = 308.15K	T = 318.15K
DEGMME + 0.00 $mol \cdot kg^{-1}$ Maltitol								
0.00000	0.99926	0.99705	0.99404	0.99036				
0.09897	1.00043	0.99821	0.99521	0.99154	108.27	108.56	108.77	109.00
0.20115	1.00145	0.99923	0.99623	0.99256	109.11	109.38	109.63	109.92
0.30955	1.00231	1.00008	0.99708	0.99346	110.04	110.33	110.58	110.78
0.39951	1.00290	1.00067	0.99766	0.99403	110.71	111.00	111.29	111.54
0.50172	1.00345	1.00119	0.99818	0.99452	111.41	111.74	112.05	112.40
DEGMME + 0.04 $mol \cdot kg^{-1}$ Maltitol								
0.00000	1.00467	1.00258	1.00021	0.99757				
0.09996	1.00578	1.00368	1.00131	0.99867	108.46	108.75	109.02	109.30
0.19994	1.00669	1.00459	1.00221	0.99957	109.37	109.62	109.91	110.17
0.29999	1.00742	1.00532	1.00293	1.00030	110.20	110.46	110.75	111.00
0.39989	1.00800	1.00587	1.00349	1.00086	110.99	111.28	111.56	111.81
0.49979	1.00841	1.00627	1.00387	1.00122	111.76	112.07	112.39	112.69
DEGMME + 0.06 $mol \cdot kg^{-1}$ Maltitol								
0.00000	1.00682	1.00449	1.00221	0.99930				

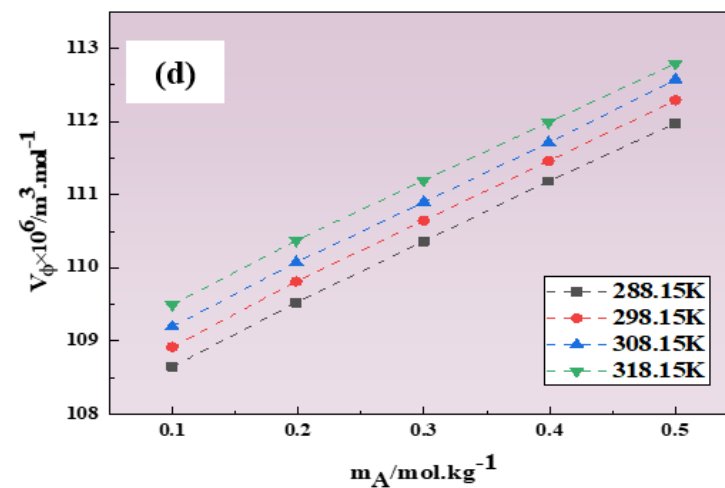
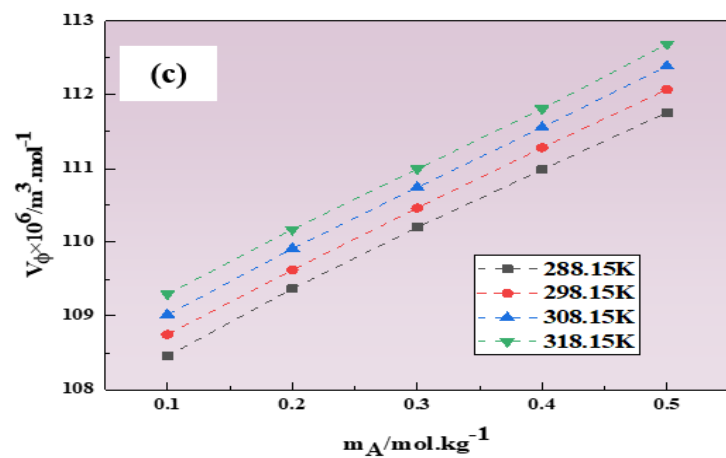
0.09999	1.00789	1.00556	1.00327	1.00036	108.65	108.92	109.20	109.50
0.19849	1.00875	1.00641	1.00412	1.00121	109.52	109.81	110.07	110.37
0.29984	1.00946	1.00712	1.00483	1.00192	110.36	110.65	110.90	111.20
0.39920	1.00998	1.00763	1.00535	1.00245	111.18	111.46	111.71	111.99
0.49990	1.01035	1.00799	1.00569	1.00282	111.97	112.29	112.57	112.79
DEGMME + 0.08 mol · kg ⁻¹ Maltitol								
0.00000	1.00874	1.00631	1.00397	1.00094				
0.09953	1.00977	1.00734	1.00499	1.00196	108.82	109.10	109.40	109.70
0.19830	1.01059	1.00816	1.00581	1.00278	109.71	109.97	110.27	110.57
0.30000	1.01127	1.00884	1.00648	1.00345	110.55	110.80	111.10	111.40
0.39976	1.01176	1.00933	1.00697	1.00395	111.36	111.61	111.89	112.19
0.50004	1.01207	1.00963	1.00730	1.00428	112.19	112.47	112.69	112.99
DEGMEE + 0.00 mol · kg ⁻¹ Maltitol								
0.00000	0.99926	0.99705	0.99404	0.99036				
0.09903	1.00001	0.99781	0.99482	0.99117	126.59	126.73	126.87	126.99
0.19262	1.00067	0.99848	0.99551	0.99189	126.76	126.91	127.05	127.17
0.29786	1.00135	0.99918	0.99623	0.99264	126.97	127.12	127.25	127.37
0.40279	1.00198	0.99981	0.99689	0.99333	127.17	127.32	127.46	127.58
0.49997	1.00250	1.00034	0.99744	0.99391	127.36	127.52	127.65	127.77

DEGMEE + 0.04 mol · kg ⁻¹ Maltitol								
0.00000	1.00467	1.00258	1.00021	0.99757				
0.09998	1.00535	1.00327	1.00092	0.99830	126.72	126.86	126.99	127.10
0.19894	1.00597	1.00390	1.00157	0.99896	126.90	127.05	127.16	127.28
0.29889	1.00654	1.00449	1.00217	0.99958	127.11	127.24	127.35	127.48
0.39989	1.00707	1.00502	1.00272	1.00015	127.31	127.45	127.57	127.69
0.49999	1.00754	1.00551	1.00322	1.00067	127.51	127.64	127.76	127.88
DEGMEE + 0.06 mol · kg ⁻¹ Maltitol								
0.00000	1.00682	1.00449	1.00221	0.99930				
0.10002	1.00746	1.00515	1.00289	1.00000	126.84	126.96	127.08	127.17
0.19849	1.00805	1.00575	1.00350	1.00064	127.03	127.14	127.26	127.36
0.30061	1.00860	1.00632	1.00408	1.00124	127.22	127.33	127.46	127.56
0.39820	1.00907	1.00680	1.00458	1.00177	127.42	127.53	127.66	127.75
0.49890	1.00951	1.00726	1.00505	1.00226	127.62	127.73	127.86	127.96
DEGMEE + 0.08 mol · kg ⁻¹ Maltitol								
0.00000	1.00874	1.00631	1.00397	1.00094				
0.10001	1.00935	1.00694	1.00462	1.00161	126.94	127.06	127.15	127.25
0.19990	1.00991	1.00751	1.00521	1.00223	127.12	127.24	127.34	127.43
0.30011	1.01042	1.00804	1.00575	1.00280	127.31	127.44	127.54	127.63

0.39996	1.01087	1.00851	1.00624	1.00331	127.51	127.64	127.73	127.83
0.50014	1.01128	1.00893	1.00667	1.0377	127.71	127.84	127.94	128.04

(I)





(II)

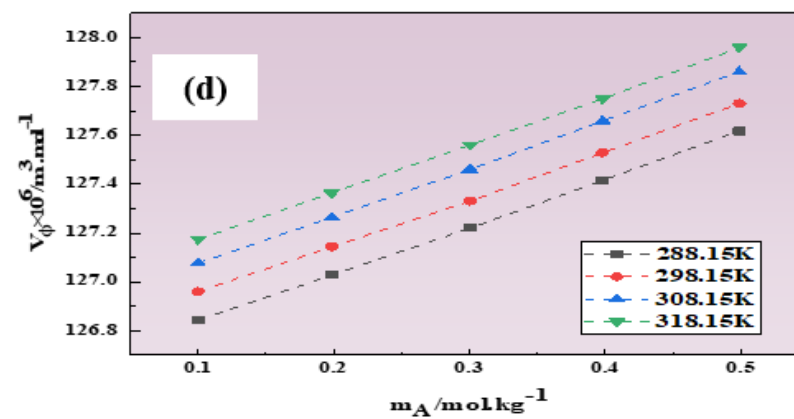
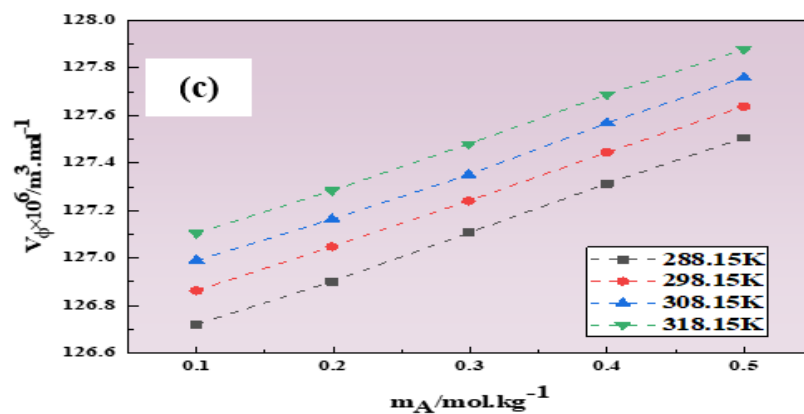
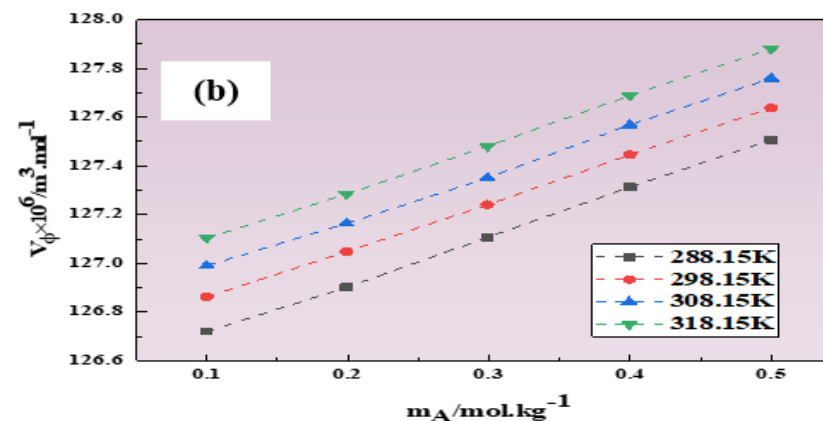
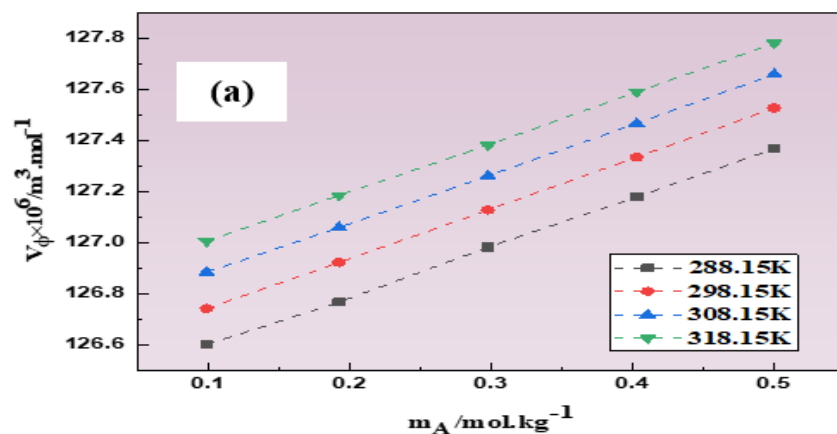


Figure 4.18 Plot of V_ϕ of (I) DEGMME and (II) DEGMEE at different temperatures and different concentrations of Maltitol: (a) 0.00 Maltitol, (b) 0.04 Maltitol, (c) 0.06 Maltitol, and (d) 0.08 Maltitol ($\text{mol} \cdot \text{kg}^{-1}$).

Partial molar volume

The V_{ϕ}^0 values calculated by using values of V_{ϕ} and equation 4.2 utilised to obtained the values for the system containing DEGMME/DEGMEE + maltitol (aq). The V_{ϕ}^0 values are given in **Table 4.24** with experimental slope (S_V^*). The positive values of V_{ϕ}^0 gradually upsurges with rise in of the maltitol concentration, that is represented in **Figure 4.19**. According to the co-sphere overlap model, interactions between ions and hydrophobic groups, as well as between two hydrophobic groups, contribute negatively to the overall volume. In contrast, interactions between ions and hydrophilic groups, or between two hydrophilic groups, lead to positive contributions. In this study, the observed positive V_{ϕ}^0 values suggest that hydrophilic-related interactions are more significant than those between hydrophobic groups [45,46]. Observed positive values for V_{ϕ}^0 are primarily due to the dominance of associations over ion-hydrophilic associations, along with system packing effects. Strong hydrogen bonding between water's hydrogen atoms and glycol ethers' oxygen atoms is also influential [47,48]. Moreover, the experimental slope remains positive across temperatures and maltitol concentrations, highlighting solute-2 associations [49,50]. However, the size of S_V^* is very small as compared to V_{ϕ}^0 indicates that solute-solvent associations take precedence over solute-2 associations in the DEGMME/DEGMEE + maltitol aqueous mixture.

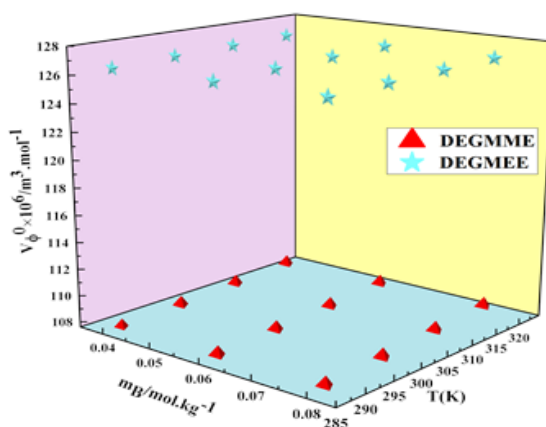


Figure 4.19 Partial molar volume, V_{ϕ}^0 , for DEGMME (red) and DEGMEE (sky blue) within an maltitol aqueous solution at various temperatures.

Table 4.24. Calculated partial molar volume (V_{ϕ}^0) values along with experimental slope (S_V^*) for (DEGMME/ DEGMEE + maltitol) at (288.15- 318.15) K temperatures.

$^a m_B / (mol \cdot kg^{-1})$	$V_{\phi}^0 \times 10^6 (m^3 \cdot mol^{-1})$				$S_V^* \times 10^6 (m^3 \cdot kg \cdot mol^{-2})$			
	T = 288.15K	T = 298.15K	T = 308.15K	T = 318.15K	T = 288.15K	T = 298.15K	T = 308.15K	T = 318.15K
DEGMME								
0.00	107.54(±0.07)	107.80(±0.06)	107.99(±0.05)	108.19(±0.03)	7.84(±0.20)	7.96(±0.18)	8.20(±0.16)	8.39(±0.10)
0.04	107.69(±0.05)	107.95(±0.03)	108.21(±0.03)	108.47(±0.02)	8.23(±0.16)	8.31(±0.09)	8.40(±0.09)	8.43(±0.07)
0.06	107.85(±0.04)	108.11(±0.03)	108.38(±0.02)	108.71(±0.04)	8.30(±0.11)	8.39(±0.10)	8.38(±0.07)	8.20(±0.11)
0.08	108.02(±0.03)	108.28(±0.03)	108.62(±0.04)	108.92(±0.04)	8.37(±0.10)	8.36(±0.08)	8.18(±0.11)	8.18(±0.11)
DEGMEE								
0.00	126.40(±0.01)	126.55(±0.00)	126.69(±0.00)	126.81(±0.00)	1.92(±0.02)	1.96(±0.01)	1.93(±0.01)	1.93(±0.01)
0.04	126.52(±0.01)	126.66(±0.01)	126.79(±0.01)	126.90(±0.01)	1.98(±0.02)	1.95(±0.02)	1.94(±0.04)	1.95(±0.02)
0.06	126.64(±0.01)	126.76(±0.01)	126.88(±0.01)	126.98(±0.01)	1.94(±0.02)	1.93(±0.02)	1.96(±0.02)	1.96(±0.02)
0.08	126.74(±0.01)	126.86(±0.00)	126.96(±0.01)	127.05(±0.01)	1.92(±0.02)	1.96(±0.01)	1.95(±0.02)	1.96(±0.03)

Partial molar volume of transfer

By using the equation 4.3, ΔV_{ϕ}^0 values for glycol ethers is determined at infinite dilution. Calculated values of ΔV_{ϕ}^0 at different temperature and concentration provided in **Table 4.25**. All the values of ΔV_{ϕ}^0 depicts that, in the system strong ion-ion interaction exist. All the value of ΔV_{ϕ}^0 are positives. So, all positives values describe that molecular associations of maltitol with glycol ethers are weak as compared to associations of water with glycol ethers [12,51]. Moreover, as per co-sphere overlap modal, the ΔV_{ϕ}^0 data indicates that solute-2 are negligible and it provides the strong solute-solvent associations. Additionally, as per the modal of co-sphere, positive ΔV_{ϕ}^0 values indicate a structure composition. With the positive's values of ΔV_{ϕ}^0 associations such as ion-hydrophilic and hydrophilic-2 are linked [52].

Table 4.25 Calculated ΔV_{ϕ}^0 values for (DEGMME/ DEGMEE + maltitol) at 0.1 MPa pressure.

$m_B / (\text{mol} \cdot \text{kg}^{-1})$	$\Delta V_{\phi}^0 \times 10^6 (\text{m}^3 \cdot \text{mol}^{-1})$			
	T = 288.15K	T = 298.15K	T = 308.15K	T = 318.15K
DEGMME				
0.04	0.15	0.15	0.22	0.27
0.06	0.31	0.32	0.39	0.52
0.08	0.48	0.49	0.63	0.73
DEGMEE				
0.04	0.11	0.12	0.10	0.09
0.06	0.24	0.22	0.19	0.16
0.08	0.34	0.31	0.27	0.24

Temperature-Dependent Partial Molar Volume

It is examining through relationship 4.4. In this relation T_{ref} is set to 298.15 K. The a, b, and c values are listed in **Table 4.26**. Furthermore, the partial molar expansibility has been obtained through equation 4.5. The E_{ϕ}^0 values are included in **Table 4.27**. All E_{ϕ}^0 are positives. Additionally, E_{ϕ}^0 is arises due to two components. In this $E_{\phi}^0(elect)$ is

Table 4.26 Calculated values for empirical parameters for (DEGMME/ DEGMEE + maltitol) at (288.15- 318.15) K temperatures.

$m_B/(mol \cdot kg^{-1})$	$a \times 10^6(m^3.mol^{-1})$	$b \times 10^6(m^3.mol^{-1}.K^{-1})$	$c \times 10^6(m^3.mol^{-1}.K^{-2})$	R^2	ARD
DEGMME					
0.04	107.947	0.026	0.000	0.999	0.0000
0.06	108.104	0.027	0.000	0.999	0.0000
0.08	108.299	0.030	0.000	0.999	0.0001
DEGMEE					
0.04	126.661	0.014	0.000	0.999	0.0000
0.06	126.764	0.012	0.000	0.999	0.0000
0.08	126.855	0.011	0.000	0.999	0.0000

Table 4.27 Calculated partial molar expansibilities, (E_{ϕ}^0) values for (DEGMME/DEGMEE + maltitol) at 0.1 MPa pressure.

^a <i>m_B</i>	<i>E</i> _ϕ ⁰ × 10 ⁶ (<i>m</i> ³ · <i>mol</i> ^{−1} · <i>K</i> ^{−1})				<i>(∂E</i> _ϕ ⁰ / <i>∂T</i>) _{<i>p</i>} / (<i>m</i> ³ · <i>mol</i> ^{−1} · <i>K</i> ^{−2})	
(<i>mol</i> · <i>kg</i> ^{−1})	T	=	T	=	T	=
	288.15K		298.15K		308.15K	318.15K
DEGMME						
0.04	0.026		0.026		0.026	0.0000
0.06	0.023		0.027		0.030	0.0004
0.08	0.028		0.030		0.031	0.0558
DEGMEE						
0.04	0.015		0.014		0.012	−0.0002
0.06	0.012		0.012		0.011	−0.0001
0.08	0.012		0.011		0.010	0.0236

expansivity due to electrostriction change (around the solute, contribution of hydration) and $E_{\phi}^0(str)$ is due to change in structure of solvent molecules. The $E_{\phi}^0(str)$ is predominant at lower temperature. On the other hand, $E_{\phi}^0(etc)$ is predominant at higher temperatures. In the case of DEGMME values of E_{ϕ}^0 is lower at lower temperature, this indicates that temperature influences the outer hydration layer of water molecules, leading to an increase in E_{ϕ}^0 values as temperature rises. On the other hand, for DEGMEE values decreasing with increase in temperature, suggest that there is less interaction at higher temperature [53,54]. Moreover, by the equation 4.6, the temperature derivative of E_{ϕ}^0 was calculated. The values of temperature derivative of $(\partial E_{\phi}^0 / \partial T)_p$, given in **Table 4.27**. Values of $(\partial E_{\phi}^0 / \partial T)_p$ are all positive for solute DEGMME, but for solute DEGMEE are negative except at 0.08 concentration of maltitol. When solutes dissolved in solvent, it acts as either structure maker or structure breaker. It can be found by sign of $(\partial E_{\phi}^0 / \partial T)_p$ values. It is helpful to assess the solute's capability to disrupt or enhance the structural organization within the solvent [23]. This leads to the fact that structural effects play a significant role to determine the solutes-solvent associations in ternary mixtures.

Apparent molar isentropic compression

Experimentally obtained values c for ternary mixtures (DEGMME/DEGMEE + maltitol) has been used to calculate $K_{\phi,s}$ values. Values of c (sound speeds) increasing with increase in concentration of maltitol. **Figure 4.20** graphically represents comparison between literature and experimental values for binary mixture (maltitol + Water) [41]. After that, experimentally measured density and sound velocity values are employed in Newton's Laplace equation 4.7 to calculate the isentropic compressibility, K_S . The calculated value of K_S was then used to determine $K_{\phi,s}$ using the equation 4.8. **Table 4.28.** provides data on the speed of sound alongside the calculated $K_{\phi,s}$ values. The derived $K_{\phi,s}$ values are negative, as depicted in **Figure 4.21**, which shows the trend of $K_{\phi,s}$ with molality at different temperatures. Moreover, these $\kappa_{\phi,s}$ values become less negative at higher temperatures and more negative as the glycol concentration increases. The negative $\kappa_{\phi,s}$ values suggest a decrease in water compressibility near charged groups, contrasting with the more ordered structure in the bulk solution [24,55,7]. This negativity in $K_{\phi,s}$ indicates significant disruption of water's structural arrangement, highlighting strong solvent-solute interactions. Negative $K_{\phi,s}$ values suggest a predominance of interactions between hydrophilic and ionic components [56,57].

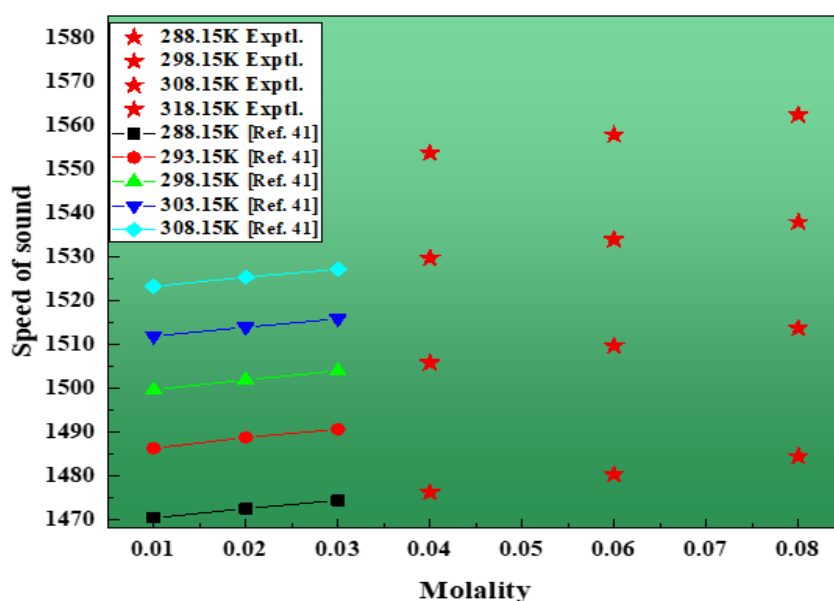


Figure 4.20 Plot of 'c' values for Maltitol + water with existing previous values [41].

Table 4.28 Values of sound speeds and $K_{\phi,S}$ values for (DEGMME/ DEGMEE + Maltitol).

$^a m_A / (mol \cdot kg^{-1})$	$c / (m \cdot s^{-1})$				$K_{\phi,S} \times 10^6 / (m^3 \cdot mol^{-1} \cdot GPa^{-1})$			
	T = 288.15K	T = 298.15K	T = 308.15K	T = 318.15K	T = 288.15K	T = 298.15K	T = 308.15K	T = 318.15K
DEGMME + 0.00 $mol \cdot kg^{-1}$ Maltitol								
0.00000	1466.59	1495.85	1519.14	1536.02				
0.09897	1473.79	1503.79	1526.14	1543.44	-46.08	-44.30	-42.95	-42.01
0.20115	1481.09	1511.02	1533.01	1551.11	-46.37	-44.57	-43.21	-42.27
0.30955	1488.46	1519.01	1540.79	1559.29	-46.49	-44.69	-43.33	-42.38
0.39951	1495.19	1525.21	1546.79	1565.79	-46.55	-44.75	-43.38	-42.44
0.50172	1502.64	1532.12	1554.15	1573.25	-46.60	-44.79	-43.43	-42.48
DEGMME + 0.04 $mol \cdot kg^{-1}$ Maltitol								
0.00000	1476.22	1505.81	1529.74	1553.79				
0.09996	1483.79	1513.71	1536.99	1560.88	-45.49	-43.72	-42.36	-41.05
0.19994	1491.01	1520.94	1544.25	1568.48	-45.76	-43.98	-42.61	-41.30
0.29999	1498.28	1528.61	1551.47	1576.00	-45.87	-44.08	-42.71	-41.40
0.39989	1505.42	1535.65	1558.25	1583.88	-45.93	-44.14	-42.77	-41.46
0.49979	1512.80	1542.24	1565.59	1591.22	-45.97	-44.18	-42.81	-41.49
DEGMME + 0.06 $mol \cdot kg^{-1}$ Maltitol								
0.00000	1480.27	1509.71	1533.99	1557.94				

0.09999	1488.15	1517.46	1541.25	1565.41	-45.24	-43.49	-42.12	-40.84
0.19849	1495.31	1524.91	1548.56	1572.66	-45.50	-43.74	-42.37	-41.08
0.29984	1502.88	1532.44	1555.59	1580.49	-45.61	-43.85	-42.47	-41.17
0.39920	1510.27	1539.19	1562.62	1588.00	-45.67	-43.91	-42.53	-41.23
0.49990	1517.74	1546.17	1570.11	1595.66	-45.71	-43.94	-42.56	-41.27
DEGMME + 0.08 mol · kg ⁻¹ Maltitol								
0.00000	1484.44	1513.77	1537.98	1562.49				
0.09953	1491.97	1521.26	1545.26	1570.29	-44.98	-43.25	-41.90	-40.60
0.19830	1499.02	1528.79	1552.36	1577.59	-45.24	-43.51	-42.15	-40.83
0.30000	1506.78	1536.36	1559.75	1585.62	-45.35	-43.61	-42.25	-40.93
0.39976	1514.27	1543.18	1567.06	1593.31	-45.41	-43.67	-42.30	-40.99
0.50004	1521.85	1550.14	1574.24	1600.75	-45.45	-43.70	-42.34	-41.02
DEGMEE + 0.00 mol · kg ⁻¹ Maltitol								
0.00000	1466.59	1495.85	1519.14	1536.02				
0.09903	1478.19	1506.99	1530.13	1546.99	-46.07	-44.28	-42.93	-41.99
0.19262	1487.09	1516.99	1539.12	1556.44	-46.32	-44.53	-43.18	-42.23
0.29786	1496.86	1527.42	1550.23	1568.15	-46.44	-44.64	-43.29	-42.34
0.40279	1505.94	1537.88	1560.55	1579.25	-46.51	-44.71	-43.35	-42.41
0.49997	1514.94	1547.99	1570.15	1589.56	-46.56	-44.76	-43.40	-42.46

DEGMEE + 0.04 mol · kg ⁻¹ Maltitol								
0.00000	1476.22	1505.81	1529.74	1553.79				
0.09998	1487.05	1516.71	1539.99	1563.88	-45.47	-43.70	-42.34	-41.04
0.19894	1496.31	1526.94	1549.55	1573.48	-45.72	-43.95	-42.58	-41.27
0.29889	1505.88	1537.61	1559.97	1584.00	-45.83	-44.05	-42.68	-41.37
0.39989	1515.27	1547.65	1569.75	1593.88	-45.89	-44.11	-42.74	-41.43
0.49999	1524.74	1557.24	1579.79	1603.22	-45.93	-44.15	-42.78	-41.47
DEGMEE + 0.06 mol · kg ⁻¹ Maltitol								
0.00000	1480.27	1509.71	1533.99	1557.94				
0.10002	1488.15	1520.95	1544.21	1567.89	-45.22	-43.47	-42.11	-40.82
0.19849	1495.31	1531.16	1553.99	1578.14	-45.47	-43.72	-42.34	-41.05
0.30061	1502.88	1541.87	1564.51	1588.56	-45.57	-43.82	-42.44	-41.15
0.39820	1510.27	1552.14	1573.49	1598.01	-45.63	-43.87	-42.50	-41.20
0.49890	1517.74	1562.08	1583.64	1608.56	-45.67	-43.91	-42.54	-41.24
DEGMEE + 0.08 mol · kg ⁻¹ Maltitol								
0.00000	1484.44	1513.77	1537.98	1562.49				
0.10001	1495.08	1524.99	1547.99	1573.26	-44.97	-43.24	-41.89	-40.58
0.19990	1504.19	1535.76	1558.01	1582.65	-45.21	-43.48	-42.12	-40.81
0.30011	1513.49	1545.69	1567.99	1592.58	-45.31	-43.58	-42.22	-40.91

0.39996	1522.69	1555.99	1577.51	1602.84	-45.37	-43.63	-42.27	-40.96
0.50014	1532.46	1566.01	1587.31	1612.56	-45.41	-43.67	-42.31	-41.00

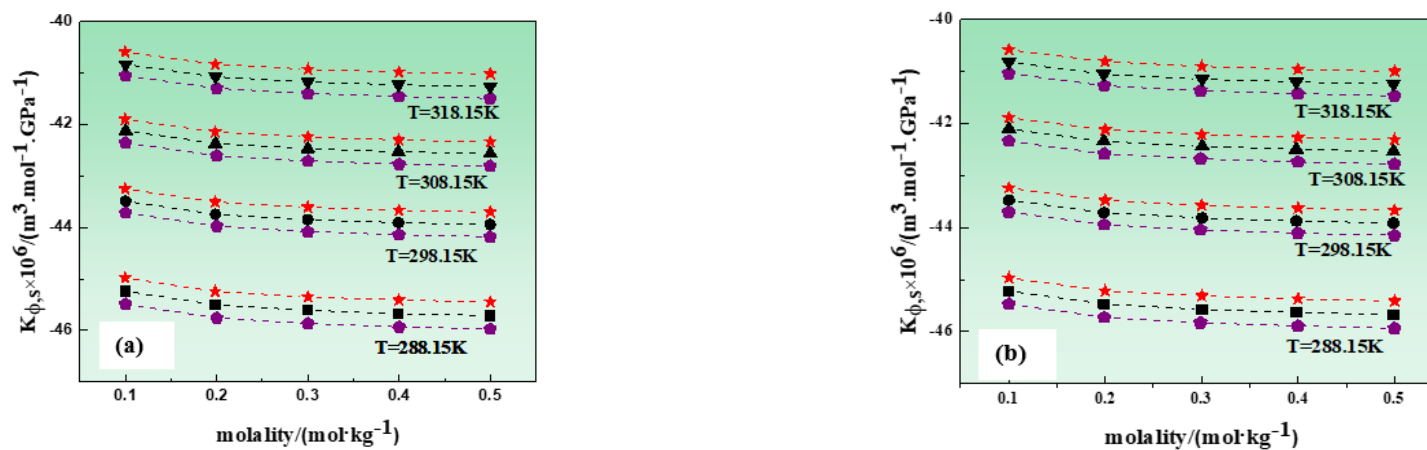


Figure 4.21 Plot of $K_{\phi,s}$, v/s molality, for (a) DEGMME and (b) DEGMEE at different temperatures and concentrations ($\text{mol} \cdot \text{kg}^{-1}$), 0.04 Maltitol (purple), 0.06 Maltitol (black), and 0.08 Maltitol (red).

Partial molar isentropic compression

The $K_{\phi,s}^0$ values are calculated by means of equation 4.9. Table 4.29. presents the $K_{\phi,s}^0$ values with their corresponding standard errors and the S_K^* values which were determined using a least-squares fitting method. The small magnitude of S_K^* suggests that solute-solute interactions at infinite dilution are minimal. Additionally, all $K_{\phi,s}^0$ values less than zero, and they tend to become less negative as the solvent concentration increases. This trend indicates that the H₂O molecules surrounding the glycol ether are not as much compressible. The relatively small value of S_K^* as compared to $K_{\phi,s}^0$, highlights the importance of $K_{\phi,s}^0$ in assessing the strength of solute-solvent interactions. Moreover, these values provide great insights into solute-solute interactions [29,17,10]. Figure 4.22 graphically represented to the variation of $K_{\phi,s}^0$ with molality.

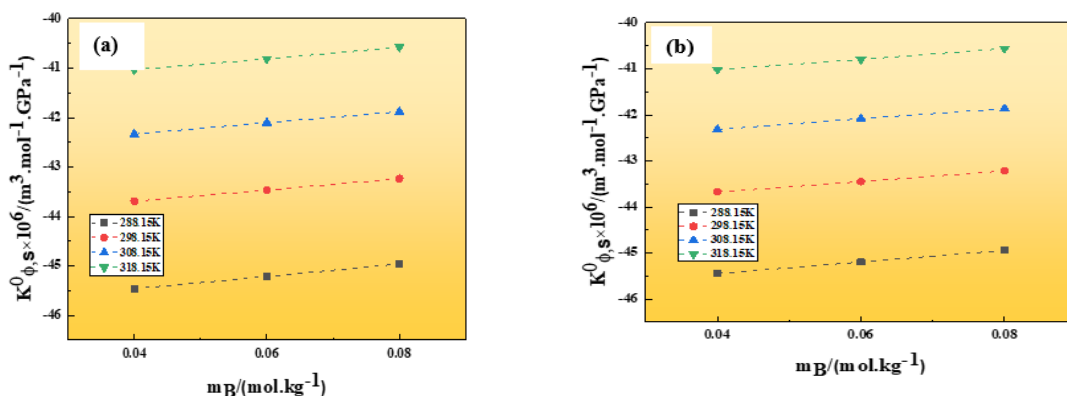


Figure 4.22 Plot of $K_{\phi,s}^0$ v/s molality, for (a) DEGMME and (b) DEGMEE in maltitol (aq) solutions at different temperatures.

Table 4.29 Calculated partial molar isentropic compression ($K_{\phi,s}^0$) values along with experimental slope (S_K^*) for (DEGMME/ DEGMEE + maltitol) at (288.15- 318.15) K temperatures.

$^a m_B / (mol \cdot kg^{-1})$	$K_{\phi,s}^0 \times 10^6 / (m^3 \cdot mol^{-1} \cdot GPa^{-1})$				$S_K^* \times 10^6 (kg \cdot m^3 \cdot mol^{-2} \cdot GPa^{-1})$			
	T = 288.15K	T = 298.15K	T = 308.15K	T = 318.15K	T = 288.15K	T = 298.15K	T = 308.15K	T = 318.15K
DEGMME								
0.00	-46.05(±0.09)	-44.27(±0.08)	-42.92(±0.08)	-41.98(±0.08)	-1.22(±0.26)	-1.17(±0.25)	-1.14(±0.25)	-1.12(±0.25)
0.04	-45.46(±0.09)	-43.69(±0.08)	-42.33(±0.08)	-41.03(±0.08)	-1.14(±0.26)	-1.10(±0.25)	-1.06(±0.24)	-1.03(±0.24)
0.06	-45.21(±0.08)	-43.47(±0.08)	-42.10(±0.08)	-40.81(±0.08)	-1.12(±0.26)	-1.07(±0.25)	-1.04(±0.24)	-1.02(±0.23)
0.08	-44.96(±0.08)	-43.23(±0.08)	-41.88(±0.08)	-40.57(±0.08)	-1.09(±0.26)	-1.05(±0.25)	-1.02(±0.24)	-1.00(±0.23)
DEGMEE								
0.00	-46.04(±0.08)	-44.25(±0.08)	-42.90(±0.08)	-41.96(±0.07)	-1.15(±0.24)	-1.11(±0.24)	-1.09(±0.23)	-1.09(±0.23)
0.04	-45.44(±0.08)	-43.67(±0.08)	-42.32(±0.07)	-41.01(±0.07)	-1.09(±0.24)	-1.06(±0.23)	-1.03(±0.23)	-1.01(±0.22)
0.06	-45.19(±0.08)	-43.45(±0.08)	-42.08(±0.07)	-40.80(±0.07)	-1.07(±0.24)	-1.04(±0.23)	-1.02(±0.22)	-1.00(±0.22)
0.08	-44.94(±0.08)	-43.22(±0.08)	-41.86(±0.07)	-40.56(±0.07)	-1.05(±0.24)	-1.02(±0.23)	-0.99(±0.22)	-0.98(±0.22)

Partial molar isentropic compression of transfer

The ΔK_{ϕ}^0 , values for DEGMME/DEGMEE in aqueous maltitol was calculated using the equation 4.10. **Table 4.30.** presents the values of ΔK_{ϕ}^0 , which consistently show positive values that increase with concentration of the solvent mixture (water + maltitol). As per a model (co-sphere), which describes the effects of volume expansion due to interactions among solute molecules. The positive ΔK_{ϕ}^0 values mainly suggest that volume expansion is occurring due to the displacement of water molecules at hydrophilic centres, and indicates to strong solute-solvent associations [58,59]. These associations are particularly visible at lower temperatures and maltitol concentrations, where the association of water molecules with the solute, especially ions, becomes more pronounced [60]. The rising ΔK_{ϕ}^0 values with concentration's, indicate a shift in the distribution of the hydration sphere around the charged end center, suggesting that hydrophilic-ionic associations are more significant than hydrophobic-2 associations.

Table 4.30 Calculated $\Delta K_{\phi,s}^0$ values for (DEGMME/ DEGMEE + maltitol) 0.1 MPa pressure.

^a m_B (mol · kg ⁻¹)	$\Delta K_{\phi,s}^0 \times 10^6 (m^3 \cdot mol^{-1} GPa^{-1})$			
	T = 288.15K	T = 298.15K	T = 308.15K	T = 318.15K
DEGMME				
0.04	0.84	0.80	0.82	1.17
0.06	1.09	1.03	1.04	1.40
0.08	1.34	1.22	1.27	1.59
DEGMEE				
0.04	0.84	0.80	0.82	1.17
0.06	1.10	1.04	1.04	1.40
0.08	1.34	1.22	1.27	1.59

Interaction Coefficients

McMillian theory of solutions provides a method to analyse solution behaviour by separation of the effects due to molecular interactions among pair and more solutes molecules [37]. This modal was further rectified by Krishnan and Friedman [38]. This

Table 4.31 Pair (V_{AB} , K_{AB}) and triplet (V_{ABB} , K_{ABB}) interaction coefficients for (DEGMME/ DEGMEE + maltitol) at 0.1 MPa pressure.

T/K	$V_{AB} \times 10^6 (m^3 \cdot mol^{-2} \cdot kg)$	$V_{ABB} \times 10^6 (m^3 \cdot mol^{-3} \cdot kg^2)$	$K_{AB} \times 10^6 (m^3 \cdot mol^{-2} \cdot kg \cdot GPa^{-1})$	$K_{ABB} \times 10^6 (m^3 \cdot mol^{-3} \cdot kg^2 \cdot GPa^{-1})$
DEGMME				
288.15	1.27	13.81	7.61	-6.33
298.15	0.92	17.98	7.75	-11.03
308.15	1.97	14.88	7.68	-9.15
318.15	3.31	9.20	13.32	-36.51
DEGMEE				
288.15	1.07	3.00	7.72	-6.98
298.15	1.21	3.27	7.83	-11.56
308.15	1.43	3.66	7.75	-9.66
318.15	1.30	6.26	13.37	-36.89

theory helpful for the calculation of ΔV_ϕ^0 , which helps in understanding how the volume of a solution changes with the addition of a solutes. This is also suggesting that the V_ϕ^0 of a solute is affected by its interactions with solvent molecules. By using these interactions into pairwise effects, the theory allows for a detailed quantification of each interaction's contribution to the partial molar volume, for equations **4.11** and **4.12** it has been calculated. All the values for volumetric coefficients (V_{AB} , V_{ABB}) are positives for both solutes (DEGMME and DEGMEE) at all temperatures. There is irregular trend in the calculated values. On the other hand, compression pair interaction coefficients (K_{AB}) are positives but compression triplet coefficients (K_{ABB}) are negatives at all thermal conditions [61]. The values for pair and triplet coefficients show the hydrophilic-hydrophilic interactions among solutes and co-solutes. The values of V_{AB} , K_{AB} and V_{ABB} , K_{ABB} are shown in **Table 4.31**. The interactions among the solute and co-solute arise because of overlapping hydration spheres.

Thermal expansion coefficients

Thermal expansion coefficients (α_p) indicates to volume change of a substance with temperature. Thermal expansions coefficients for ternary mixtures of (maltitol+ DEGMME/DEGMEE) was calculated by equation **4.13**. In **Table 4.32**. values of thermal expansion coefficients are reported at various temperatures. To interpret the solute-solvent associations, thermal expansion coefficients can be used [62,63].

Table 4.32 Calculated isothermal expansion coefficients for (DEGMME/ DEGMEE + maltitol).

$^a m_B / (mol \cdot kg^{-1})$	$\alpha_p \times 10^3 / (K^{-1})$			
	T=288.15K	T=298.15K	T=308.15K	T=318.15K
DEGMME				
0.04	0.241	0.241	0.240	0.239
0.06	0.213	0.247	0.280	0.313
0.08	0.258	0.273	0.287	0.301
DEGMEE				
0.04	0.119	0.107	0.095	0.083
0.06	0.099	0.091	0.084	0.076
0.08	0.093	0.084	0.076	0.068

References

1. Y. Ma, Zhu and C. Zhou, *J. Chem. Eng. Data* 55, 3882–3885 (2010).
2. N. Chakraborty, K.C. Juglan and H. Kumar, *J. Mol. Liq.* 337, 116605 (2021).
3. H. Kumar, R. Sharma and M. Singla, *J. Mol. Liq.* 342, 117022 (2021).
4. H. Kaur, N. Chakraborty, K.C. Juglan and H. Kumar, *J. Sol. Chem.* 50 1079–1102 (2021).
5. P. Kaur, N. Chakraborty, H. Kumar, M. Singla and K.C. Juglan, *J. Sol. Chem.* 51, 1268–1291 (2022).
6. P. Anila, K.R. Reddy, G.S. Rao, P.V.S. Sairam, D. Ramachandran and C. Rambabu, *Thermochim. Acta* 620, 1–9 (2015).
7. K.D. Amirchand, S. Kaur, T.S. Banipal and V. Singh, *J. Mol. Liq.* 334, 116077 (2021).
8. N. Chakraborty, K. Kaur, K.C. Juglan and H. Kumar, *J. Chem. Eng. Data* 65, 1435–1446 (2020).
9. R. Rani, A. Kumar, T. Sharma, T. Sharma and R.K. Bamezai, *J. Chem. Thermodyn.* 135, 260–277 (2019),
10. K. Kaur, K.C. Juglan and H. Kumar, *J. Mol. Liq.* 268, 700–706 (2018).
11. C. Das, *J. Chem. Eng. Data*, 59, 168–175 (2014).
12. M.J. Iqbal and M.A. Chaudhry, *J. Chem. Thermodyn.* 42, 951–956 (2010).
13. N. Chakraborty, K.C. Juglan and H. Kumar, *ACS Omega*, 5, 32357–32365 (2020).
14. C. Zhu, X. Ren and Y. Ma, *J. Chem. Eng. Data*, 62, 477–490 (2017).
15. P.A. Leduc, J.L. Fortier and J.E. Desnoyers, *J. Phys. Chem.* 78, 1217–1225 (1974).
16. A.K. Mishra and J.C. Ahluwalia, *J. Phys. Chem.* 88, 86–92 (1984).
17. N. Chakraborty, H. Kumar, K. Kaur and K.C. Juglan, *J. Chem. Thermodyn.* 126, 137–146 (2018).
18. Y. Marcus, *Chem. Rev.* 109, 1346–1370 (2009).
19. F. Shahidi, P.G. Farrell and J.T. Edward, *J. Sol. Chem.* 5, 807–816 (1976).
20. S. Devi, M. Kumar, N. Sawhney, U. Syal, A.K. Sharma and M. Sharma, *J. Chem. Thermodyn.* 154, 106321 (2021).
21. R.S. Sah, P. Pradhan and M.N. Roy, *Thermochim. Acta* 499, 149–154 (2010).
22. H. Shekaari, S.S. Mousavi and Y. Mansoori, *Int. J. Thermophys.* 30, 499–514 (2009).

23. L.G. Hepler, *Can. J. Chem.* 47, 4613–4617 (1969).
24. R. Gaba, A. Pal, D. Sharma and D.A. Khajuria, *J. Mol. Liq.* 234, 187–193 (2017).
25. Q.M. Omar, J.N. Jaubert and J. A. Awan, *Int. J. Chem. Eng.* 1–10 (2018).
26. M.S. Raman, M. Kesavan, K. Senthilkumar and V. Ponnuswamy, *J. Mol. Liq.* 202, 115–124 (2015).
27. K.C. Juglan and H. Kumar, *Results Chem.* 2, (2020).
28. T.S. Banipal, D. Kaur, P.K. Banipal and G. Singh, *J. Chem. Thermodyn.* 39, 371–384 (2007).
29. R. Sadeghi and A. Gholamireza, *J. Chem. Thermodyn.* 43, 200–215 (2011).
30. S.S. Dhondge, R.L. Paliwal and N.S. Bhawe, *J. Chem. Thermodyn.* 59, 158–165 (2013).
31. A.K. Nain and R. Pal, *J. Chem. Thermodyn.* 64, 172–181 (2013).
32. C.M. Romero, J.M. Lozano and G.I. Giraldo, *Phys. Chem. Liq.* 46, 78–85 (2008).
33. S. Baluja and S. Oza, *Fluid Phase Equilib.* 178, 233–238 (2001).
34. A. Salabat, L. Shamshiri and F. Sahrakar, *J. Mol. Liq.* 118, 7–70 (2005).
35. R. Sadeghi and F. Ziamajidi, *J. Chem. Eng. Data* 52, 1037–1044 (2007).
36. H. Kumar, M. Singla and R. Jindal, *Monat. Chem.-Chem. Monthly* 145, 1063–1082 (2014).
37. W.G. McMillan Jr and J.E. Mayer, *J. Chem. Phys.* 13, 276–305 (1945).
38. C.V. Krishnan and H.L. Friedman, *J. Sol. Chem.* 2, 37–51 (1973).
39. M.A. Mohamed, J. Jaafar, A.F. Ismail, M.H.D. Othman and M.A. Rahman, 3–29 (2017).
40. V. Abbot and P. Sharma, *J. Mol. Liq.* 328, 115489 (2021).
41. H. Kaur, N. Chakraborty, K.C. Juglan and A. Upmanyu, *J. Mol. Liq.* 392, 123403 (2013).
42. K. Bhakri N. Chakraborty, K.C. Juglan, H. Kumar and R. Sharma, *J. Therm. Analys. Calorim.* 148, 7185–7205 (2023).
43. S. Chauhan, M.S. Chauhan, D. Kaushal, V.K. Syal and J. Jyoti, *J. Sol. Chem.* 39, 622–638 (2010).
44. K. Kaur, K.C. Juglan and H. Kumar, *J. Chem. Eng. Data* 127, 8–16 (2018).
45. S.K. Lomesh, M. Bala, D. Kumar and I. Kumar, *J. Mol. Liq.* 289, 109479 (2019).
46. R.C. Thakur, R. Sharma and M. Bala, *J. Mater. Environ. Sci.* 7, 3415–3420 (2016).

47. R.C. Thakur, R. Sharma, A. Kumar, S. Kumar and M.L. Parmar Orient. J. Chem 30, 2037-2041 (2014).
48. I. Banik and M.N. Roy, J. Mol. Liq. 203, 66-79 (2015).
49. D. Brahman and B. Sinha, J. Chem. Thermodyn. 75, 136-144 (2014).
50. M.N. Roy, B. Sinha, R. Dey and A. Sinha, Inter. J. Thermophys. 26, 1549-1563 (2005).
51. P. Kaur, N. Chakraborty, K.C. Juglan and H. Kumar, J. Mol. Liq. 315, 113763 (2020).
52. B. Naseem, I. Arif and M.A. Jamal, Arab. J. Chem. 14, 103405 (2021).
53. M.N. Roy, V.K. Dakua and B. Sinha, Inter. J. Thermophys. 28, 1275-1284 (2007).
54. R.L. Gardas, D.H. Dagade, J.A. Coutinho and K.J. Patil J. Phy. Chem. B 112, 3380-3389 (2008).
55. H.S. Frank and M.W. Evans, J. Chem. phys. 13, 507-532 (1945).
56. H. Kumar, M. Singla and R. Jindal, J. Mol. Liq. 199, 385-392 (2014).
57. J. G. Kirkwood, Chem. Reviews 24, 233-251 (1939).
58. P. Ramasami and R. Kakkar, J. Chem. Thermodyn. 38, 1385-1395 (2006).
59. R. Sadeghi and F. Ziamajidi J. Chem. Eng. Data 52, 1037-1044 (2007).
60. U. Gazal, Ameri. J. Analyt. Chem. 14, 72-94 (2023).
61. M. Lamba, N. Chakraborty, K.C. Juglan, M. Singla and R. Sharma, J. Mol. Liq. 390, 123045 (2023).
62. S.S. Dhondge, S.P. Zodape and D.V. Parwate J. Chem. Thermodyn. 48, 207-212 (2012).
63. A. Pal, H. Kumar, B. Kumar, P. Sharma and K. Kaur, J. Chem. Thermodyn. 57, 182-188 (2013).

Section III

Problem 4

Study of Thermodynamic and Acoustic Properties of DEGMME/ DEGMEE in aqueous Erythritol solutions at different temperatures

In this problem, densities values and speed of sound values, of DEGMME/DEGMEE in (0.1, 0.2 and 0.3 mol.kg⁻¹) erythritol (aq) mixtures, were obtained at T= (288.15-318.15) K.

Apparent Molar Volume

The density and speed of sound data were used to analyse various parameters. The density data demonstrate that, the values rises as erythritol concentration rises and decreases as temperature increases. The comparison of experimental densities of a binary mixture (erythritol and water) with literature [1-3] is shown in **Figure 4.23**. Additionally, comparison of experimental densities of a binary mixture (water +DEGMME/DEGMEE) with literature [4,5] is displayed in **Figure 4.24**. **Figure 4.23** and **Figure 4.24** clearly shows that the density correlate well with literature data. Equation 4.1 is used to investigate V_ϕ . All the values of density and V_ϕ are given in **Table 4.33** at all temperatures and concentration. From the table values, it is analysing that that all the values of density decreasing with temperatures and increasing with molality and concentration. On the other side, values of V_ϕ are all positives as well as increasing with temperatures, molality, and concentration of erythritol. Additionally, it gives great insight into the behaviour of solutes in solution [6]. **Figure 4.25**. depicts the graphical trends of V_ϕ v/s molality. All the positive values of apparent molar volume indicate that solute molecules are occupying more space in the solution as compared to pure form. This is also suggesting, that there is volume increase and expansions when solute dissolved in solvent [7,8]. Furthermore, the increase in concentration leads to a corresponding increase in volume, associations among the molecules of solute and solvent. These interlinkages help to reduce the electrostriction effect exerted by water molecules within the solution bulk, ultimately contributing to the rise in the apparent molar volume [9]. **Figure 4.26** indicates to the experimental procedure and shows interactions between DEGMME/DEGMEE and Erythritol.

Table 4.33 Values of ρ and V_ϕ for solutions of DEGMME/ DEGMEE in erythritol aqueous solutions.

$^a m_A / (mol \cdot kg^{-1})$	$\rho \times 10^{-3} / (kg \cdot m^{-3})$				$V_\phi \times 10^6 / (m^3 \cdot mol^{-1})$			
	T/K=288.15	T/K=298.15	T/K=308.15	T/K=318.15	T/K=288.15	T/K=298.15	T/K=308.15	T/K=318.15
DEGMME + 0.0 $mol \cdot kg^{-1}$ Erythritol								
0.00000	0.99926	0.99705	0.99404	0.99036				
0.09897	1.00043	0.99821	0.99521	0.99154	108.27	108.56	108.77	109.00
0.20115	1.00145	0.99923	0.99623	0.99256	109.11	109.38	109.63	109.92
0.30955	1.00231	1.00008	0.99708	0.99346	110.04	110.33	110.58	110.78
0.39951	1.00290	1.00067	0.99766	0.99403	110.71	111.00	111.29	111.54
0.50172	1.00345	1.00119	0.99818	0.99452	111.41	111.74	112.05	112.40
DEGMME + 0.1 $mol \cdot kg^{-1}$ Erythritol								
0.00000	1.00306	1.00096	0.99777	0.99391				
0.09997	1.00389	1.00178	0.99860	0.99476	111.42	111.67	111.94	112.11
0.20015	1.00465	1.00253	0.99936	0.99553	111.69	112.00	112.26	112.48
0.30855	1.00538	1.00325	1.00009	0.99628	112.06	112.34	112.61	112.84
0.39911	1.00593	1.00378	1.00061	0.99682	112.31	112.65	112.94	113.15
0.50152	1.00648	1.00430	1.00114	0.99735	112.62	112.99	113.28	113.53
DEGMME + 0.2 $mol \cdot kg^{-1}$ Erythritol								

0.00000	1.00659	1.00431	1.00119	0.99728				
0.09928	1.00729	1.00501	1.00190	0.99802	112.36	112.54	112.75	112.93
0.19973	1.00794	1.00566	1.00257	0.99871	112.56	112.75	112.95	113.14
0.31045	1.00858	1.00632	1.00324	0.99941	112.81	112.98	113.18	113.36
0.39860	1.00906	1.00679	1.00373	0.99991	112.98	113.18	113.37	113.55
0.49820	1.00954	1.00727	1.00423	1.00043	113.19	113.39	113.57	113.76

DEGMME + 0.3 $\text{mol} \cdot \text{kg}^{-1}$ Erythritol

0.00000	1.01001	1.00778	1.00461	1.00068				
0.09833	1.01065	1.00842	1.00527	1.00136	112.56	112.71	112.88	113.04
0.19730	1.01124	1.00902	1.00588	1.00200	112.74	112.90	113.07	113.24
0.29999	1.01180	1.00958	1.00646	1.00261	112.93	113.10	113.28	113.43
0.39556	1.01228	1.01006	1.00696	1.00312	113.09	113.28	113.45	113.61
0.50009	1.01275	1.01054	1.00745	1.00364	113.28	113.48	113.66	113.82

DEGMEE + 0.0 $\text{mol} \cdot \text{kg}^{-1}$ Erythritol

0.00000	0.99926	0.99705	0.99404	0.99036				
0.09903	1.00001	0.99781	0.99482	0.99117	126.59	126.73	126.87	126.99
0.19262	1.00067	0.99848	0.99551	0.99189	126.76	126.91	127.05	127.17
0.29786	1.00135	0.99918	0.99623	0.99264	126.97	127.12	127.25	127.37
0.40279	1.00198	0.99981	0.99689	0.99333	127.17	127.32	127.46	127.58

0.49997	1.00250	1.00034	0.99744	0.99391	127.36	127.52	127.65	127.77
DEGMEE + 0.1 $\text{mol} \cdot \text{kg}^{-1}$ Erythritol								
0.00000	1.00306	1.00096	0.99777	0.99391				
0.10028	1.00376	1.00167	0.99851	0.99468	126.71	126.81	126.92	127.05
0.20062	1.00441	1.00234	0.99920	0.99541	126.87	126.98	127.10	127.22
0.30086	1.00501	1.00295	0.99984	0.99608	127.06	127.17	127.30	127.42
0.41279	1.00562	1.00358	1.00048	0.99676	127.27	127.38	127.52	127.63
0.49937	1.00604	1.00402	1.00094	0.99724	127.44	127.54	127.69	127.81
DEGMEE + 0.2 $\text{mol} \cdot \text{kg}^{-1}$ Erythritol								
0.00000	1.00659	1.00431	1.00119	0.99728				
0.10200	1.00725	1.00499	1.00190	0.99803	126.80	126.88	126.97	127.05
0.20282	1.00794	1.00569	1.00264	0.99881	126.96	127.04	127.13	127.21
0.29909	1.00840	1.00617	1.00314	0.99935	127.08	127.16	127.25	127.34
0.40071	1.00899	1.00678	1.00378	1.00003	127.25	127.33	127.42	127.49
0.49746	1.00939	1.00720	1.00422	1.00050	127.38	127.46	127.54	127.62
DEGMEE + 0.3 $\text{mol} \cdot \text{kg}^{-1}$ Erythritol								
0.00000	1.01001	1.00778	1.00461	1.00068				
0.10000	1.01061	1.00839	1.00525	1.00136	126.96	127.04	127.11	127.18
0.19999	1.01116	1.00896	1.00585	1.00200	127.09	127.18	127.24	127.32

0.29870	1.01166	1.00948	1.00641	1.00259	127.22	127.30	127.37	127.44
0.41360	1.01221	1.01004	1.00700	1.00323	127.37	127.46	127.54	127.60
0.49390	1.01256	1.01040	1.00738	1.00364	127.47	127.57	127.65	127.71

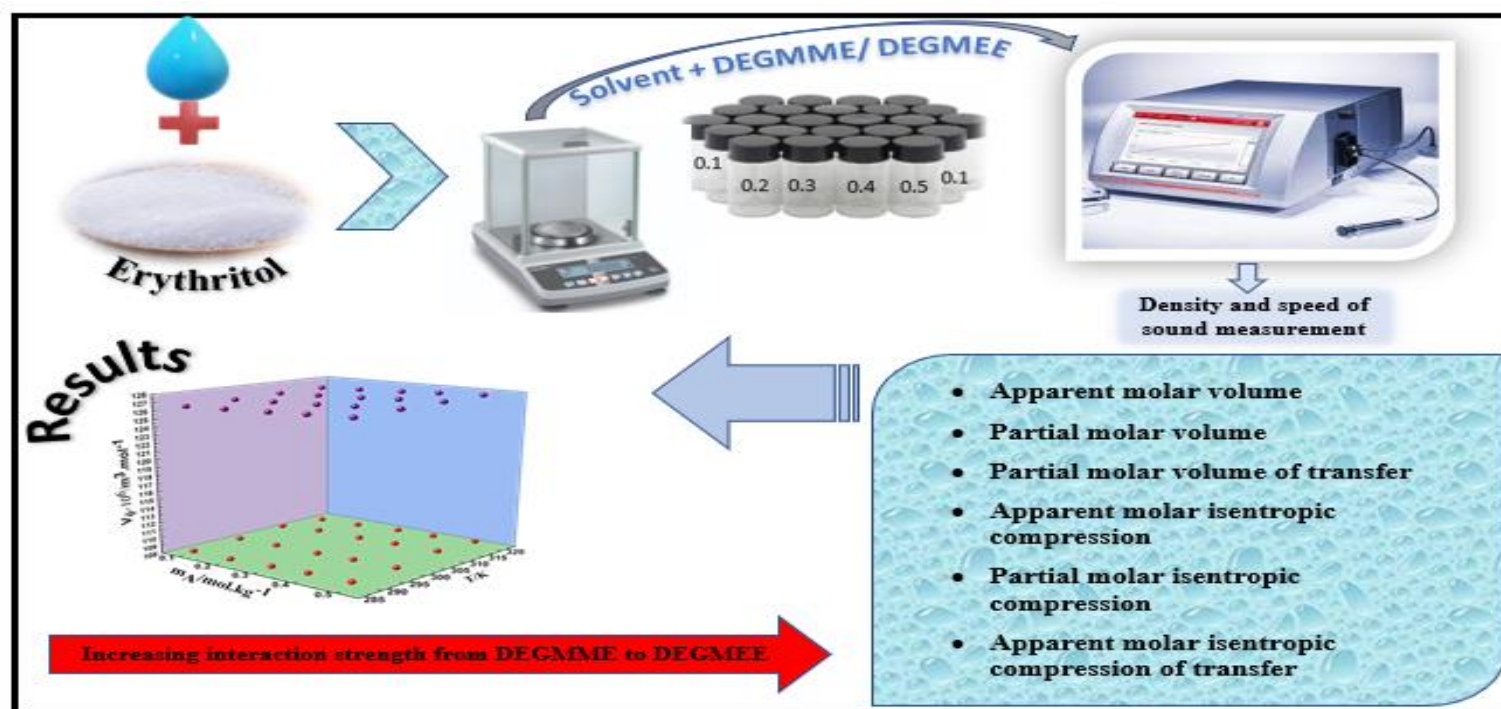


Figure 4.26 Interactions between DEGME/DEGMEE and Erythritol.

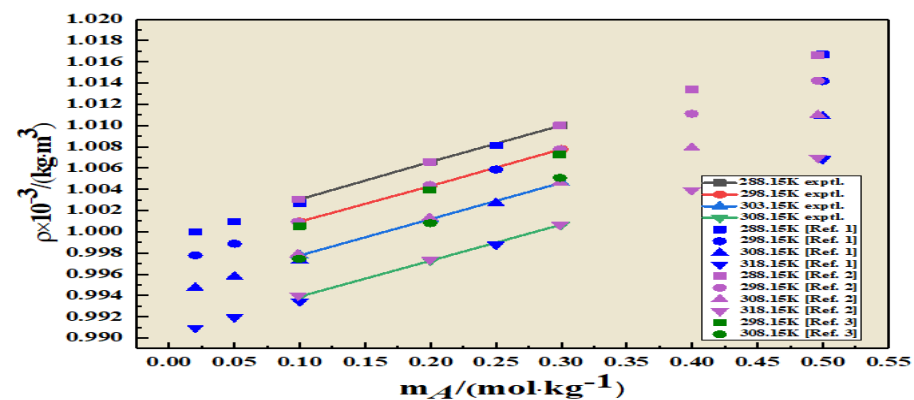


Figure 4.23 Experimental (line + symbol) and literature values (scatter) [1-3] of density for erythritol + water at different temperatures.

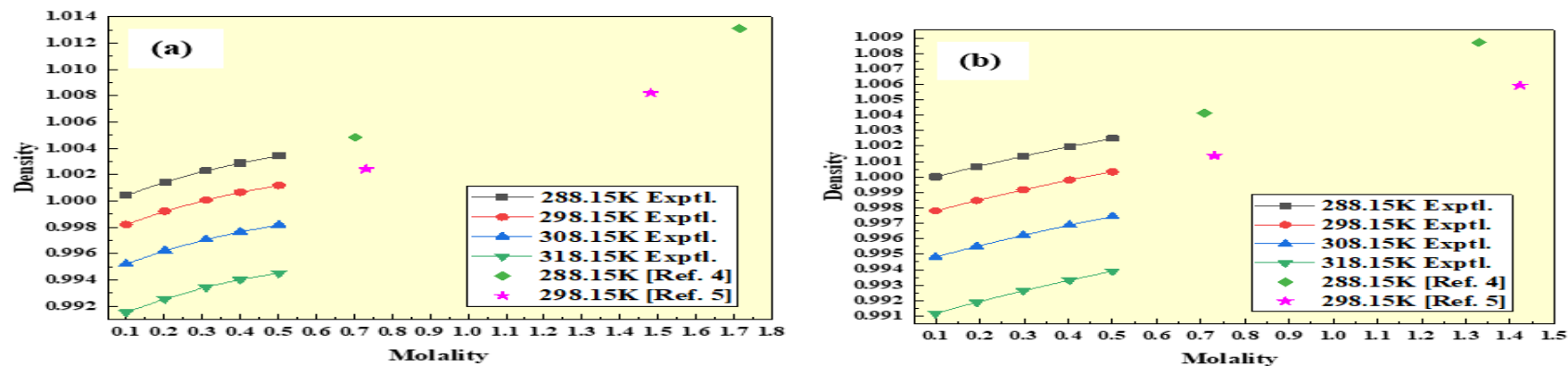
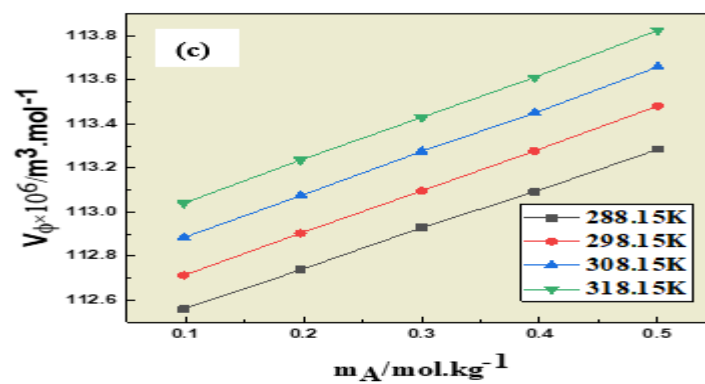
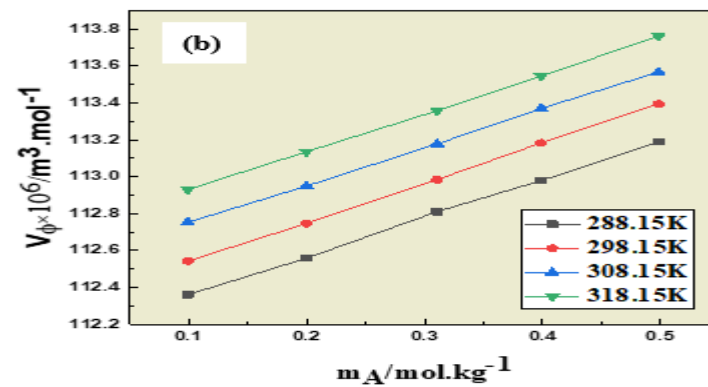
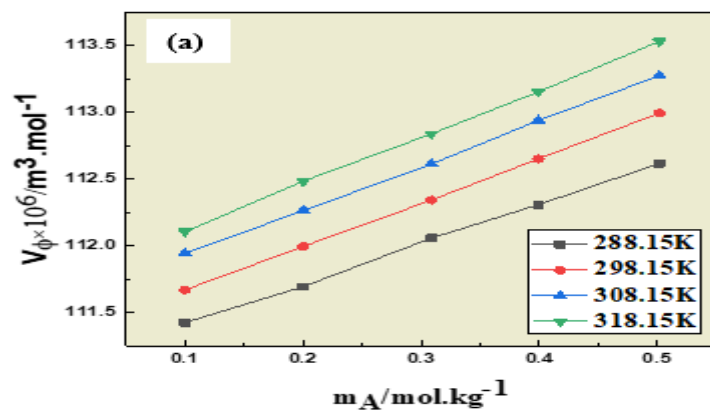


Figure 4.24 Experimental (line + symbol) and literature values (scatter) [4,5] of density for (a) DEGMME and (b) DEGMEE at different temperatures.

(I)



(II)

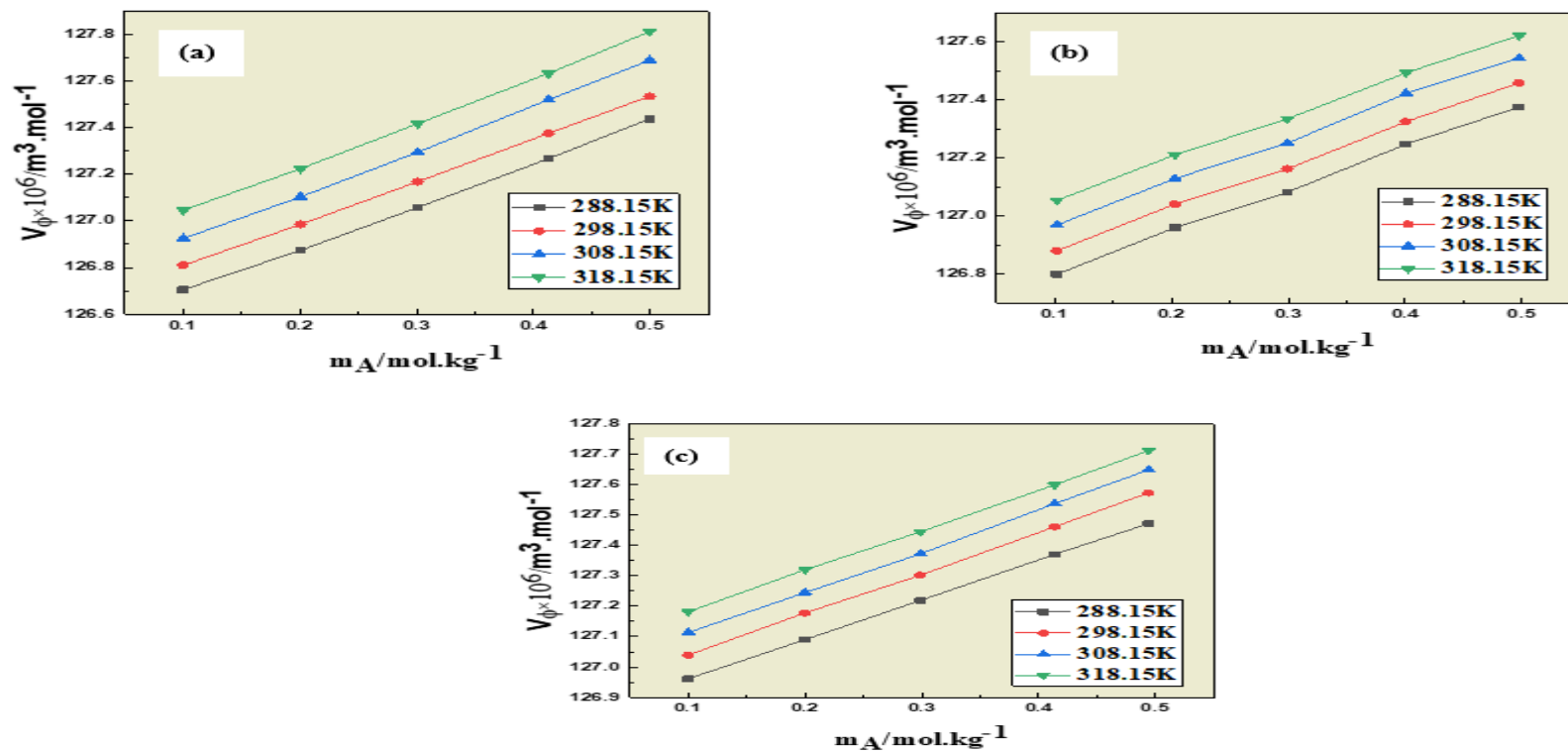


Figure 4.25 Plot of V_ϕ for (I) DEGMME and (II) DEGMEE at different temperatures and different concentrations of erythritol: (a) 0.1 Erythritol, (b) 0.2 Erythritol, and (c) 0.3 Erythritol ($\text{mol} \cdot \text{kg}^{-1}$).

Partial molar volume

It is useful in understanding solutions and mixtures and it is obtained by equation 4.2. For small concentrations, this linear relationship is valid, as the concentration, is low enough that higher-order effects can be neglected. In this case, equation (2) describes the system well. However, as the concentration increases, non-linear effects start to play a role, and the simple linear term $S_V^* m_A$ no longer captures the behaviour accurately. At high concentrations, it is important to include a non-asymptotic correction term proportional to $(m_A)^{1/2}$, which accounts for deviations from ideal behaviour. The Debye–Hückel limiting law for volumes has been used via the following equation [10].

$$V_\phi = V_\phi^0 + S_V^* m_A + C(m_A)^{1/2} \quad (4.17)$$

Here, m_A is solute's molality, and S_V^* and C , are the two adjustable parameters. **Table 4.34** presents the values of V_ϕ^0 and slope (S_V^*), and C , along with standard errors. These values are crucial for understanding the different associations. It is providing significant insights into the nature of solute-solvent associations and the behaviour of solutions at varying concentrations. The values of V_ϕ^0 , indicates that solute molecules occupy more space in the solution as compared to the pure solvent. As **Table 3.34** depicts that all the values of V_ϕ^0 are positives and rising with upsurge in the concentrations as well as with temperature. This is due to the that solute molecule's structure and size as compare to solvent molecules which leads to increase in the volume. **Figure 4.27.** represents the trend of V_ϕ^0 value with respect to temperatures and molality. The volume decreases when hydrophobic-2 and ion-hydrophobic groups overlap, volume increases when two ionic species overlap [11,12]. At infinite dilution, there are no solute-solute or ion-ion interactions. Partial molar properties depend on temperature, influencing solvent-solvent interactions and resulting in volume changes. This relationship is evident in the increasing values shown in **Table 4.34**. The positive V_ϕ^0 values suggest hydrophobic effects and strong H-bond formation [13]. The significantly smaller S_V^* values, compared to V_ϕ^0 values, indicate that solute-solvent associations predominate in this system, defining the volumetric properties of the liquid combination [14-17]

Table 4.34 Partial molar volumes, V_ϕ^0 , and parameters S_V^* , and C with standard deviations, for DEGMME/ DEGMEE in erythritol (aq) solutions at p=0.1 MPa.

Parameters	T/K			
	288.15K	298.15K	308.15K	318.15K
DEGMME + 0.0 Erythritol				
$V_\phi^0 \times 10^6 (m^3.mol^{-1})$	107.54 (± 0.06)	107.80 (± 0.06)	107.99 (± 0.05)	108.19 (± 0.03)
$S_V^* \times 10^6 (m^3.kg.mol^{-2})$	7.84 (± 0.20)	7.96 (± 0.20)	8.20 (± 0.15)	8.39 (± 0.96)
$C \times 10^6 (m^3.kg.mol^{-2})$	2.70 (± 1.17)	2.02 (± 1.31)	2.07 (± 0.92)	0.74 (± 0.92)
DEGMME + 0.1 Erythritol				
$V_\phi^0 \times 10^6 (m^3.mol^{-1})$	111.12 (± 0.02)	111.34 (± 0.07)	111.60 (± 0.01)	111.76 (± 0.02)
$S_V^* \times 10^6 (m^3.kg.mol^{-2})$	3.00 (± 0.05)	3.30 (± 0.02)	3.33 (± 0.03)	3.52 (± 0.04)
$C \times 10^6 (m^3.kg.mol^{-2})$	0.08 (± 0.51)	-0.44 (± 0.29)	-0.27 (± 0.14)	-0.15 (± 0.58)
DEGMME + 0.2 Erythritol				
$V_\phi^0 \times 10^6 (m^3.mol^{-1})$	112.15 (± 0.01)	112.32 (± 0.01)	112.54 (± 0.01)	112.72 (± 0.01)
$S_V^* \times 10^6 (m^3.kg.mol^{-2})$	2.08 (± 0.03)	2.14 (± 0.02)	2.06 (± 0.02)	2.08 (± 0.02)
$C \times 10^6 (m^3.kg.mol^{-2})$	0.01 (± 0.32)	-0.25 (± 0.13)	-0.17 (± 0.17)	-0.25 (± 0.11)
DEGMME + 0.3 Erythritol				
$V_\phi^0 \times 10^6 (m^3.mol^{-1})$	112.38 (± 0.01)	112.53(± 0.00)	112.70 (± 0.01)	112.85(± 0.01)
$S_V^* \times 10^6 (m^3.kg.mol^{-2})$	1.80 (± 0.01)	1.91 (± 0.01)	1.92 (± 0.01)	1.94 (± 0.02)

$C \times 10^6 (m^3.kg.mol^{-2})$	0.05 (± 0.15)	-0.04 (± 0.08)	-0.01 (± 0.16)	-0.08 (± 0.17)
DEGMEE + 0.0 Erythritol				
$V_\phi^0 \times 10^6 (m^3.mol^{-1})$	126.39 (± 0.01)	126.54 (± 0.00)	126.68 (± 0.00)	126.80 (± 0.00)
$S_V^* \times 10^6 (m^3.kg.mol^{-2})$	1.92 (± 0.02)	1.96 (± 0.01)	1.93 (± 0.01)	1.93 (± 0.01)
$C \times 10^6 (m^3.kg.mol^{-2})$	-0.12 (± 0.20)	-0.09 (± 0.01)	-0.18 (± 0.01)	-0.15 (± 0.09)
DEGMEE + 0.1 Erythritol				
$V_\phi^0 \times 10^6 (m^3.mol^{-1})$	126.51 (± 0.01)	126.62 (± 0.00)	126.72 (± 0.01)	126.85 (± 0.01)
$S_V^* \times 10^6 (m^3.kg.mol^{-2})$	1.84 (± 0.03)	1.82 (± 0.01)	1.93 (± 0.03)	1.92 (± 0.03)
$C \times 10^6 (m^3.kg.mol^{-2})$	-0.46 (± 0.05)	-0.18 (± 0.04)	-0.38 (± 0.08)	-0.43 (± 0.09)
DEGMEE + 0.2 Erythritol				
$V_\phi^0 \times 10^6 (m^3.mol^{-1})$	126.66 (± 0.01)	126.73 (± 0.01)	126.82 (± 0.01)	126.91 (± 0.01)
$S_V^* \times 10^6 (m^3.kg.mol^{-2})$	1.46 (± 0.03)	1.46 (± 0.03)	1.46 (± 0.04)	1.44 (± 0.02)
$C \times 10^6 (m^3.kg.mol^{-2})$	0.15 (± 0.33)	0.10 (± 0.31)	0.17 (± 0.39)	0.16 (± 0.25)
DEGMEE + 0.3 Erythritol				
$V_\phi^0 \times 10^6 (m^3.mol^{-1})$	126.83 (± 0.00)	126.90 (± 0.00)	126.97 (± 0.01)	127.05 (± 0.00)
$S_V^* \times 10^6 (m^3.kg.mol^{-2})$	1.30 (± 0.00)	1.35 (± 0.01)	1.36 (± 0.02)	1.34 (± 0.01)
$C \times 10^6 (m^3.kg.mol^{-2})$	0.00 (± 0.05)	-0.06 (± 0.14)	-0.23 (± 0.09)	-0.04 (± 0.13)

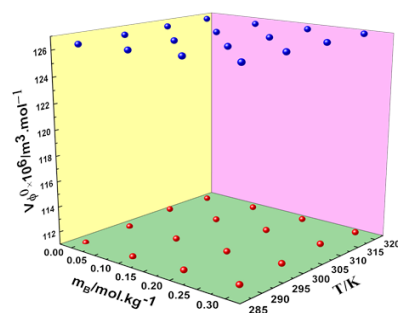


Figure 4.27 Partial molar volume, V_{ϕ}^0 , for DEGMME (red) and DEGMEE (blue) within an Erythritol aqueous solution at various temperatures.

Partial molar volume of Transfer

It is implying the variation in the partial volume of a substance when it is transferred from one phase to another. Values of ΔV_{ϕ}^0 for glycol ethers in aqueous erythritol solutions was calculated using the relation **4.3** at infinite dilution. **Table 4.35** contains the values ΔV_{ϕ}^0 at different temperatures. Values of **Table 4.35** depicts that all the value of ΔV_{ϕ}^0 are positive. All the values of ΔV_{ϕ}^0 depicts that the molecules associations of erythritol with DEGMME/ DEGMEE are weaker than the associations of H_2O +glycol ethers. All the positive values of ΔV_{ϕ}^0 indicates that the solute occupies more volume when transferred to the solution compared to an infinite dilution [18]. Additionally, with regard to these values, the contribution from solute-solute interaction is considered insignificant, allowing focus on solute-solvent interaction. According to the model, negative contributions originate from ion-hydrophobic and hydrophobic-2 associations, while positive contributions stem from other two types of interactions. Therefore, in our current investigation of erythritol in the presence of water and glycol ethers, it is evident that ion-hydrophilic associations and hydrophilic-2 associations exert a greater influence compared to the other two interactions [19-22].

Table 4.35 Values of ΔV_{ϕ}^0 , of DEGMME/ DEGMEE in aqueous solutions of erythritol.

^a $m_B/(mol \cdot kg^{-1})$	$\Delta V_{\phi}^0 \times 10^6 (m^3 \cdot mol^{-1})$			
	T = 288.15K	T = 298.15K	T = 308.15K	T = 318.15K
DEGMME				
0.1	3.578	3.539	3.613	3.569
0.2	4.614	4.528	4.555	4.528

0.3	4.845	4.729	4.706	4.656
DEGMEE				
0.1	0.117	0.088	0.046	0.044
0.2	0.261	0.200	0.146	0.110
0.3	0.437	0.369	0.296	0.247

Temperature-dependent partial molar volume

This parameter describes the change in volume of a substance when a slight quantity of it is added into a solution, accounting for the influence of temperature variations. It is an important parameter that gives great insight into the how the volume of a substance changes with temperature in a solution [23,24]. When substances are dissolved in a solution, they interact with the solvent molecules, due to which volume changes because of rearrangement of molecules and changes in intermolecular forces. The V_{ϕ}^0 quantifies the contribution of each component to the overall volume of the solution [25]. With the help of a polynomial equation 4.4 the variation of V_{ϕ}^0 with temperature calculated. **Table 4.36** contains the values of these parameters along with the deviation. The main purpose of studying V_{ϕ}^0 is to determine the E_{ϕ}^0 . The main purpose of the V_{ϕ}^0 data investigation was to use the 4.5 equation to get the E_{ϕ}^0 . In the solution, values of E_{ϕ}^0 indicates to solute- solvent interlinkage in the arrangement. The value of E_{ϕ}^0 are all positive at every temperature and compositions of the solution which indicating the interaction between the DEGMME/ DEGMEE in aqueous erythritol solution and decrease in the volume. All the value of E_{ϕ}^0 given in **Table 4.37**. The 4.6 equation was formulated to quantify the role of the solute in both building and disrupting structures within the system. The sign of $(\partial E_{\phi}^0 / \partial T)_p$, indicates whether the solute have a tendency to structure make or a structure break in the solvent. A positive or small negative value of $(\partial E_{\phi}^0 / \partial T)_p$ suggests that the solute exhibits a tendency to act as a structure maker. On the other hand, when values are negatives, it implies the structure breaking ability [26,27]. From the **Table 4.37** it can be analysing that there is no regular trend with concentration but the value of E_{ϕ}^0 is increase with temperature.

Table 4.36 Values of empirical constants for DEGMME/ DEGMEE in aqueous solutions of erythritol at p=0.1Mpa along with R² and ARD (deviations).

^a <i>m_B</i> /(mol · kg ⁻¹)	<i>a</i> × 10 ⁶ (m ³ .mol ⁻¹)	<i>b</i> × 10 ⁶ (m ³ .mol ⁻¹ .K ⁻¹)	<i>c</i> × 10 ⁶ (m ³ .mol ⁻¹ .K ⁻²)	<i>R</i> ²	ARD
DEGMME					
0.1	107.7847	0.0229	-0.00014	0.9999	0.0001
0.2	111.3582	0.0235	-0.00015	0.9999	0.0001
0.3	112.3377	0.0192	0.00001	0.9999	0.0000
DEGMEE					
0.1	126.5383	0.0141	-0.00004	0.9999	0.0000
0.2	126.6184	0.0108	0.00002	0.9999	0.0000
0.3	126.7367	0.0084	0.00002	0.9999	0.0000

Table 4.37 Partial molar expansibilities, E_{ϕ}^0 for DEGMME/ DEGMEE in erythritol (aq) solutions at different temperatures.

$^a m_B$	$E_{\phi}^0 \times 10^6 (m^3.mol^{-1}.K^{-1})$				$(\partial E_{\phi}^0 / \partial T)_p / (m^3.mol^{-1}.K^{-2})$		
$(mol \cdot kg^{-1})$	T	=	T	=	T	=	
	288.15K		298.15K		308.15K	318.15K	
DEGMME							
0.1	0.0265		0.0235		0.0206	0.0176	-0.0003
0.2	0.0189		0.0192		0.0194	0.0196	0.0000
0.3	0.0148		0.0154		0.0159	0.0165	0.0001
DEGMEE							
0.1	0.0103		0.0108		0.0113	0.0117	0.0000
0.2	0.0080		0.0084		0.0088	0.0091	0.0000
0.3	0.0071		0.0072		0.0073	0.0074	0.0000

Apparent molar isentropic compression

Experimentally measured density and sound velocity values are employed in Newton's Laplace equation 4.7 to calculate the isentropic compressibility, K_S . The obtained value of K_S was utilized to calculate the $K_{\phi,s}$ with the equation 4.8. **Table 4.38** presents the 'c' data alongside the determined $K_{\phi,s}$ values. The comparison of 'c' data for obtained values of a binary mixture (erythritol and water) with literature [2] is shown in **Figures. 4.28**. Additionally, speed of sound values for water + DEGMME/DEGMEE with literature [4,5] is presented in **Figure 4.29**. **Figure 4.28** and **Figure 4.29** clearly shows that the speed of sound correlates well with literature data. The derived $\kappa_{\phi,s}$ values consistently exhibit negativity across all temperatures and concentrations. **Figure 4.30** shown the trend of $K_{\phi,s}$ with molality at different temperatures. Additionally, these $K_{\phi,s}$ values exhibit a trend of becoming less negative with higher thermal condition, while increasing in negativity with glycol ethers. This negative $K_{\phi,s}$ value suggests reduced compressibility of water near charge groups, contrasting with its more ordered arrangement in the bulk solution [28-31]. The negative $K_{\phi,s}$ values indicate significant disruption to water's structural alignment, indicating notable solvent-solute interactions [32].

Table 4.38 Values of c , and $K_{\phi,S}$ of DEGMME/ DEGMEE in water and aqueous solutions of erythritol.

$^a m_A / (mol \cdot kg^{-1})$	$c / (m \cdot s^{-1})$		$K_{\phi,S} \times 10^6 / (m^3 \cdot mol^{-1} \cdot GPa^{-1})$					
	T/K=288.15	T/K=298.15	T/K=308.15	T/K=318.15	T/K=288.15	T/K=298.15	T/K=308.15	T/K=318.15
DEGMME + 0.0 $mol \cdot kg^{-1}$ Erythritol								
0.00000	1466.59	1495.85	1519.14	1536.02				
0.09897	1473.79	1503.79	1526.14	1543.44	-45.82	-44.30	-42.94	-42.00
0.20115	1481.09	1511.02	1533.01	1551.11	-46.11	-44.57	-43.21	-42.27
0.30955	1488.46	1519.01	1540.79	1559.29	-46.23	-44.69	-43.33	-42.38
0.39951	1495.19	1525.21	1546.79	1565.79	-46.29	-44.75	-43.38	-42.44
0.50172	1502.64	1532.12	1554.15	1573.25	-46.34	-44.79	-43.43	-42.48
DEGMME + 0.1 $mol \cdot kg^{-1}$ Erythritol								
0.00000	1470.72	1500.39	1523.11	1539.48				
0.09999	1478.43	1507.89	1529.47	1547.04	-45.82	-44.02	-42.71	-41.81
0.20015	1485.51	1514.78	1536.33	1554.29	-46.08	-44.27	-42.96	-42.05
0.30855	1493.54	1522.41	1543.63	1562.48	-46.19	-44.38	-43.07	-42.16
0.39911	1500.25	1528.87	1549.78	1569.33	-46.25	-44.44	-43.12	-42.22
0.50152	1507.95	1536.21	1556.71	1576.72	-46.30	-44.49	-43.17	-42.26
DEGMME + 0.2 $mol \cdot kg^{-1}$ Erythritol								
0.00000	1476.35	1505.54	1527.82	1543.881				

0.09928	1483.63	1512.37	1534.06	1551.03	-45.46	-43.71	-42.44	-41.56
0.19973	1491.08	1519.54	1540.57	1557.99	-45.72	-43.96	-42.69	-41.81
0.31045	1498.87	1527.13	1547.83	1566.11	-45.83	-44.07	-42.79	-41.91
0.39860	1505.5	1533.58	1553.56	1572.49	-45.88	-44.12	-42.85	-41.96
0.49820	1512.29	1540.24	1559.99	1579.97	-45.93	-44.16	-42.89	-42.01
DEGMME + 0.3 mol · kg ⁻¹ Erythritol								
0.00000	1481.55	1510.29	1532.16	1547.81				
0.09833	1488.63	1517.17	1538.06	1555.03	-45.14	-43.43	-42.20	-41.35
0.19730	1495.98	1523.54	1544.57	1561.99	-45.39	-43.68	-42.44	-41.59
0.29999	1503.67	1531.13	1550.93	1569.51	-45.49	-43.78	-42.54	-41.69
0.39556	1510.5	1537.58	1556.96	1576.49	-45.55	-43.84	-42.60	-41.74
0.50009	1517.79	1545.14	1563.89	1583.97	-45.60	-43.88	-42.64	-41.79
DEGMEE + 0.0 mol · kg ⁻¹ Erythritol								
0.00000	1466.59	1495.85	1519.14	1536.02				
0.09902	1478.19	1506.99	1530.13	1546.99	-46.07	-44.28	-42.86	-41.99
0.19262	1487.09	1516.99	1539.12	1556.44	-46.32	-44.53	-43.10	-42.23
0.29786	1496.86	1527.42	1550.23	1568.15	-46.44	-44.64	-43.21	-42.34
0.40279	1505.94	1537.88	1560.55	1579.25	-46.51	-44.71	-43.28	-42.41
0.49997	1514.94	1547.99	1570.15	1589.56	-46.56	-44.76	-43.33	-42.46

DEGMEE + 0.1 mol · kg ⁻¹ Erythritol								
0.00000	1470.72	1500.39	1523.11	1539.48				
0.10028	1481.55	1511.59	1533.87	1550.24	-45.81	-44.02	-42.71	-41.81
0.20062	1490.87	1522.11	1543.91	1561.18	-46.07	-44.27	-42.96	-42.05
0.30086	1500.58	1532.44	1554.55	1571.58	-46.18	-44.37	-43.06	-42.15
0.41279	1511.13	1543.92	1565.71	1583.54	-46.24	-44.44	-43.12	-42.22
0.49937	1519.15	1552.55	1574.22	1592.55	-46.28	-44.47	-43.16	-42.26
DEGMEE + 0.2 mol · kg ⁻¹ Erythritol								
0.00000	1476.35	1505.54	1527.82	1543.88				
0.10200	1486.05	1516.19	1537.87	1554.51	-45.47	-43.73	-42.46	-41.58
0.20282	1496.25	1528.03	1549.81	1566.47	-45.72	-43.97	-42.70	-41.82
0.29909	1504.18	1536.75	1558.29	1575.08	-45.82	-44.06	-42.79	-41.91
0.40071	1514.89	1548.46	1569.87	1587.18	-45.88	-44.12	-42.85	-41.97
0.49746	1522.4	1557.62	1578.91	1596.37	-45.92	-44.16	-42.89	-42.01
DEGMEE + 0.3 mol · kg ⁻¹ Erythritol								
0.00000	1481.55	1510.29	1532.16	1547.81				
0.09999	1491.25	1521.19	1541.99	1558.51	-45.14	-43.44	-42.21	-41.36
0.19999	1500.05	1531.03	1552.15	1568.77	-45.39	-43.68	-42.45	-41.59
0.29870	1509.58	1541.75	1561.88	1579.18	-45.49	-43.78	-42.54	-41.69

0.41360	1519.89	1553.46	1573.55	1591.18	-45.55	-43.84	-42.60	-41.75
0.49390	1527.4	1561.62	1582.45	1599.77	-45.59	-43.87	-42.64	-41.79

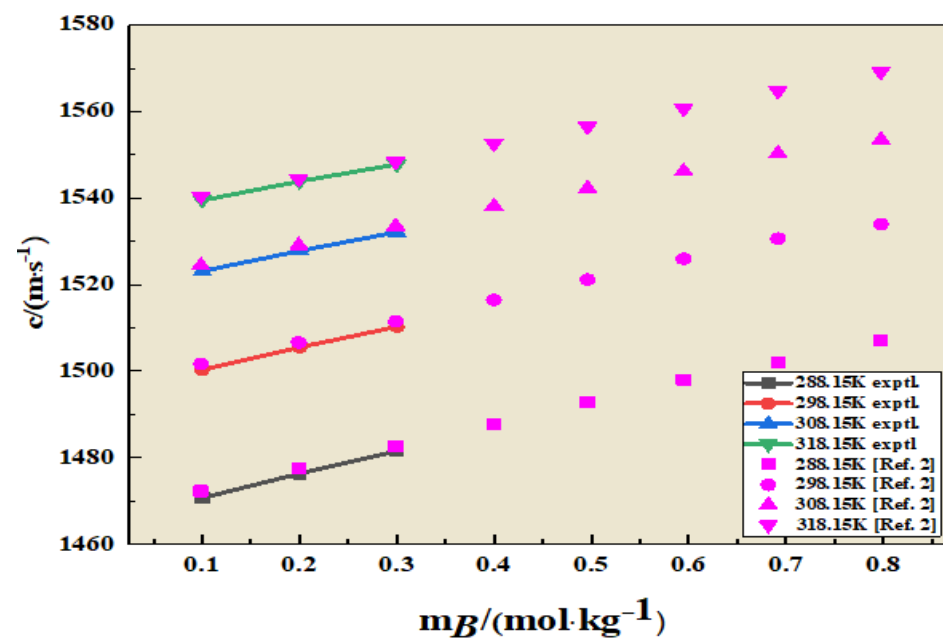


Figure 4.28 Experimental (line + symbol) and existing values (scatter) [2] of speed of sound for erythritol + water.

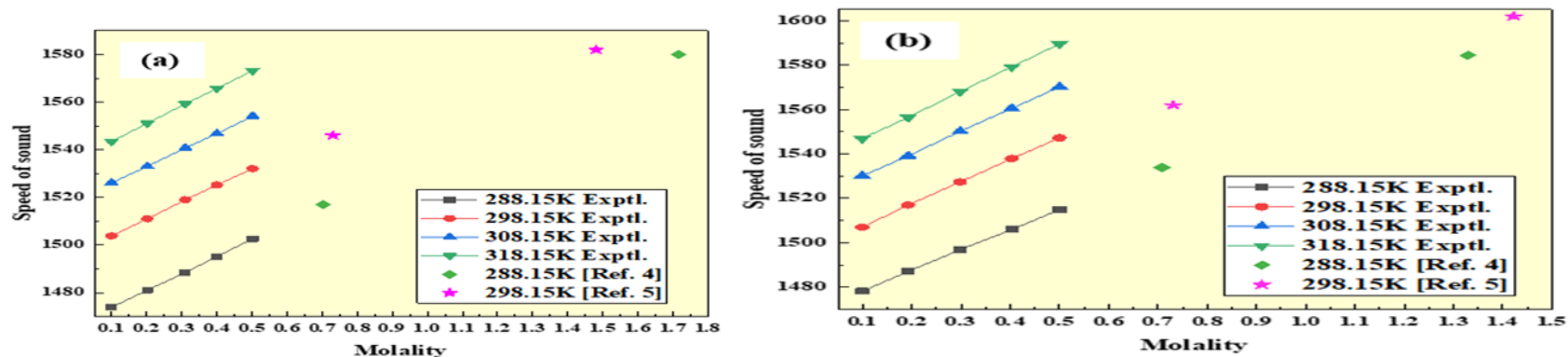


Figure 4.29 Experimental (line + symbol) and literature values(scatter) [4,5] of speed of sound for (a) DEGMME and (b) DEGMEE at different temperatures.

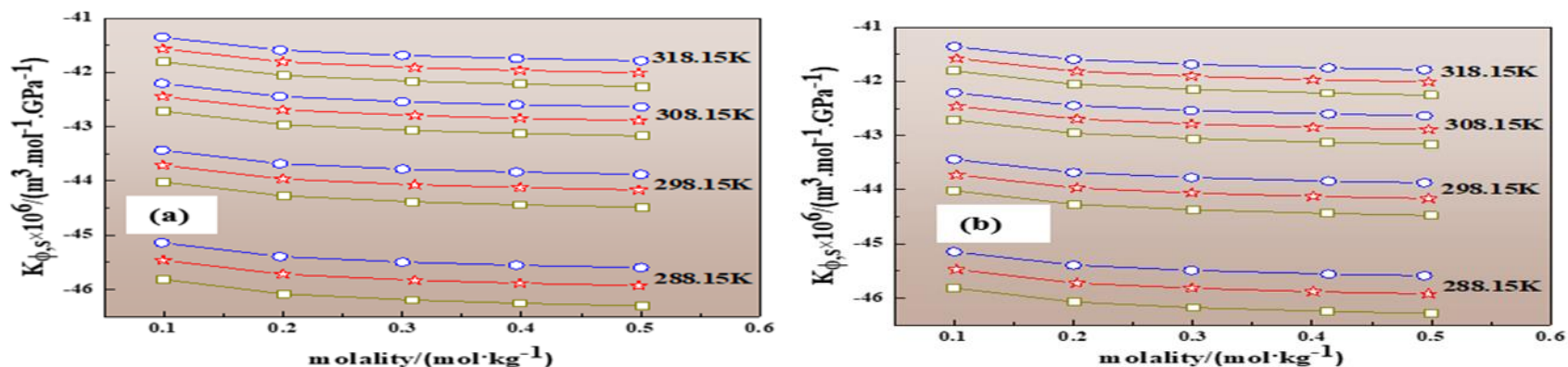


Figure 4.30 Values of $K_{\phi,s}$, v/s molality, for (a) DEGMME and (b) DEGMEE at different temperatures and concentrations, ($\text{mol} \cdot \text{kg}^{-1}$), 0.1 Erythritol (Square), 0.2 Erythritol (Star), and 0.3 Erythritol (circle).

Partial molar isentropic compression

It is obtained by using the equation 4.9. In Table 4.39 the $K_{\phi,s}^0$ values are provided alongside their associated standard errors and values of S_K^* . These values were determined using the least-squares fitting approach. Due to the small size of S_K^* , it suggests minimal solute-solute interaction at infinite dilution [33]. Notably, all $K_{\phi,s}^0$ values becoming less negative with rising values of temperature and solvent concentration. This trend suggests that some water molecules surrounding the glycol ether are less compressible. The small magnitude of S_K^* compared to $K_{\phi,s}^0$ underscores the latter's significance in gauging solute-solvent interaction strength. Furthermore, these values offer valuable insights into solute-2 associations, with solute-solvent associations prevailing in the solution [34-36]. The graphical representation of the values of $K_{\phi,s}^0$, shown in Figure 4.31.

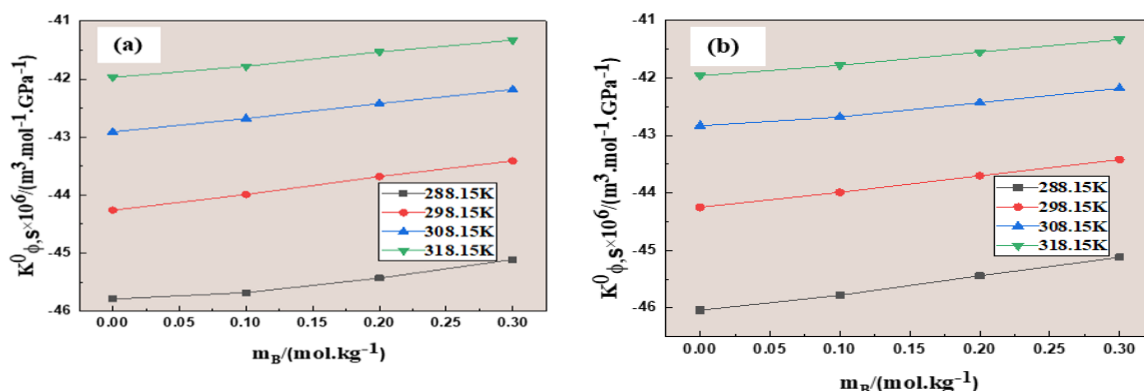


Figure 4.31. Plot of $K_{\phi,s}^0$ v/s molality, for (a) DEGMME and (b) DEGMEE in erythritol (aq) solutions at different temperatures.

Table 4.39 Values of $K_{\phi,s}^0$, experimental slopes, S_K^* , of DEGMME/ DEGMEE in water and erythritol (aq) solutions at p=0.1 MPa.

$^a m_B / (mol \cdot kg^{-1})$	$K_{\phi,s}^0 \times 10^6 / (m^3 \cdot mol^{-1} \cdot GPa^{-1})$				$S_K^* \times 10^6 (kg \cdot m^3 \cdot mol^{-2} \cdot GPa^{-1})$			
	T = 288.15K	T = 298.15K	T = 308.15K	T = 318.15K	T = 288.15K	T = 298.15K	T = 308.15K	T = 318.15K
DEGMME								
0.0	-45.79(±0.09)	-44.26(±0.09)	-42.91(±0.08)	-41.97(±0.09)	-1.22(±0.26)	-1.17(±0.25)	-1.14(±0.25)	-1.13(±0.25)
0.1	-45.78(±0.08)	-43.99(±0.08)	-42.68(±0.08)	-41.78(±0.08)	-1.15(±0.24)	-1.10(±0.24)	-1.08(±0.23)	-1.07(±0.23)
0.2	-45.43(±0.08)	-43.68(±0.08)	-42.42(±0.08)	-41.53(±0.07)	-1.11(±0.24)	-1.07(±0.23)	-1.05(±0.23)	-1.05(±0.22)
0.3	-45.11(±0.08)	-43.41(±0.08)	-42.18(±0.08)	-41.33(±0.07)	-1.08(±0.24)	-1.04(±0.23)	-1.02(±0.23)	-1.02(±0.23)
DEGMEE								
0.0	-46.04(±0.08)	-44.25(±0.08)	-42.83(±0.08)	-41.96(±0.08)	-1.15(±0.24)	-1.12(±0.24)	-1.10(±0.23)	-1.09(±0.23)
0.1	-45.78(±0.08)	-43.99(±0.08)	-42.68(±0.08)	-41.78(±0.07)	-1.10(±0.24)	-1.07(±0.23)	-1.06(±0.22)	-1.05(±0.22)
0.2	-45.44(±0.08)	-43.70(±0.08)	-42.43(±0.07)	-41.55(±0.07)	-1.07(±0.24)	-1.04(±0.23)	-1.03(±0.22)	-1.03(±0.22)
0.3	-45.12(±0.08)	-43.42(±0.07)	-42.18(±0.07)	-41.33(±0.07)	-1.05(±0.23)	-1.02(±0.22)	-1.01(±0.22)	-1.01(±0.21)

Partial molar isentropic compression of transfer

For DEGMME and DEGMEE in erythritol (aq), ΔK_{ϕ}^0 was calculated by using the equation 4.10. **Table 4.40** showcases the values for ΔK_{ϕ}^0 , which consistently exhibit positivity, escalating as the solvent concentration (erythritol + water) rises. This phenomenon finds explanation in the co-sphere overlap model, shedding light on volume expansion effects arising from interactions between solute molecules. Positive ΔK_{ϕ}^0 values indicate volume expansion due to water molecules dispensation hydrophilic centres, suggestive of robust solute-solvent interactions [37-39]. Particularly apparent at low temperatures and erythritol concentrations, these interactions foster increased water molecule association with the solute, notably ions, as elucidated by ΔK_{ϕ}^0 values.

Table 4.40 Values of ΔK_{ϕ}^0 of DEGMME/ DEGMEE in erythritol (aq) solutions at different for temperatures.

$^a m_B / (mol \cdot kg^{-1})$	$\Delta K_{\phi}^0 \times 10^6 (m^3 \cdot mol^{-1})$			
	T = 288.15K	T = 298.15K	T = 308.15K	T = 318.15K
DEGMME				
0.1	0.01	0.28	0.23	0.20
0.2	0.36	0.58	0.50	0.44
0.3	0.68	0.85	0.74	0.65
DEGMEE				
0.1	0.25	0.26	0.15	0.18
0.2	0.59	0.55	0.40	0.41
0.3	0.92	0.83	0.65	0.63

Pair and Triplet Coefficients

Friedman and Krishnan [40] expanded upon McMillian and Mayer's [41] hypothesis to elucidate a solute's transfer properties in aqueous erythritol solution. They proposed a methodology for determining solute and co-solute interaction coefficients. This relationship between ΔV_{ϕ}^0 , and ΔK_{ϕ}^0 is stated by equation 4.11 and 4.12 respectively. To attain the values for coefficients, the values of ΔV_{ϕ}^0 and $\Delta K_{\phi,s}^0$ must be fitted into the equations [42,43]. The values of V_{AB} , K_{AB} and V_{ABB} , K_{ABB} are shown in **Table 4.41**. The pair coefficients for both volume and compressibility are all positive except at all temperature 288.15K for DEGMME. In addition, triplet coefficients for volume have

Table 4.41 Pair (V_{AB} , K_{AB}) and triplet (V_{ABB} , K_{ABB}) interaction coefficients of DEGMME and DEGMEE in erythritol (aq) mixes.

T/K	$V_{AB} \times 10^6 (m^3 \cdot mol^{-2} \cdot kg)$	$V_{ABB} \times 10^6 (m^3 \cdot mol^{-3} \cdot kg^2)$	$K_{AB} \times 10^6 (m^3 \cdot mol^{-2} \cdot kg \cdot GPa^{-1})$	$K_{ABB} \times 10^6 (m^3 \cdot mol^{-3} \cdot kg^2 \cdot GPa^{-1})$
DEGMME				
288.15	20.81	-28.65	-0.06	2.73
298.15	20.59	-28.59	1.43	0.00
308.15	21.03	-29.67	1.20	0.08
318.15	20.86	-29.46	1.03	0.13
DEGMEE				
288.15	0.51	0.49	1.25	0.65
298.15	0.31	0.66	1.32	0.18
308.15	0.10	0.87	0.69	0.89
318.15	0.07	0.76	0.92	0.31

T/K is the temperatures.

negative for DEGMME at all temperatures and positive for DEGMEE and K_{ABB} are all positive. **Table 4.41** shows that V_{AB} , and K_{AB} are all positive except 288.15 K for DEGMME with temperature, which illustrates the pairwise association among DEGMME, DEGMEE, and erythritol. The interactions among the solute and co-solute arise because of overlapping hydration spheres. Furthermore, values of the triplet coefficient (V_{ABB} , K_{ABB}) are positive except at all four temperatures (288.15, 298.15, 308.15, and 318.15) K for DEGMME.

Isobaric thermal expansion coefficients

It is denoted by α_p , that measures the fractional change in volume of a material per unit change in temperature at constant pressure. Mathematically, it's expressed as equation **4.13**. It indicates how much a material expands or contracts per degree change in temperature, while keeping the pressure constant. All the values of α_p given in **Table 4.42** It is a measure of the sensitivity of a material's volume to temperature changes under constant pressure conditions. For DEGMME/ DEGMEE + Erythritol values of α_p are all positive but not consistent with temperature and with concentration [44]. Hepler's theory introduces the concept of Hepler's constant, denoted as $\left(\frac{\partial V_{\phi}^0}{\partial T}\right)$, which serves to categorise a solute into two distinct roles: as a builder or a breaker of structure. All values indicate that the solutes promote the formation or enhancement of structure.

Table 4.42 Isothermal expansion coefficients for DEGMME/ DEGMEE in erythritol (aq) solutions.

$^a m_B / (\text{mol} \cdot \text{kg}^{-1})$	$\alpha_p \times 10^3 / (K^{-1})$			
	T=288.15K	T=298.15K	T=308.15K	T=318.15K
DEGMME				
0.1	0.2382	0.2113	0.1845	0.1579
0.2	0.1689	0.1705	0.1721	0.1737
0.3	0.1317	0.1365	0.1413	0.1462
DEGMEE				
0.1	0.0813	0.0850	0.0888	0.0926
0.2	0.0634	0.0663	0.0691	0.0719
0.3	0.0557	0.0565	0.0572	0.0579

References

1. M.B. Blodgett, S.P. Ziemer, B.R. Brown, T.L. Niederhauser and E.M. Woolley, J. Chem. Thermodyn. 39, 627-644 (2007).
2. R. Gaba, N. Kaur, A. Pal and D. Sharma, J. Mol. Liq. 380, 121766 (2023).
3. C.M. Romero, M.S. Páez and M.J. Puchana, J. Mol. Liq. 223, 1192-1196 (2016).
4. C.P. Pandhurnekar, D.V. Parwate and S.S. Dhondge, J. Mol. Liq. 183, 94-101 (2013).
5. S.S. Dhondge, C.P. Pandhurnekar and D.V. Parwate, J. Chem. Eng. Data 41, 577-585 (2009).
6. H. Kaur, N. Chakraborty, K.C. Juglan and A. Upmanyu, J. Mol. Liq. 392, 123403 (2023).
7. H. Kumar, I. Behal and M. Singla, J. Chem. Thermodyn. 95, 1-14 (2016).
8. T. Sharma, R. Rani, A. Kumar and R.K. Bamezai, J. Mol. Liq. 300, 111985 (2020).
9. P. Kaur, N. Chakraborty, K.C. Juglan and H. Kumar, J. Mol. Liq. 315, 113763 (2020).
10. S.P. Jengathe, S.S. Dhondge, L.J. Paliwal, V.M. Tangde and S. Mondal, J. Chem. Thermodyn. 87, 78-87 (2015).
11. N. Chakraborty, K. Kaur, H. Kumar and K.C. Juglan, J. Chem. Eng. Data 65, 1435-1446 (2020).
12. P. Rajput, T. Sharma and A. Kumar, J. Mol. Liq. 326, 115210 (2021).
13. A. Thakur, K.C. Juglan, H. Kumar and K. Kaur, J. Mol. Liq. 288, 111014 (2019).
14. I. Banik and M.N. Roy, J. Mol. Liq. 203, 66–79 (2015).
15. M.N. Roy, B. Sinha, R. Dey and A. Sinha, Int. J. Thermophys. 26, 1549–1563 (2005).
16. D. Brahman and B. Sinha, J. Chem. Thermodyn. 75, 136–144 (2014).
17. M. Lamba, N. Chakraborty, K.C. Juglan, M. Singla and R. Sharma, J. Mol. Liq. 390, 123045 (2023).
18. Y. Marcus, Chem. Reviews, 109, 1346-1370 (2009).
19. A.K. Mishra and J.C. Ahluwalia, J. Phys. Chem. 88, 86–92 (1984).
20. M. Iqbal and M.A. Chaudhary, J. Chem. Thermodyn. 42, 951–956 (2010).
21. H. Kumar, M. Singla and R. Jindal, Monatshefte fur Chemie-Chemical Monthly 145, 1063–1082 (2014).

22. H. Kumar and I. Behal, *J. Mol. Liq.* 219, 756–764 (2016).
23. Z. Yan, J.J. Wang, H. Zheng, D. Liu, *J. Sol. Chem.* 27, 473–477 (1998).
24. K. Kaur, K.C. Juglan and H. Kumar, *J. Chem. Eng. Data* 62, 3769-3782 (2017).
25. B. Sinha, A. Sarkar, P. Roy and D. Brahman, *Int. J. Thermophys.* 32, 2062 -2078 (2011).
26. Ashima, K.C. Juglan and H. Kumar, *J. Chem. Thermodyn.* 140, 105916 (2020).
27. M.N. Roy, V.K. Dakua and B. Sinha, *Int. J. Thermophys.* 28, 1275 -1284 (2007).
28. H. Kumar, M. Singla and R. Jindal, *J. Mol. Liq.* 199, 385-392 (2014).
29. R. Sadeghi and A. Gholamireza, *J. Chem. Thermodyn.* 43, 200-215 (2011).
30. S.S. Dhondge, R. Paliwal N.S.S. Bhawe, *J. Chem. Thermodyn.* 59, 158-165 (2013).
31. A.K. Nain, R. Pal and Neetu, *J. Chem. Thermodyn.* 64, 172-181 (2013).
32. H.S. Frank and M.W. Evans, *J. Chem. Phys.* 13, 507–532 (1945).
33. H. Kumar, K. Kaur, S. Arti and M. Singla, *J. Mol. Liq.* 221, 526–534 (2016).
34. N. Chakraborty, H. Kumar, K. Kaur, K.C. Juglan, *J. Chem. Thermodyn.* 126, 137-146 (2018).
35. K. Kaur, K.C. Juglan and H. Kumar. *J. Mol. Liq.* 268, 700-706 (2018).
36. J.G. Kirkwood, *Chem. Rev.* 24, 233–251 (1939).
37. P. Ramasami and R. Kakkar, *J. Chem. Thermodyn.* 38, 1385–1395 (2006).
38. R. Sadheghi and F. Ziamajidi, *J. Chem. Eng. Data* 52, 1037–1044 (2007).
39. U. Gazal, Ameri. *J. Analy. Chem.* 14, 72-94 (2023).
40. C.V. Krishnan and H.L. Friedman, *J. Sol. Chem.* 2, 37-51 (1973).
41. W.G. McMillan Jr and J.E. Mayer, *J. Chem. Phys.* 13, 276-305 (1945).
42. A. Pal, H. Kumar, R. Maan, H. K. Sharma, *J. Sol. Chem.* 42, 1988-2011 (2013).
43. M.J. Iqbal and M.A. Chaudhry, *J. Chem. Thermodyn.* 42, 951-956 (2010).
44. Q.M. Omar, J.N. Jaubert and J. A. Awan, *Inter. J. Chem. Eng. Data* 1-10 (2018).

SUMMARY AND CONCLUSIONS

The thesis titled “Acoustic and thermodynamic study of glycol ethers in aqueous solution of sugar alcohols” describes the acoustic and thermodynamic properties of ternary mixtures consisting polyol components (maltitol, erythritol, and inositol) with water and six different glycol ethers. The research deals with the acoustic and thermodynamic properties of ternary mixtures based on polyols: maltitol, erythritol, and inositol, water, and glycol ethers. Density and ultrasonic velocity measurements were carried out at different temperatures and concentrations to derive some important thermodynamic parameters like apparent molar volumes, isentropic compressibility, and thermal expansion coefficients. Such parameters have offered deep insights into the interaction of a solute with a solvent, the role of the molecular structure, and the effects of temperature. The DSA 5000 M from Anton Paar can measure the density and the speed of sound in liquid mixtures from which further acoustic and thermodynamic parameters are calculated. In problem 1, after analyzing the results of volumetric and acoustic studies for the glycol ethers (2-ME and 2-EE) in an aqueous solution of inositol at different concentrations (0.01, 0.03, and 0.05) mol·kg⁻¹, four different temperatures (288.15–318.15 K), and a constant pressure 0.1 MPa, it is observed that when temperature and inositol concentration rise, solute-solvent interactions also increase. Density data are used to calculate the apparent and partial molar volumes. On the other hand, the speed of sound values was used to calculate the apparent and partial molar isentropic compression. The apparent molar expansibilities are very significant in both solutes and the solvent. Furthermore, the sign of $(\partial E_{\phi}^0/\partial T)_p$ denotes the ability to build and demolish structures. It can be determined from the apparent molar properties that in the liquid system, strong solute-solvent interactions occur. Additionally, mixtures contain intramolecular hydrogen bonds, dipole-induced dipole interactions, and dipole-dipole interactions. Additionally, hydrophobic hydration and hydrophobic impact are seen in these specifications. As determined by the transfer characteristics, it can be concluded that between solute and solvent molecules, hydrophilic-hydrophilic interactions predominate over hydrophobic interactions. Positive values for the apparent and partial molar volumes indicate a strong solute-solvent interaction in ternary combinations. It has been discovered that this

ternary mixture compresses more readily than do the pure components. All K_{ϕ}^0 values are negative. The K_{ϕ}^0 values become less negative as the temperature and solvent (water and inositol) concentrations rise. With this trend of decreasing negativity of the K_{ϕ}^0 values, there is an increase in the temperature, which implies a reduction of electrostriction and the emission of molecules of water into the bulk. FTIR spectroscopy can determine the type of interaction that is taking place during the IR measurements. A ternary mixture's spectroscopic data is also gathered, which is useful for revealing interactions and different structural alterations within the molecules. So, in this study, FTIR gives information about the shift in the band above 3000 cm^{-1} , which indicates the presence of an intermolecular hydrogen bond in a binary mixture. Furthermore, in problem 2, measurements of density and speed of sound for 2-butoxyethanol and 2-phenoxyethanol in maltitol aqueous solutions is provided. The experimental results have been utilised to calculate partial and apparent molar volumes. The analysis of the data provides clear insights into the interactions between maltitol and glycol ethers. The extent of these interactions increases as the concentration of the maltitol solution rises. The pair and triplet coefficients offer valuable insights as well. All $K_{\phi,s}$ values are negative, but they become less negative with increasing temperature and solvent concentration (water + maltitol). The apparent molar properties indicate the occurrence of strong solute-solvent interactions in the liquid system. The mixtures exhibit intramolecular hydrogen bonds, dipole-induced dipole interactions, dipole-dipole interactions, hydrophobic hydration, and hydrophobic impact. Analysis of the transfer characteristics $(\Delta V_{\phi}^0, \Delta K_{\phi}^0)$, reveals that hydrophilic-hydrophilic interactions predominate over hydrophobic interactions between the solute and solvent molecules. The decrease in negativity of the $K_{\phi,s}^0$ values is associated with an increase in temperature, suggesting a reduction in electrostriction and the release of water molecules into the bulk. The coefficient of thermal expansion is essential for interpreting solute-solvent interactions, while FTIR spectroscopy helps identify the type of interaction during IR readings. Furthermore, spectroscopic information on a ternary mixture is obtained, which facilitates the identification of interactions and structural modifications within the molecules. Therefore, the order, intensity, and position of the -OH band strongly support the conclusion derived from acoustic and

thermodynamic studies, indicating that molecular interactions reach their peak at these specific concentrations. Problem 3, provides volumetric and acoustic studies of glycol ethers, specifically diethylene glycol monomethyl ether (DEGMME) and diethylene glycol monoethyl ether (DEGMEE), in aqueous maltitol solutions. The experiments were conducted at different concentrations (0.04 , 0.06 , and $0.08 \text{ mol} \cdot \text{kg}^{-1}$) and temperature range of 288.15 to 318.15 K , under a constant pressure of 0.1 MPa . The results discovered that an increase in both temperature and maltitol concentration led to greater solute-solvent interactions. Density measurements allowed for the calculation of both apparent and partial molar volumes, denoted as V_ϕ and V_ϕ^0 , respectively. In corresponding, speed of sound data enabled the determination of apparent and partial molar isentropic compressions, represented as $K_{\phi,s}^0$ and $K_{\phi,s}^0$, respectively. The study found that the apparent molar expansibilities were significant for both the solutes and the solvent. The sign of $(\partial E_\phi^0/\partial T)_p$ provided some information related to the ability of the system to build or to destroy structures: strong interactions between the solute and solvent were present within the liquid system. Indeed, all the observed transfer properties agreed with dominant hydrophilic-hydrophilic against hydrophobic solute-solvent and, by consequence, solute-solute interactions. From this, both apparent and partial molar volumes have significant, positive values, indicating excellent interactions of the solute with the solvent in ternary mixtures. All the $K_{\phi,s}^0$ values calculated were negative in values, pointing to higher compressibility of the ternary solution than in pure components. These results have profound implications to understand the behaviors of such ternary systems especially in applications where solution properties must be controlled with high accuracy. In problem 4, volumetric and acoustic analyses on glycol ethers (specifically, DEGMME and DEGMEE) dissolved in an aqueous solution of erythritol at various concentrations (0.1 , 0.2 , and $0.3 \text{ mol} \cdot \text{kg}^{-1}$), across a range of temperatures (288.15 - 318.15 K) and at a constant pressure of 0.1 MPa , it was observed that as both temperature and erythritol concentration increased, there was a corresponding increase in solute-solvent interactions. Density measurements were utilized to compute both apparent and partial molar volumes (denoted as V_ϕ and V_ϕ^0 , respectively). Similarly, the speed of sound values was employed to calculate apparent and partial molar isentropic compressions

(denoted as $K_{\phi,s}^0$ and $K_{\phi,s}^0$ respectively). The apparent molar expansibilities were found to be significant for both the solutes and the solvent. The sign of $(\partial E_{\phi}^0/\partial T)_p$ signifies the system's capability to form or break down structures. Based on the analysis of molar properties, it was determined that the liquid system exhibits strong interactions between the solute and solvent. Investigation of transfer characteristics (ΔV_{ϕ}^0 and $\Delta K_{\phi,s}^0$) indicates that hydrophilic-hydrophilic interactions are more significant than hydrophobic interactions between the solute and solvent molecules. Positive values for apparent and partial molar volumes indicated strong solute-solvent interactions in ternary combinations. It was noted that this ternary mixture compresses more readily than its pure components. All $K_{\phi,s}^0$ values were found to be negative, with less negativity observed as temperature and solvent concentrations increased. The ultrasonic technique has proven to be a powerful, non-destructive tool for studying intermolecular interactions in ternary liquid mixtures. This study investigates the acoustic and thermodynamic behavior of polyols (maltitol, erythritol, inositol) with glycol ethers in aqueous solutions, revealing both expected and unusual interaction patterns. These findings deepen the theoretical understanding of ternary mixtures, which are often oversimplified in binary studies. Beyond theory, the results have practical relevance across industries-enhancing drug formulation in pharmaceuticals, improving texture and stability in cosmetics and food products, and optimizing solvent systems in chemical and polymer processing. This work underscores the importance of molecular-level insight for designing stable, efficient, and responsive industrial formulations.

Future Scope of the Present Work

The ultrasonic technique has gained prominence across various scientific sectors due to its ability to non-destructively analyse the thermodynamic and acoustic properties of binary and ternary liquid mixtures. This method provides valuable insights into the molecular interactions, including binding forces between atoms and molecules within liquid mixtures, making it an effective tool for understanding complex fluids. Its non-invasive nature allows for precise measurements without altering the components, which is particularly advantageous for applications in industries such as food, cosmetics, and pharmaceuticals. While pure solvents have well-established uses across these sectors, the study of combinations of these pure liquids opens up new opportunities for innovation. There are numerous potential combinations of pure solvents that remain unexplored, which could lead to the development of novel mixtures with enhanced properties. Understanding the interactions within these mixtures can optimize formulations, improve product performance, and create more effective solutions for industrial and household applications. Hence, further research on these solvent combinations could significantly benefit various industries, paving the way for new and improved chemical processes and products.

List of publications

1. **Harsimaran Kaur**, Nabaparna Chakraborty, and K.C. Juglan, “Volumetric and “Ultrasonic Studies on Interactions of 2-Methoxyethanol/2-Ethoxyethanol in Aqueous Solutions of Inositol at Different Temperatures” (2024) published in *Journal of Chemical and Engineering Data* (American Chemical Society) with impact factor **2.3**.
<https://doi.org/10.1021/acs.jced.4c00088>
2. **Harsimaran Kaur**, Nabaparna Chakraborty, K.C. Juglan, and Arun Upmanyu “Thermodynamic and physicochemical characteristics of 2-butoxyethanol/ 2-phenoxyethanol in aqueous maltitol solutions” (2023) published in *Journal of Molecular Liquids* (Elsevier publications) with impact factor **5.3**.
<https://doi.org/10.1016/j.molliq.2023.123403>
3. **Harsimaran Kaur**, Nabaparna Chakraborty, K. C. Juglan, Arun Upmanyu “Study of Thermodynamic and Acoustic Properties of DEGMME/ DEGMEE in aqueous Erythritol solutions at different temperatures” (2024) published in *Journal of Chemical Thermodynamics* (Elsevier publications) with impact factor **2.2**. <https://doi.org/10.1016/j.jct.2024.107446>
4. **Harsimaran Kaur**, Nabaparna Chakraborty, and K. C. Juglan “Characteristics of a temperature dependent aqueous solution of Maltitol with DEGMME/ DEGMEE: An acoustic and volumetric approach” (2025) is published in “Journal of Chemical and Engineering data” with impact factor **2.3**.
<https://doi.org/10.1021/acs.jced.4c00638>
5. **Harsimaran Kaur**, Nabaparna Chakraborty, Kailash Chandra Juglan, Parminder Kaur and Harsh Kumar, “Study of Molecular Interaction of PEG-200 and PEG-600 in Aqueous D-Mannitol Solutions at Different Temperatures” 1-14 (2022), published in *Letters in Applied NanoBioscience*.
6. Pallvee Thakur, **Harsimaran Kaur**, Kailash Chandra Juglan, and Harsh Kumar “Investigation of acoustical properties of glycols with D-Mannitol mixture” (2024) published in *AIP conference proceeding* (AIP)
<https://doi.org/10.1063/5.0192673>
7. **Harsimaran Kaur**, Kailash Chandra Juglan, and Nabaparna Chakraborty “A Review on the Acoustic and Thermodynamic Properties of Sugar Alcohols”

- (2024) published in *Cutting-Edge Applications of Nanomaterials in Biomedical Sciences* (IGI Global).
8. **Harsimaran Kaur**, Prachi Patnaik, and Harsh Kumar “**Study of Molecular interactions of glycols with D-Mannitol at different temperature**” (2021) **Journal of Physics: Conference Series (IOP publishing)**.
<https://doi.org/10.1088/1742-6596/2267/1/012047>
 9. Kanika Bhakri, K.C. Juglan, Nabaparna Chakraborty, and **Harsimran Kaur**, **An Investigation to Display Galactose's Physico-Chemical Behaviour with PEGs: A Thermo-Acoustical and Spectroscopic Study**” published in **International Journal of Thermophysics (Springer)** with Impact factor **2.5**.
 10. Harsimaran Kaur, Nabaparna Chakraborty, K.C. Juglan, Harsh Kumar “**Volumetric and Acoustic Behavior of PEG-200 and PEG-600 in Aqueous D-Mannitol solutions at Different Temperatures**” published in *Journal of solution chemistry* (Springer) with Impact factor **1.5**.
 11. Ashima Thakur, Harsimaran Kaur, Nabaparna Chakraborty, K.C. Juglan, Harsh Kumar “**Molecular interactions in ternary system of ethane-1, 2-diol with methanol and methyl 4-hydroxybenzoate at 298 K: An acoustic approach**” published in **Journal of Physics: Conference Series (IOP)**.

List of communicated papers

1. **Harsimaran Kaur**, Nabaparna Chakraborty, and K. C. Juglan “**Effect of Temperature on the Volumetric and Acoustic Properties of Alkoxyethanol’s in Aqueous Maltitol Solution**” submitted to *Journal of Solution Chemistry*.
2. **Harsimaran Kaur**, Nabaparna Chakraborty, and K. C. Juglan “**Analysis of physical properties of glycol ethers in aqueous erythritol solution through thermo-acoustic approach**” submitted to *Journal of Chemical Thermodynamics*.
3. **Harsimaran Kaur**, Nabaparna Chakraborty, and K. C. Juglan “**Physicochemical and spectroscopic studies of molecular interactions for 2-methoxyethanol and 2-ethoxyethanol in aqueous erythritol mixtures at different temperatures**” submitted to *The Journal of Chemical and engineering data*.
4. **Harsimaran Kaur**, Nabaparna Chakraborty, and K. C. Juglan “**A Comprehensive Study of Ternary Mixtures: Acoustic, Thermodynamic, and Spectroscopic Analysis of Glycol Ethers and Inositol Interactions**” submitted to *Journal of Molecular Liquids*.

List of Conferences

Attended Conferences

1. **Recent Advances in Fundamental and Applied Sciences**, Lovely Professional University, Phagwara, Punjab, 19th and 20th April 2024, “Investigation on molecular interaction glycol ether in aqueous erythritol solution at different temperatures through thermo-acoustical analysis”
2. **Recent Advances in Fundamental and Applied Sciences**, Lovely Professional University, Phagwara, Punjab, 24th and 25th March 2023, “Acoustic and thermodynamic investigations of sugar alcohol: A Review”
3. **Fundamental and Applied Sciences**, Sardar Vallabhbhai national Institute of technology, Surat, 20th and 21th October 2021, “Study of Molecular Interaction of PEG-200 and PEG-600 in Aqueous D-Mannitol Solutions at Different Temperatures”